RAS AND RHO CO-REGULATE LIVER DEVELOPMENT AND HEPATOCELLULAR CARCINOMA IN ZEBRAFISH

CHEW TI WENG
(B.Sc. (Hons.), NUS)

A THESIS SUBMITTED

FOR THE DEGREE OF DOCTOR OF PHILOSOPHY

DEPARTMENT OF BIOLOGICAL SCIENCES

NATIONAL UNIVERSITY OF SINGAPORE

2012

Acknowledgements

The work presented in this thesis has been carried out at the Department of Biological Sciences, Faculty of Science, National University of Singapore, from 2007 to 2011. It has been my privilege and honor to have the opportunity to work with so many brilliant, diligent and helpful colleagues and friends during these five years.

First and foremost, I would like to express my utmost gratitude to my thesis supervisors Associate Professor Low Boon Chuan and Professor Gong Zhiyuan for their continuous support, creative insights, invaluable guidance, encouragement throughout the study, and also the room needed for myself to develop in own way and pace. If not for their foresight and unsurpassed knowledge of cell signaling and zebrafish biology, this work would have never have been achieved.

I would like to thank my mentors, Dr Liu Lihui and Dr Liu Xingjun, for their precious time, their constant mentoring and valuable insights especially during the budding phase of this study.

I would also like to thank collaborator Dr Jan Spitsbergen from Oregon State University for her invaluable advice and professional contribution, which are vital for this study.

Next, I will like to thank Dr Zhou Yiting, Dr Chew Li Li, and Dr Unice Soh for always being so kind and helpful in rendering help and advice when most needed, Kenny Lim and Jasmine Chin for the huge moral support and friendship throughout these years. I must also thank Mr. Balan of the zebrafish husbandry for the technical support, insight

on zebrafish maintenance and friendship for the past few years. It has been an honor and blessing for me to be able to work with a group of cheerful, youthful and helpful people in the two different laboratories. Many thanks to you people, Doreen, Catherine, Aarthi, Jennifer, Dandan, Denise, Pearl, Shuting, Shizhen, Jichao, Huang Lu, Zhenghua, Shelly, Archna, Akila, Anjali, Pan Meng, TingTing, Jiawei, Xuahua, Tong Yan, Huiqing, Tina, Caixia, Grace, Lili, JianZhou, Lizhen, Weiling, Zhou Li, Xiaoqian, Hendrian, Xiaoyan, Hong Yan, Shen Yuan, Sahar, Anh Tuan, Qing Hua and many others who have helped me in one way or another.

I would like to thank all my family members and loved ones for their continuous support and patience during the course of this study, especially my beloved wife, Aileen, and my parents.

Last but not least, I would like to acknowledge the National University of Singapore for awarding the Graduate Research Scholarship during the course of my studies, and the biomedical research council (BMRC), A-Star, Singapore who has funded the study.

Table of contents

Summary

Aberrant RAS signaling, caused by activating mutations of the *RAS* genes (H-, K- and NRAS), has been implicated in approximately 30% of all human cancers with the vast majority of these mutations occurring in the *KRAS*. Approximately five percent of human liver cancers are attributed to activating mutations of the KRAS. Hepatocellular carcinoma (HCC), a common form of primary liver tumor, is one of the most common and aggressive tumors worldwide. Capitalizing on the growing importance and relevance of zebrafish, *Danio rerio*, as an alternate cancer model, it was used to model human HCC in this study.

The Tg(*lfabp*-rtTA2s-M2; *TRE2*-eGFP-Kras G12V) line expressed eGFP-Kras G12V in a liver-specific manner under the control of the Tet-on system. Ectopically expressed eGFP-Kras G12V was predominantly localized at the plasma membrane and was biologically active. Based on quantitative bio-imaging and molecular markers for genetic and signaling aberrations, we showed that oncogenic Kras expression during early development caused liver enlargement, concomitant with elevated RAF/MAPK and PI3K/AKT signaling. Kras G12V expression in adult transgenic resulted in the development of HCC associated with increased RAF/MAPK signaling. Thus, this model could be useful as a platform for small molecule screen or the study of oncogenic Kras signaling.

Like the KRAS GTPase, RhoA also acts as a key molecular switch in the signal-transduction cascade that controls and regulates many important biological processes ranging from proliferation and survival, to migration. It is also implicated in many human cancers. While much has been learnt about their individual functions in cell and animal

models, the physiological/pathophysiological consequences of their signaling crosstalk in multi-cellular context *in vivo* remains undefined, especially in liver development and cancers. Furthermore, the roles of RhoA in RAS-mediated transformation remain controversial. Herein, I generated transgenic fish that expressed RhoA, constitutively active RhoA G14V or dominant-negative RhoA T19N in a liver restricted manner under the control of the Tet-on system. They were used to study the crosstalk of Kras and RhoA in the context of liver development and tumorigenesis.

Double transgenic fish harboring Kras G12V and RhoA or its mutants were obtained by the crossing of selected transgenic lines. The oncogenic Kras-mediated liver overgrowth was augmented significantly by dominant-negative RhoA T19N, but was significantly reduced by constitutively active RhoA G14V. These changes correlated well with changes in hepatocyte proliferation in the respective transgenic lines. It could be, in part, attributed to the upregulation of Akt2 expression/activities by reduced RhoA signaling, and the downregulation of Akt2 expression/activities by increased RhoA signaling, in the respective double transgenic larvae.

Survival studies further revealed that co-expression of dominant-negative RhoA T19N with oncogenic Kras increased the mortality rate (due to HCC development) significantly as compared to the other single and double transgenic lines. Interestingly, the double transgenic Tg(*lfabp*-rtTA2s-M2; *TRE2*-eGFP-Kras G12V; *lfabp*-rtTAs-M2-*TRE2*-mCherry-RhoA G14V) did not result in any significant increase in its survival compared to the Tg(*lfabp*-rtTA2s-M2; *TRE2*-eGFP-Kras G12V) despite its ability to downregulate Kras-mediated liver enlargement in the larvae.

In this study, I reported the first *in vivo* vertebrate animal model of Ras and Rho crosstalk in regulating liver development and tumorigenesis. My findings could eventually influence the development and use of therapeutic intervention targeting RhoA signaling for the treatment of RAS-driven cancers.

Key findings:

- I have established a zebrafish HCC model, driven by oncogenic Kras signaling, with potential as a platform for chemical compound library screening for drug development.
- I demonstrated that the liver-specific ectopic expression of either RhoA or its mutant could cause the development of HCC in transgenic zebrafish.
- I have established the first *in vivo* vertebrate model of crosstalk between Kras and RhoA in regulating liver development and tumorigenesis.

List of Figures

List of Tables

List of Abbreviations

AKT	v-akt murine thymoma viral oncogene homolog
ALL-1	Leukemia, acute lymphocytic, susceptibility to -1
ARF	ADP ribosylation factor
BAD	BCL2-associated agonist of cell death
BCL	Associated agonist of cell death
BSA	Bovine serum albumin
Cdc42	Cell division cycle 42
CE	Convergence and extension
Chp	Calcium binding protein P22
DAG	Diacylglycerol
DLC-1	Deleted in liver cancer -1
DMBA	7,12-dimethylbenz(a)anthracene
Dox	Doxycycline
dpf	Days post fertilization
E-cadherin	Epithelial-cadherin
EGF	Epithelial growth factor
eGFP	Enhanced green fluorescent protein
EGFR	Epithelial growth factor receptor
EMT	Epithelial mesenchymal transition
ERK	Mitogen-activated protein kinase kinase
GAP	GTPase activating protein
GDI	GDP dissociation inhibitor
GDP	Guanosine diphosphate

GDS	GDP dissociation stimulator
GEF	Guanine nucleotide exchange factor
GFP	Green fluorescence protein
GTP	Guanosine triphosphate
H&E	Hematoxylin and eosin
HCA	Hepatocellular adenoma
HCC	Hepatocellular carcinoma
HIF1α	Hypoxia-inducible factor 1α
HP	Hyperplasia
HRAS	Harvey RAS
IF	Immunofluorescence
IHC	Immuno-histochemistry
IKK	IκB kinase
iNOS	Inducible nitrate oxide synthase
KRAS	Kirsten RAS
lfabp	Liver fatty acid binding protein
LIM-kinase	LIM domain kinase
MAPK	Mitogen-activated protein kinase
mDia	Mammalian diaphanous
MEK	Mitogen-activated protein kinase
MET	Met proto-oncogene (hepatocyte growth factor)
MLC	Myosin light chain
MMP	Matrix metalloproteinase
MST1	Macrophage stimulating 1
mTORC2	Mammalian target of rapamycin C2

MYC	v-myc myelocytomatosis viral oncogene homolog
NF-κB	Nuclear factor kappa-light-chain-enhancer of activated B cells
ng	Nano gram
nm	Nano meter
NRAS	Neuroblastoma RAS
PAR4	Prostate apoptosis response 4
PBS	Phosphate buffered saline
PBST	Phosphate buffered saline with 0.1% Tween20
PCNA	Proliferating cell nuclear antigen
PCR	Polymerase chain reaction
PDK1	Phosphoinositide dependent kinase 1
PH domain	Pleckstrin homology domain
pH3	Phospho-histone 3
PI3K	phosphoinositide-3-kinase
PIP2	Phosphatidylinositol 4,5-bisphosphate
PIP3	Phosphatidylinositol 3,4,5- triphosphate
PKA	Protein kinase A
PLCε	phospholipase C, epsilon
RAB	Member RAS oncogene family
RAC	Ras-related C3 botulinum toxin substrate
RAF	v-raf murine sarcoma viral oncogene homolog
RAL1	v-ral simian leukemia viral oncogene homolog 1
RALGEF	v-ral simian leukemia viral oncogene homolog guanine exchange factor
RAN	RAS-related nuclear protein
RAS	Rat sarcoma viral oncogene homolog

RASGAP	RAS GTPase activating protein
RASGEF	RAS guanine exchange factor
RASSF	Ras-dissociated domain family
RBD	Ras binding domain
RHO	Ras homology protein
RIN1	RAS and RAB interactor 1
RKIP	RAF-1 kinase inhibitory protein
ROCK	Rho-associated coiled-coiled containing protein kinase
RTK	Receptor tyrosine kinase
rtTA	Reverse Tet-controlled transcriptional activator
SDS-PAGE	Sodium dodecyl sulphate polyacrylamide gel electrophoresis
Smurf1	SMAD specific E3 ubiquitin protein ligase 1
SOS	Son of sevenless
TBS	Tris-buffered saline
TBST	Tris-buffered saline with 0.1% Tween20
Tet	Tetracycline
TGFβ	Transforming growth factor beta
TIAM1	T-cell lymphoma invasion and metastasis-1
TRE	Tetracycline response element
tTA	Tet-controlled transcriptional activator
VEGFA	Vascular endothelial growth factor A
WT	Wild type
µl	Micro litre
µm	Micro meter

List of Conferences

Poster from the current thesis presented in conference

1. 5th Mechanobiology conference. 9-11th November 2011. NUS, Singapore

Chapter 1 Introduction

1.1 RAS superfamily of small guanine nucleotide triphosphatases (GTPases)

Early research in the 1960s on the oncogenic Harvey murine sarcomas virus and Kirsten murine sarcomas virus provided vast early insight into oncogenic genetics elements which were later established as human *HRAS* and *KRAS* oncogene, respectively. They got their name RAS because of their ability to cause rat sarcomas (Cox and Der, 2010). It was not until 1982 that HRAS, the first human mutated active oncogene, was identified in human cancer (Cox and Der, 2010; Shih and Weinberg, 1982). Since then numerous efforts were spent characterizing the RAS oncogene, identifying its role as a master regulator of many aspects of cell biology, including proliferation, differentiation, cytoskeleton reorganization, nucleocytoplasmic transport, microtubule organization, vesicle trafficking and gene expression (Takai et al., 2001). It also triggered future studies that led to the identification and characterization of many small GTPase members of the RAS superfamily.

The RAS superfamily of small guanine nucleotide triphosphatases (GTPases) consists of monomeric G-proteins with molecular masses of 20-40 kDa and comprises over 150 members in humans (Figure 1.1). Many of the members are highly conserved among eukaryotes. They are divided into five major branches, namely the RAS, RHO, RAB, RAN and the ARF family, based on their sequence and functional similarities (Wennerberg et al., 2005). The RAB family is the largest with 61 members while RAN is the smallest with only one member. Each family such as the RAS family can be further classified into many sub-families, as illustrated in Figure 1.2. Structurally, members of the RAS superfamily share a conserved G domain that is made up of five sets of G box

GDP/GTP binding motif elements starting at the N-terminus, called G1 to G5 motifs (Bourne et al., 1991; Wennerberg et al., 2005).

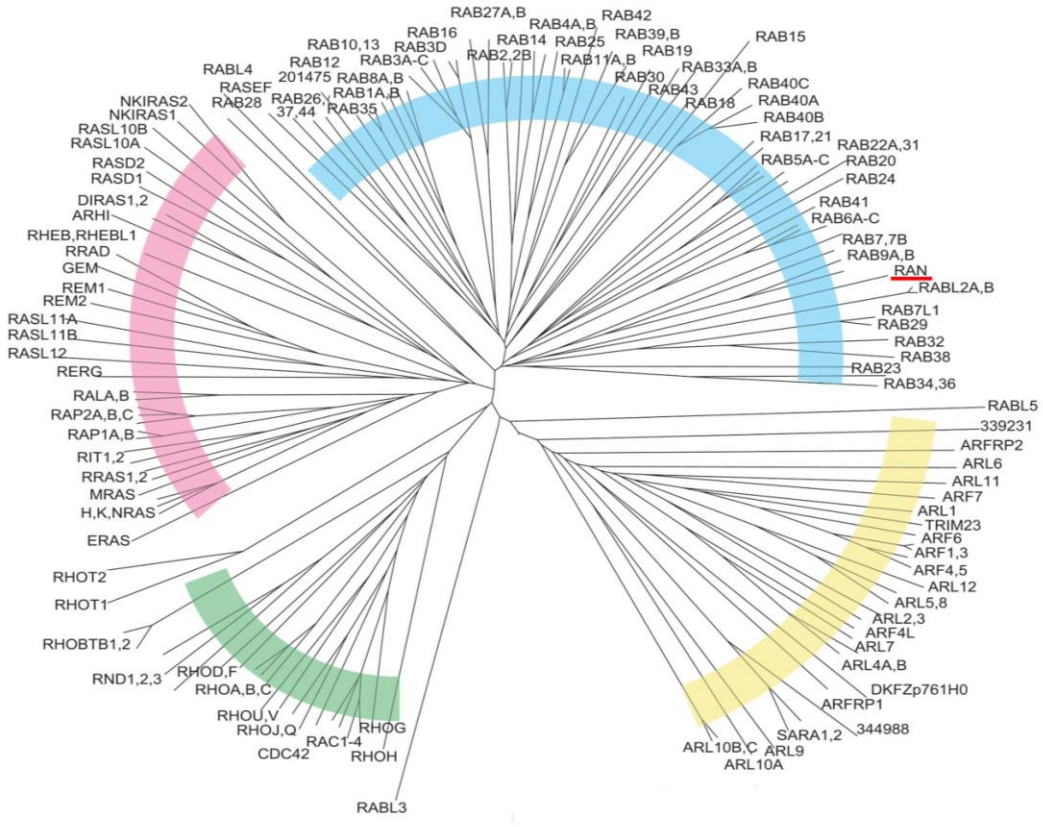

Figure 1.1: Dendrogram of Human RAS superfamily members. RAS superfamily members are divided into five families, namely the RAS, RHO, RAN, RAB and ARF family. The RAB family comprises of the largest number of members with 61 members (blue), followed by the RAS family with 36 members (pink), the ARF family with 27 members (yellow), the RHO family with 20 members (green) and the smallest family being the RAN subfamily with only one member (underlined in red) (Colicelli, 2004). RAN is grouped together in the RAB family.

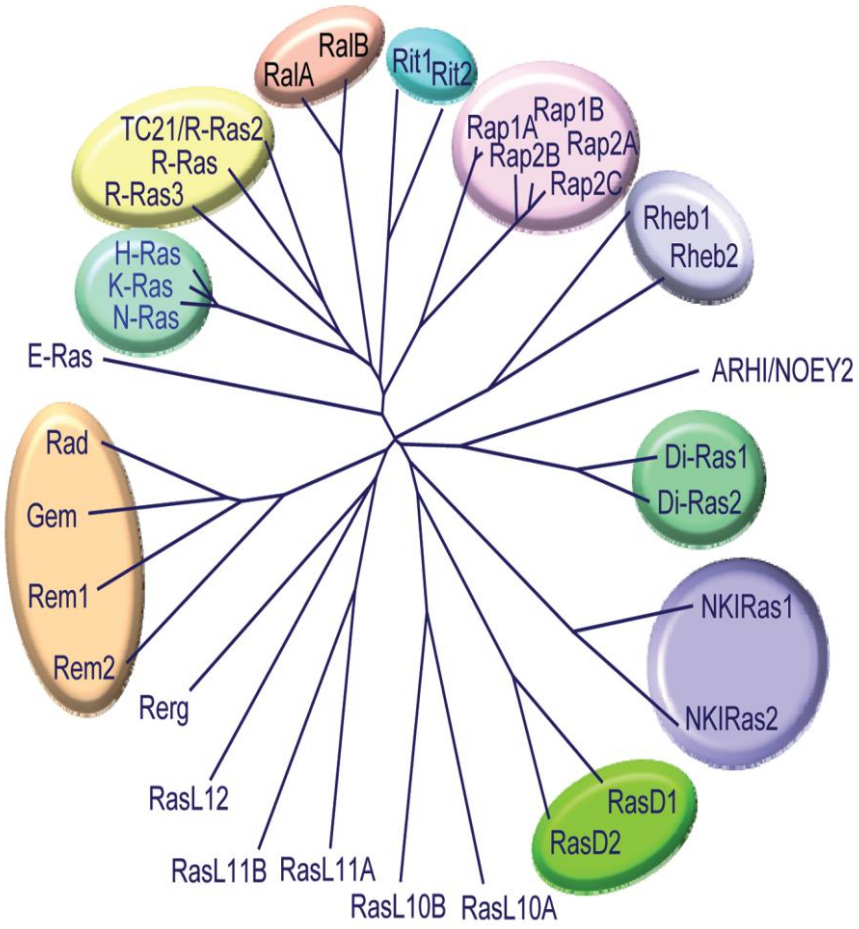

Figure 1.2: Dendrogram of members from the RAS family. The RAS family radial tree was generated using matrices derived from a ClustalW multiple sequence alignment of the various RAS family members (Modified from Karnoub and Weinberg, 2008). The H-, N-, and KRAS proteins are grouped together in a cluster. They represent the better characterized members of the RAS family.

The small GTPases can be considered as binary molecular switches, cycling between the GTP-bound active form and the GDP-bound inactive form. The GTPases possess low intrinsic GTP hydrolysis activity and high affinity for free GDP and GTP (Wennerberg et al., 2005). The activity of the small GTPases is tightly regulated by two

groups of proteins, namely the guanine exchange factors (GEFs) and the GTPase-activating proteins (GAPs). The small GTPases are activated by the GEFs which promote GDP release and the subsequent binding to the more abundant GTP. Once activated, the small GTPases can bind to different effectors and trigger cascades of signaling to elicit various cellular responses. The GAPs are negative regulators of the small GTPase signaling. The GAP serves to increase the intrinsic GTPase activity of the small GTPases, hydrolyzing the GTP to GDP, thus rendering the GTPase inactive (Figure 1.3). GTPases within each family are regulated by common and unique GEFs and GAPs, emphasizing the specificity and redundancy in GTPase signaling. The GTP-bound GTPases and GDP-bound GTPases displayed significant conformation similarities except in the region of switch I and switch II. The differences in these two switch regions allow regulatory proteins and effectors to determine the activation status of the GTPases (Wennerberg et al., 2005).

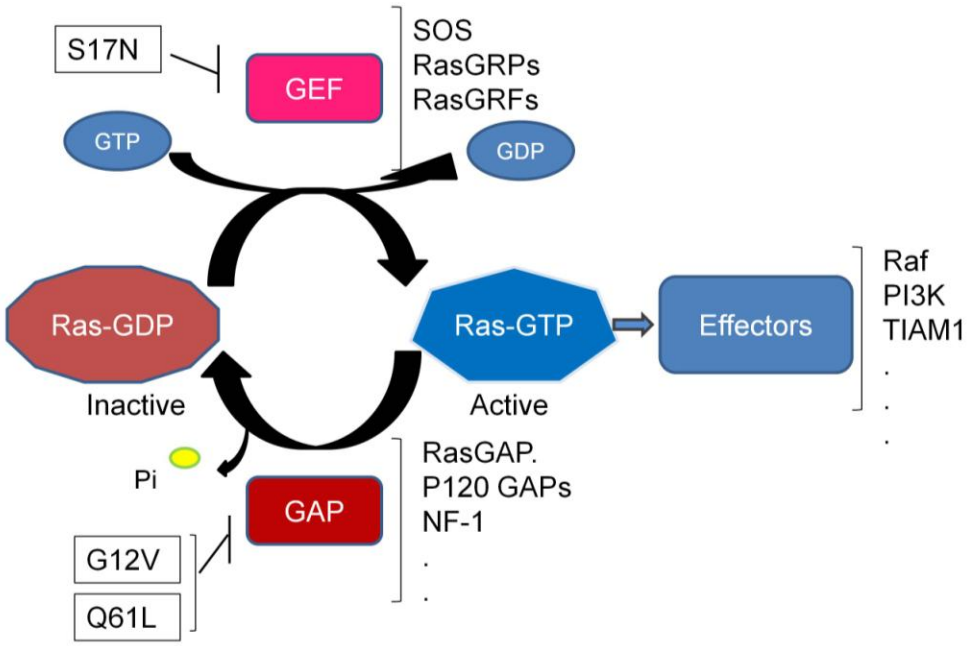

Figure 1.3: Regulation of RAS signaling networks. RAS proteins are binary molecular switches that cycle between the active GTP-bound state and the inactive GTP-bound state. They are negatively regulated by GAP proteins such as RASGAP, p120GAP, and NF-1. They are activated by GEF such as the Son of sevenless (SOS), Ras GTP-releasing proteins/factors (RasGRPs/RasGRFs). The binding of GTP activates RAS and enables its high affinity interactions with downstream targets, called effectors. RAS proteins act as signal transducers to convey and convert extracellular cues into biological responses. Growth factor stimulation of the receptor tyrosine kinase activates the RAS proteins, and through its interaction with downstream effectors initiates several signaling cascades. Activating mutation in codon 12 or 61 renders the RAS protein resistant to negative regulation by the GAP proteins, thus remains constitutively active. Mutation in codon 17 of the RAS protein renders it resistant to GEF activity and thus acts as a dominant negative mutant to downregulate RAS signaling (Cox and Der, 2010).

Post-translational modification by lipids represents another level of regulation for the majority of the RAS superfamily members. Many members of the RAS and Rho families possess a C-terminal CAAX tetrapeptide sequence (C = Cys, A = aliphatic amino acid and X = any amino acid) (Cox and Der, 2002; Wennerberg et al., 2005). The

CAAX sequence is the recognition sequence for lipid modification by farnesyltransferase or geranylgeranyltransferase. The lipid modified CAAX sequence coupled with an upstream secondary signal provides the membrane targeting signals, which determine the subcellular location of the small GTPases. Membrane anchoring for many members of the RAS super-family is a prerequisite for their activity (Olofsson, 1999). In addition, the activity of certain small GTPase, for example, RAB and RHO/RAC families, can also be regulated by guanine-nucleotide-dissociation inhibitors (GDIs). GDI does so by binding to the C-terminal of these small GTPases and extracting it from the membrane and sequestering it in its GDP-bound inactive form (Olofsson, 1999) in the cytosol.

1.1.1 RAS family of GTPases

The RAS family of GTPases encompasses 36 genes which encode 39 RAS proteins in the human genome (Karnoub and Weinberg, 2008). The RAS proteins are tightly regulated by the RASGAP and RASGEF proteins. To date, there are nine known RASGEF genes and eight RASGAP genes in the human genome (Grewal et al., 2011; Lahoz and Hall, 2008). Out of the 36 *RAS* genes, three *RAS* genes namely, *K*-, *N*-, *HRAS* were better characterized than other members of the family. These three members form the RAS sub-family in the RAS family of GTPases. These RAS proteins mainly act as signal transducers, transmitting and translating extracellular signals into cellular processes.

The differential biology of the three RAS isoforms is largely attributed to their respective distinct membrane targeting sequences and post-translational lipid processing (Figure 1.4). They share a highly conserved N-terminal domain (1-165aa) with 90-95% identity. The C-terminal sequence (166-188/9aa), which is also known as the hypervariable region, differs significantly among the three members. The hypervariable region consists of the anchor sequences that act as the RAS trafficking signals. The anchor sequence is made of the CAAX motif and a secondary signal. The NRAS and HRAS have a single palmitoylation site (C181) and double palmitoylation sites (C181 & C184), respectively, as the secondary signal. In KRAS, the poly-lysine sequence (K175-180) serves as the secondary signal (Hancock, 2003). The H-, N- and KRAS undergo farnesylation at the endoplasmic reticulum catalyzed by the ER-associated acyltransferase. The first lipid modification occurs on the cysteine residue in the CAAX motif. The H- and NRAS, but not KRAS, are palmitoylated at the ER and traffic through the Golgi to the plasma membrane. The KRAS exits the ER after the initial farnesylation and traffic to the plasma membrane by an uncharacterized mechanism (Hancock, 2003). It anchors itself to the plasma membrane through lipid modification and the poly-lysine sequence interaction with negatively charged head group of phosphatidylserine and phosphatidylinositol (Cox and Der, 2010). KRAS, like other RAS family members, needs to be membrane-bound for effective signaling to occur. Plasma-membrane-tethered KRAS can induce transformation, while mitochondrial bound KRAS can induce apoptosis (Bivona et al., 2006). Under normal/resting conditions, quiescent cells have only 5% of their total Ras proteins in the GTP-bound active form as compared to 50%

upon mutagenic activation (Osterop et al., 1993). Once in its GTP-bound active form, RAS can initiate cascades of signaling pathway by interacting with its many effectors.

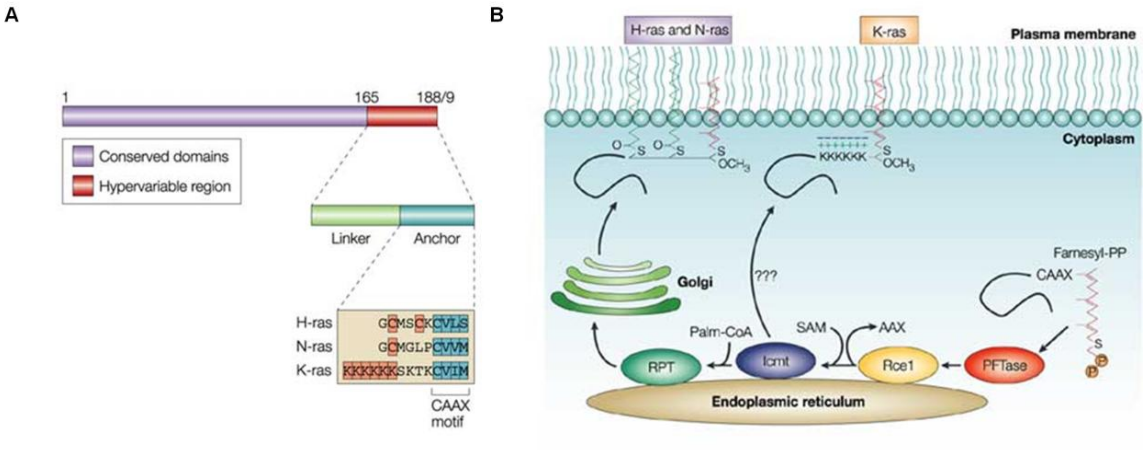

Figure 1.4: Domain architecture of the RAS protein and its membrane trafficking. (A) The three RAS proteins shared a conserved N-terminal of the first 165 amino acids, with 90-95% identity. They vary significantly at the C-terminus which is also known as the hypervariable region. The hypervariable region comprises the RAS anchor sequence, which consist of the CAAX motif and a secondary signal (highlighted in orange). The RAS anchor sequence acts as the RAS trafficking signal. The secondary signal in the H- and NRAS is made up of two and one palmitoylation sites, respectively. The poly-lysine stretch is the secondary signal in the KRAS. (B) The CAAX motif is processed in a step-wise manner. It starts with the protein farnesyltransferase (PFTase) adding a farnesyl group (Farnesyl-PP) to the cysteine in the CAAX motif. The process continues at the endoplasmic reticulum with Rce1 removing the AAX tripeptide and conclude with the methylation with S-adenosylmethionine (SAM) by the Icmt. KRAS exit the ER after this step and traffic to the plasma membrane. The H- and NRAS are subsequently palmitoylated by the palmitosyltransferase (RPT), and translocate to the plasma membrane through the Golgi. (Hancock, 2003)

1.1.1.1 Effectors of the RAS signaling

The RAF/MEK/ERK and PI3K/AKT pathways are two well-characterized pathways out of the many vital signaling cascades regulated by RAS activation (Figure 1.5).

In the RAS/RAF/MEK/ERK pathway, the RAS is activated by the receptor tyrosine kinase (EGFR) through RasGEF SOS. The activated RAS recruits the RAF proteins to the plasma membrane where they are activated by phosphorylation. Active RAF phosphorylates and activates the MEK1/2 protein kinases, which in turn phosphorylate and activate the ERK1/2 proteins. Activated ERK1/2 proteins translocate to the nucleus. In the nucleus, ERK1/2 can phosphorylate and activate many transcription factors, triggering transcription of many growth-related proteins. It was also demonstrated that the MAPK signaling is both sufficient and necessary to induce cellular transformation in mouse cell lines (Leevers et al., 1994; Stokoe et al., 1994; White et al., 1995). However, one study in 1996 by Khosravi-Far and co-workers demonstrated that the engagement of the RAF/MEK pathway is not necessary for RAS-induced transformation (Khosravi-Far et al., 1996).

In the PI3K/AKT pathway, the activated RAS can activate PI3K. Activated PI3K converts PIP2 to PIP3. The PIP3 serves as signal/sites to recruit PH domain containing proteins to the plasma membrane. AKT and PDK1 are examples of proteins with PH domain. At the plasma membrane, the AKT protein is phosphorylated by PDK1 and mTORC2, which renders it catalytically active. Overactive AKT is implicated in cellular transformation and survival (Heron-Milhavet et al., 2011).

Many years of intense research on the RAS also led to the identification of many other RAS effectors, which play many vital roles in RAS transformation. These include RalGEF, phospholipase Cε, TIAM1, RIN1, ALL-1 and the RASSF (Karnoub and Weinberg, 2008). The RalGEF-Ral pathway was demonstrated to be sufficient for the RAS-mediated transformation in human cell line (Hamad et al., 2002), which could be attributed to their ability to promote proliferation and evade apoptosis (Chien and White, 2003). TIAM1 knock-out mice show resistance to 7, 12 dimethylbenz(a)anthracene (DMBA)-induced tumorigenesis (Malliri et al., 2002). DMBA are carcinogens known to cause oncogenic RAS activation which resulted in skin tumorigenesis.

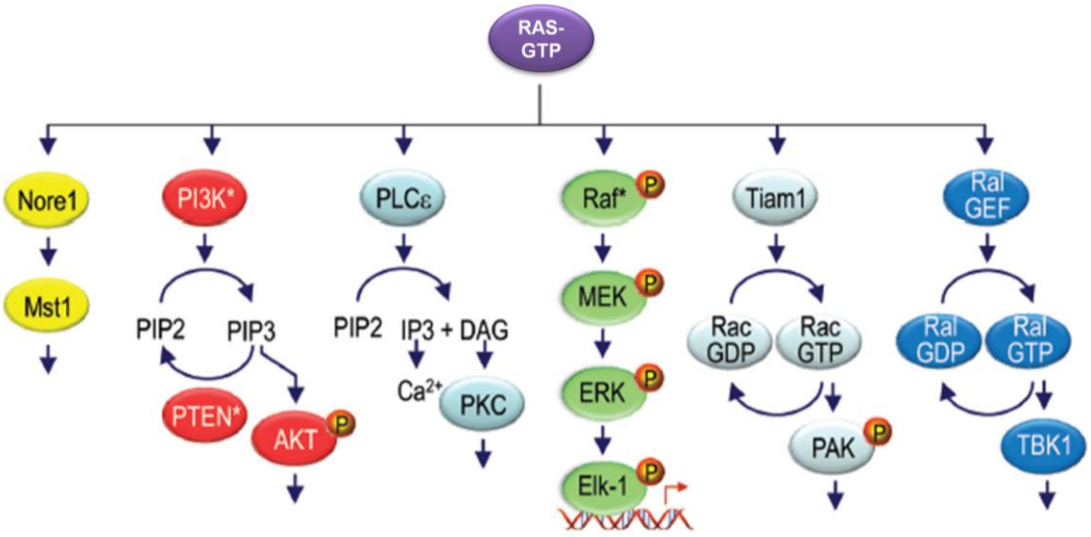

Figure 1.5: Ras signaling networks. RAS proteins serve to relay extracellular cues to cytoplasmic signalling cascades. GTP-bound activated Ras engages effector molecules — belonging to multiple effector families — that initiate several signal-transduction cascades which translate into various cellular processes. Adopted from (Cox and Der, 2010).

1.1.1.2 RAS in tumorigenesis

The RAS signaling cascade is mis-regulated in approximately 30% of all human tumors. In addition, *RAS* genes are the most frequently mutated oncogenes that can be detected in human tumors. Mutations in codons 12, 13 or 61 of any one of the three RAS, KRAS, NRAS and HRAS, transform them into active oncogenes. The KRAS and HRAS are more frequently mutated at glycine 12 while the NRAS is frequently mutated at glutamine 61. These activating mutations can be found in a variety of tumor types (Bos, 1989; Karnoub and Weinberg, 2008; Pylayeva-Gupta et al., 2011). Mutations at these codons render the RAS GTPase unable to hydrolyse the bound-GTP to GDP and become locked in the active form. Mutation at Q61 prevents the proper association of a water molecule that is required for the hydrolysis. Mutations at G12 or G13 hinder the interaction of the GTPase with the GAP protein and thus prevent the proper orientation of Q61, resulting in the attenuation of GTP hydrolysis (Pylayeva-Gupta et al., 2011).

The three human *RAS* genes (*H*-, *K*- and *NRAS*) share a high degree of sequence identity. Yet, the frequency of monogenic mutation is almost tissue and tumor-dependent (Janssen et al., 2005). The frequency of mutations is not evenly or randomly spread out to the three *RAS* genes. The vast majority of these mutations take place in the *KRAS* genes (Janssen et al., 2005; Pylayeva-Gupta et al., 2011) as shown in Table 1. Mutations in *KRAS* genes are more frequently observed in the cancer of organs forming the digestive system, with the pancreas (~60%) being highly targeted. Approximately five percent of human liver cancers were found with activating mutation of the *KRAS* gene (Table 1).

Table 1: Distribution and frequency of RAS mutations in human cancers

Tissue	*HRAS**	*KRAS**	*NRAS**
Endocrine	3% (535)	0% (670)	5% (570)
Biliary tract	0% (153)	31% (1,679)	1% (287)
Bone	2% (199)	1% (252)	0% (207)
Breast	1% (716)	4% (782)	2% (504)
Central nervous system	0% (964)	1% (1,054)	1% (1,017)
Cervix	9% (264)	7% (637)	2% (132)
Endometrium	1% (291)	14% (2,251)	0% (314)
Eye	0% (33)	4% (90)	1% (106)
Haematopoietic and lymphoid tissue	0% (3,076)	5% (5,978)	10% (8,753)
Kidney	0% (273)	1% (704)	0% (435)
Large intestine	0% (617)	33% (34,013)	2% (1,570)
Liver	0% (270)	5% (461)	3% (310)
Lung	0% (2,091)	17% (16,348)	1% (3,081)
Oesophagus	1% (161)	4% (375)	0% (161)
Ovary	0% (152)	14% (3,181)	5% (191)
Pancreas	0% (278)	57% (5,329)	2% (305)
Pleura	0% (19)	0% (45)	0% (30)
Prostate	6% (558)	8% (1,184)	2% (588)
Salivary gland	15% (161)	3% (170)	0% (45)
Skin	6% (2,100)	3% (1,462)	18% (4,956)
Small intestine	0% (5)	20% (316)	0% (5)
Stomach	4% (384)	6% (2,793)	2% (215)
Testis	4% (130)	4% (432)	3% (283)
Thymus	2% (46)	2% (186)	0% (46)
Thyroid	3% (4,137)	2% (5,166)	8% (4,662)
Upper aerodigestive tract	9% (1,083)	3% (1,582)	3% (836)
Urinary tract	11% (1,765)	5% (1,099)	2% (873)

Adopted and modified from (Pylayeva-Gupta et al., 2011) - Numbers in parentheses indicate total unique samples sequenced. KRAS mutation frequency in liver cancers is highlighted in the red oval. * denotes activating mutation.

1.1.1.3 RAS in cell growth and survival

Sustaining proliferative signaling and resisting cell death are two of the many hallmarks of cancer (Hanahan and Weinberg, 2011), and RAS has been largely implicated in both the promotion of proliferation and the evasion of cell death.

As RAS is the main signal transducers/executors of extracellular mitogenic stimulation, it is not unexpected that oncogenic RAS promotes cell proliferation. After its identification as the first human oncogene, early work demonstrated that the ectopic expression of HRAS could drive the proliferation of quiescent cells (Feramisco et al., 1984; Stacey and Kung, 1984). Moreover, it was later shown that oncogenic RAS-driven proliferation involves complex signaling networks that regulate expression of growth factors, growth factor receptors, cell cycle progression related genes. For instance, the expression of cyclin-D1, a G1 cyclin, was upregulated by oncogenic RAS signaling (Filmus et al., 1994; Liu et al., 1995). In addition, oncogenic RAS signaling also prolonged cyclin-D1 protein stability by preventing its degradation (Diehl et al., 1998). In 1998, Robles and co-workers demonstrated that cyclin-D1 deficient mice had increased resistance to RAS-induced skin cancer (Robles et al., 1998) .

Apoptosis functions as one of the key mechanisms against malignancy, and the mis-regulation of this process is often implicated in many cancers. Apoptosis is a complex process, which is tightly regulated by a balance of pro-death and pro-survival factors. Oncogenic RAS signaling has been well-known for the erosion of pro-apoptotic mechanisms. Activation of RAF and PI3K pathways by RAS can downregulate pro-apoptotic mediators and/or upregulate anti-apoptotic molecules (Pylayeva-Gupta et al., 2011). For instance, RAF can upregulate anti-apoptotic protein BCL-2 (Kinoshita et al.,

1995) and downregulate pro-apoptotic transcriptional repressor PAR-4 (prostate apoptosis response 4) (Ahmed et al., 2008). PI3K and RAF pathways were also shown to mediate phosphorylation of pro-apoptotic BAD (BCL-2 associated agonist of cell death) protein which resulted in its inactivation (Datta et al., 1997; Fang et al., 1999). Thus, oncogenic RAS signaling tipped the balance in favour of cellular survival.

1.1.1.4 RAS in microenvironment remodelling and metastasis

Inducing angiogenesis, activating invasion and metastasis are another three hallmarks of cancer (Hanahan and Weinberg, 2011). It is not too surprising that RAS oncogenic signaling has vital roles to play in these contexts too.

As the tumor grows, its access to oxygen and nutrients become a limiting factor in its quest to develop further. Also, it was well-documented that cancer cells, which are highly proliferative, require more nutrients than normal healthy cells. In order to gain more access to oxygen and nutrients, the tumor will need to induce the formation of new blood vessels. The vascular endothelial growth factor A (VEGFA) is a well-known target of RAS signaling. VEGFA is involved in the regulation of endothelial proliferation and formation of new blood vessels. VEGFA expression is upregulated by RAS/RAF/MEK/ERK signaling through the increased stabilization of the pro-angiogenic transcription factor, HIF1α (hypoxia-inducible factor-1α) (Lee et al., 2002; Richard et al., 1999). VEGFA expression can also be increased via the COX-2 production of prostaglandins, which is caused by RAS signaling (Kranenburg et al., 2004).

Clinically, metastasis of the tumor from its primary site usually represents the last stage of the cancers. This is when the tumor acquires the ability to invade into the surrounding tissues and distant organs. Metastatic cancers usually indicate unfavourable prognosis for the patients. The metastasis process requires the loss of cell-cell contact, loss of adhesion to the matrix and the acquisition of a more motile phenotype, which can be collectively known as epithelial-mesenchymal transition (EMT). This process usually requires the downregulation of E-cadherin, a cell-cell adhesion molecule, which weaken the cell attachment. RAS has been demonstrated to increase the expression of E-cadherin transcriptional repressors such as the SNAIL and SLUG, which reduces the expression of E-cadherin (Horiguchi et al., 2009; Schmidt et al., 2005). Another vital step is for the cell to lose its attachment to the extra-cellular matrix. Activated RAS has also been reported to downregulate the expression of integrin, a cell-matrix adhesion molecule, expression (Schramm et al., 2000). Taken together, activated RAS signaling can induce the "detachment" of the cancer cell from its primary site. Coupled with other signaling pathways, such as the TGFβ signaling, activated RAS can create a more metastatic phenotype (Pylayeva-Gupta et al., 2011).

1.1.1.5 Kras in zebrafish (*Danio rerio*)

My laboratory recently demonstrated that the knockdown of Kras (gene: *kras*; NM_001003744) with morpholinos resulted in specific hematopoietic and angiogenic defects, including impaired expression of erythroid-specific gene *gata1* (GATA binding protein 1) and *hbbe3* (haemoglobin beta embryonic-3), reduced blood circulation and disorganized blood vessels. We have also established that the PI3K/Akt plays a crucial role in mediating Kras signaling during these processes *in vivo* (Liu et al., 2008). Based on current database search and to the best of our knowledge, there is no paralog of *Kras* gene found in the zebrafish genome.

A zebrafish model of embryonic rhabdomyosarcoma (ERMS), a very aggressive childhood cancer, was reported by Langenau and co-workers in 2007. This model was generated by the ectopic expression of human activated KRAS G12D under the *rag2* promoter. Another zebrafish cancer model mediated by KRAS G12D was also reported in 2007 by Le and colleagues. In this study, the expression of KRAS G12D is driven by *β-actin* promoter after the excision of the *loxP*-green fluorescence gene-*loxP* cassette by heat-shock-induced Cre recombinase expression. Four types of malignancy were reported in this study, namely, skeletal muscle tumors, myeloproliferative disorder, intestinal epithelial hyperplasia and malignant peripheral nerve sheath tumors. In another study, Park *et al*. (2008) reported the creation of a zebrafish pancreatic cancer model mediated by pancreas-specific expression of the Kras G12V. Collectively, they illustrated that the zebrafish is a good model for the study of Ras signaling and Ras-driven processes.

1.1.2 Rho GTPases family

RAS homologous (Rho) GTPases belong to a distinct family within the RAS superfamily. They were first discovered in 1985 in the snail *Aplysia* (Madaule and Axel, 1985). Rho GTPases can be characterized by the presence of a Rho-specific insert domain (Valencia et al., 1991), which is absent in other members of the RAS superfamily. To date, there are 20 mammalian members in this family that can be further classified into eight subfamilies (Figure 1.6A) (Vega and Ridley, 2008). Of the 20 members in this family, RhoA, Rac and Cdc42 are the better studied and characterized members. They not only play important roles in regulating cell morphology and actin cytoskeleton but also in many other key aspects of cell biology, including gene expression, cell proliferation, cell survival and even the promotion of tumorigenesis (Sahai and Marshall, 2002). Earlier studies have shown that RhoA activation causes stress fiber formation, Rac1 activation results in lamellipodia formation, and Cdc42 activation causes formation of filopodia (Figure 1.6B) (Jaffe and Hall, 2002).

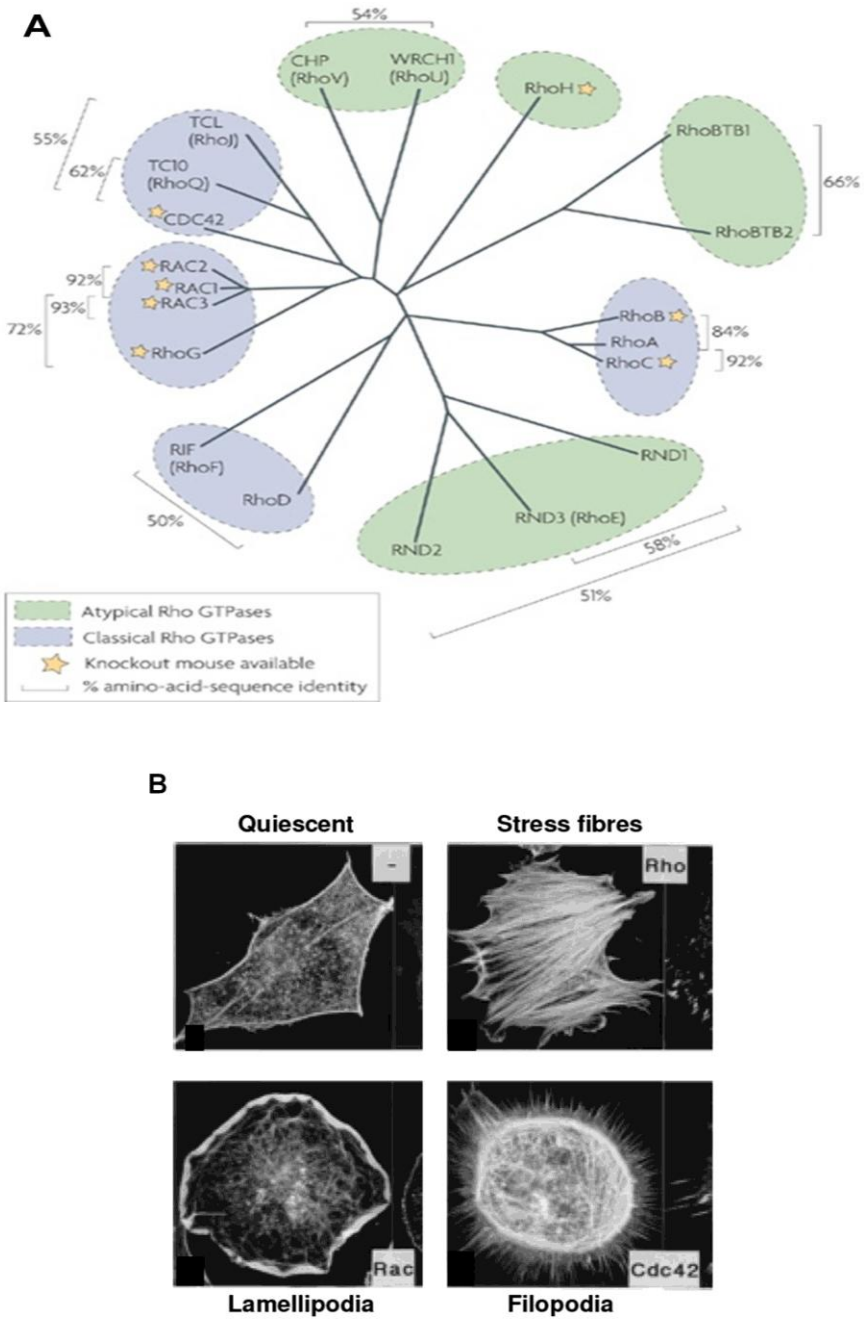

Figure 1.6: Rho family of small GTPases. (A) Dendrogram of the 20 Rho GTPase proteins. The tree demonstrates the relationship between the different family members. Members of the Rho GTPases family can be classified into 8 subfamilies (Heasman and Ridley, 2008). (B) Rho, Rac and Cdc42 control the assembly and organization of the actin cytoskeleton. The effects of Rho, Rac, or Cdc42 activation observed in Swiss 3T3 fibroblasts. Activation of RhoA leads to stress fibers and focal adhesion formation. Activation of Rac induces lamellipodia. While the activation of Cdc42 leads to the formation of filopodia. Cdc42 activates Rac; hence, filopodia are intimately associated with lamellipodia (Jaffe and Hall, 2002).

Like RAS, most Rho GTPases also exist as binary molecular switches. They cycle between active GTP-bound form and inactive GDP-bound form. Rho GTPases are tightly regulated by three groups of proteins namely the GEF, GAP, and GDI (Figure 1.7). To date, there are 82 known GEFs, 67 GAPs and three GDIs (Vega and Ridley, 2008). Atypical Rho GTPases like the RhoH, Wrch-1, Chp and RhoBTB have amino acid substitutions that make them lose their GTPase activity and thus keeping them in the constitutively active state (Aspenstrom et al., 2007). These atypical Rho GTPases might be regulated by expression level, phosphorylation and protein-protein interactions with other molecules. The activity of Rho A had also been shown to be regulated by phosphorylation by PKA by Rolli-Derkinderen and colleagues (2005). RhoA signaling can also be regulated through ubiquitination. Smurf1 ubiquitin ligase had been demonstrated to ubiquitinate RhoA, leading to its degradation (Bryan et al., 2005; Sahai et al., 2007).

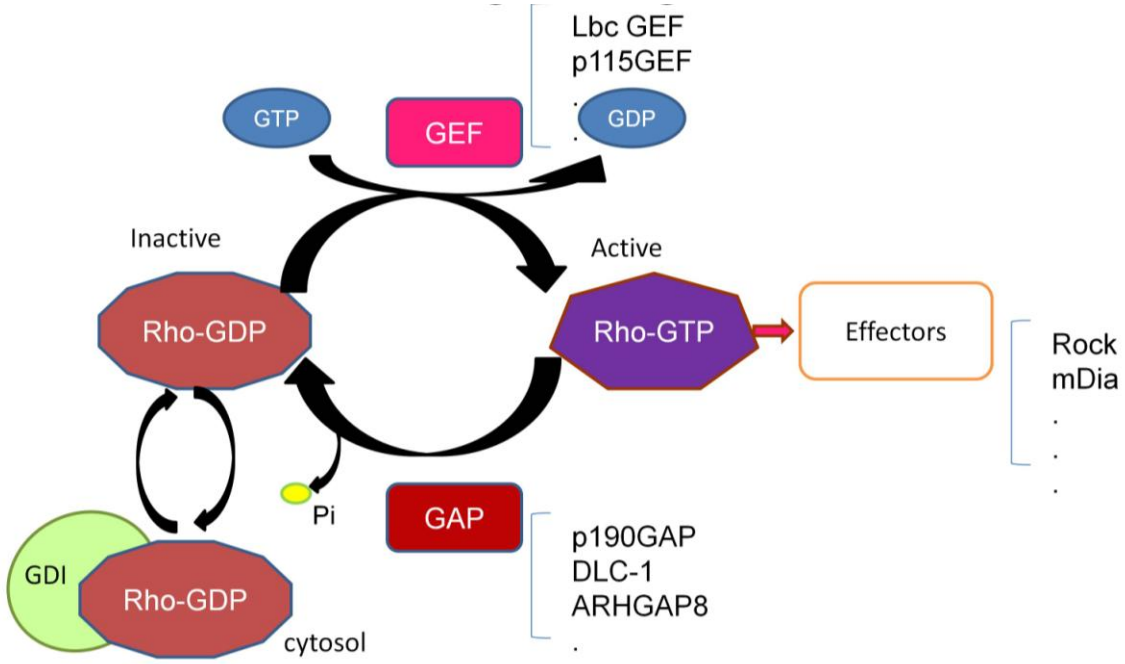

Figure 1.7: Regulation of Rho GTPase signaling networks. Inactive GDP bound GTPases reside mainly in the cytosol, maintained there by GDIs masking the C-terminal tail required for plasma membrane localization. Upon dissociation of the GDI, the Rho GTPases translocate to the plasma membrane, where they can be activated by GEFs (upon external stimuli). GEFs kick out the GDP and aids in the exchange for GTP which activates the Rho GTPase. Upon activation by GEFs, GTP bound Rho GTPases can bind different effector proteins, and induce downstream signaling pathways. GAPs inactivate the Rho GTPases by catalyzing the hydrolysis of the bound GTP, thus switching off the downstream signaling.

1.1.2.1 Effectors of RhoA GTPases

In the last two decades, many RhoA downstream effectors have been identified by means of yeast two hybrid selection, affinity chromatography or specific interactions with active RhoA-GTP (Hall, 1998; Kaibuchi et al., 1999). Interactions between the effectors and the RhoGTPases, like the RhoGEFs and RhoGAP interactions, occur largely through the conserved switch I and II regions. This implies that the three Rho proteins, RhoA,

Rho B and Rho C, might share overlapping effectors (Wheeler and Ridley, 2004). However, there are some differences in the amino acid sequences in the Rho-binding domain of some of the effectors. These differences suggest that the affinity/interaction of effectors with the RhoGTPases can vary (Kaibuchi et al., 1999), where preferential binding can take place. In addition, the sub-cellular location of the Rho proteins could also determine its interaction with a specific group of effectors. For instance, the RhoB proteins are found primarily on the endosomes where it regulates endosomal transport (Fernandez-Borja et al., 2005).

ROCK (Rho-associated coiled-coiled containing protein kinase) is the first kinase effector of RhoA to be identified. It has been identified to be responsible for the majority of RhoA signaling, such as the formation of stress fiber, assembly of focal adhesion and actomyosin contractility (Ishizaki et al., 1996; Leung et al., 1995). There are currently two known ROCK proteins in the human genome, namely ROCK1 and ROCK2. They are multi-domains proteins with a highly conserved kinase domain at the N-terminus, a Rho binding domain at the C-terminus, and a coiled-coil domain sandwiched in between the two domains. ROCKs are serine/threonine kinases that can phosphorylate many different substrates upon activation (Riento and Ridley, 2003). ROCKs are key modulators of actomyosin formation and contractility which are essential for the formation of stress fibers and focal adhesion. They do so by increasing the level of phosphorylated myosin-light chain. ROCKs act through the inhibitory phosphorylation of the myosin binding subunit of the MLC phosphatase, which inactivates it (Kimura et al., 1996). ROCKs can also phosphorylate the myosin-light chain directly (Amano et al.,

1996). Besides the formation of the filamentous actin, ROCKs also stabilize it by the inactivation of cofilin through the LIM-kinase activation (Maekawa et al., 1999).

Other than ROCKs, another key effector of Rho in the regulation of the stress fiber and focal adhesion formation is the mDia (mammalian homologues of *Drosophila Diaphanous*). The combined effect of mDia and ROCK is vital for proper assembly of actomyosin bundles such as the stress fibers. mDia is a formin molecule that catalyse the nucleation and polymerization of actin monomer to form long actin filament (Narumiya et al., 2009). ROCKs phosphorylate the myosin molecules to activate the cross-linking between myosin and actin filaments, resulting in the formation of actomyosin bundles (Narumiya et al., 2009) .

Beside ROCK and mDia, many other Rho effectors were also identified. They include protein kinases (citron kinase, PI4p5K, protein kinase N), scaffolds (Rhotekin, Rhophilin), and lipid kinases (DAG kinase, phospholipase D) (Bishop and Hall, 2000). Some of them have also been demonstrated to be involved in the regulation of actin cytoskeleton reorganization. For instance, citron kinase controls actomyosin contractility during cytokinesis (Madaule et al., 1998). The numerous effectors of Rho indicate the importance of Rho signaling cascades in mediating various biological processes.

1.1.2.2 RhoA in tumorigenesis

Rho GTPases are involved in nearly all stages of cancer progression and were reported to be involved in the acquisition of unlimited proliferative potential, survival and

evasion from apoptosis, tissue invasion and the establishment of metastases (Vega and Ridley, 2008). It is not surprising as the Rho GTPases are vital in controlling many aspects of cell dynamics, and thus they must be tightly regulated spatially and temporally.

The misregulations of Rho GTPases signaling are often implicated in tumor progression. The RhoA expression level and activity were elevated in various types of malignancies, for example in liver tumors (Gomez del Pulgar et al., 2005) (Table 2). Studies demonstrated that over-expression of RhoA in rat hepatoma cells promotes invasiveness both *in vitro* and *in vivo* (Itoh et al., 1999; Yoshioka et al., 1998). RhoA has also been suggested to play a role in governing cell/tumor proliferation, and the promotion of survival and metastasis through many of its effectors. Unlike the RAS proteins, activating mutations of Rho GTPases have never been identified (Narumiya et al., 2009; Vega and Ridley, 2008). These might suggest that the up-regulation of RhoA expression may be enough to promote tumorigenesis (Karlsson et al., 2009). Conversely, these might also suggest that the activating mutant of RhoA does not yield any significant tumorigenic properties (Karlsson et al., 2009). Studies utilizing the overexpression of RhoA or its constitutively active mutants (G14V or Q61L) only exhibited little or weak transforming activities (Narumiya et al., 2009).

The value of RhoA as a prognostic marker for HCC was investigated by many studies (Fukui et al., 2006; Li et al., 2006; Wang et al., 2007). Their results (by qPCR and immunobloting of patients' tumor and peri-tumor specimen) suggested that RhoA is significantly overexpressed in HCC and even more in tissues with high invasive potential. Thus, increased levels of RhoA are associated with poor prognosis. Fukui and co-workers (2006) further demonstrated in their studies that not only did RhoA

expression level increase; the active GTP-bound form was also found to be elevated. A recent study by Gou and colleagues (2011) described significant increase in RhoA (plasma membrane bound) expression in HCC sample compared to normal liver tissue by proteomic analyses. They also reported that a RNAi knockdown of RhoA in HepG2 and HepG3 cells can lead to significant inhibition of growth, induction of apoptosis and decreased migration (Gou et al., 2011).

Table 2: Dysregulation of Rho GTPase in human cancers

	RhoC	RhoA	Rac1	Rac2	Rac3	Cdc42
Breast IBC	(P)(A)	(–)				
non-IBC	(P)	(P)	(P)		(A)	(P)
Melanoma	(R)	(A)	(A)			(A)
SCC	(R)	(P) (A) HNSCC	(P)	(P) HNSCC		(P) HNSCC
Colorectal		(P) (A)	(P) (A)			(P)
Pancreas	(P)	(A)				
Lung	(P) (A) NSCLC	(P) (A) SCLC	(P) NSCLC			
Testicular		(P)	(P)			(P)
Ovarian	(P) (A)	(P) (A)				
Gastric	(P)	(P) (A)	(P) (A)			
Liver		(P) (A)				
Pelvic ureteric		(R)				
Prostate		(A)				
Renal			(A)			
Neuroblastoma		(A)				
Bladder	(P)	(P) (A)				
Leukemias AML		(A)				
Sarcoma		(A)				
Lymphomas	(R) Hodgkin's					

Footnote: (A) represents high signaling activity, (P) represents high protein levels, whereas (R) represents high mRNA levels. Boxes containing (P) (A) represent high expression and high signaling activity. Abbreviations used are SSC (squamous cell carcinoma), HNSCC (head and neck squamous cell carcinoma), SCLC (small cell lung cancer), NSCLC (nonsmall cell lung cancer), AML (acute myeloid leukemia). (Gomez del Pulgar et al., 2005)

Compelling evidence that Rho signaling might play a significant role in tumor progression of HCC could come from studies on the Deleted-in-liver cancer-1 (DLC-1) gene. DLC-1 is a Rho-specific GAP and it has been reported by many studies to be down-regulated in many types of human cancers, especially in cancers of the liver. One study reported that cells with reduced DLC-1 expression contain elevated GTP-bound RhoA levels, and enforced expression of a constitutively activated RhoA mimics DLC-1 loss in promoting hepatocellular carcinogenesis in a background of null p53 and overexpressed Myc (Xue et al., 2008). Another study demonstrated that the DLC-1 protein can negatively regulate the RhoA/Rho-associated coiled coil-forming kinase (ROCK)/myosin-light-chain (MLC) pathway, thus suggesting that the RhoA might play a significant role in shaping the tumorigenesis process in the absence of DLC-1 regulation (Wong et al., 2008). All the above findings suggest strong association of RhoA with liver tumorigenesis.

On the other hand, the role of RhoA could also be inhibitory to tumorigenesis. One interesting study conducted by the Cantrell laboratory on mice suggested opposing roles for RhoA in tumorigenesis (Cleverley et al., 2000). They expressed the C3 transferase, a bacterial toxin derived from *Clostidium botulinum*, in the thymus of mice. C3 transferase inhibits Rho signaling by ribosylating the Rho effector domain thereby abolishing its activation of downstream signaling cascades. It was reported that the C3 transferase-expressing mice developed aggressive thymic lymphoma with early onset at an age of 4 to 8 months. Knockout of RhoB, a closely related member of the Rho GTPase family, also demonstrated increased susceptibility to transformation (Liu et al., 2001).

Knockout of Cdc42, a Rho related GTPase, in the liver of the mouse led to the development of hepatocellular carcinomas (van Hengel et al., 2008). ROCK, a key effector of RhoA, has been reported to negatively regulate epidermal growth factor receptors (EGFR) in colon and pancreatic cancer cells. Inhibition of ROCK by Y27632, a potent pharmacological inhibitor of ROCK, has been reported to enhance the activation of EGFR in both cell types thus resulting in increased proliferation (Nakashima et al., 2011; Nakashima et al., 2010). Constitutively active RhoA has also been shown to inhibit proliferation by delaying G1 to S phase cell cycle progression and impairing cytokinesis (Morin et al., 2009).

1.1.2.3 RhoA in zebrafish

Currently, there are five RhoA gene paralogs identified. They are *rhoaa*, *rhoab*, *rhoac*, *rhoad* and *rhoae*. We have demonstrated that the knockdown of zebrafish RhoA (*rhoab*, Accession number: NP_997914.2) leads to extensive apoptosis during embryogenesis, resulting in overall reduction of body size and length. These defects are associated with reduced activation of Erk and reduced expression of anti-apoptotic bcl-2 protein (Zhu et al., 2008). Earlier through the use RhoA morpholinos and convergence and extension (CE) morphants defective in Wnt signaling, we demonstrated the involvement of RhoA downstream of non-canonical Wnt5 and Wnt11 signaling to regulate CE movements through Rho Kinase and Diaphanous (Zhu et al., 2006). This

study further validated the use of zebrafish as an *in vivo* model for study of GTPase signaling.

1.1.3 Interplay of RAS and RhoA signaling in tumorigenesis

RAS and Rho small GTPases are key molecular switches that control cell dynamics, cell growth and tissue development via their distinct signaling pathways. Much has been learnt about their individual functions through cell and animal models but the physiological/pathophysiological consequences of their signaling crosstalk in multi-cellular context *in vivo* remains largely unknown, especially in liver tumorigenesis. Furthermore, the roles of RhoA in RAS-mediated transformation and their crosstalk *in vitro* remain highly controversial. To date, the molecular mechanism of crosstalk between RhoA and RAS is still not well-defined. It appears to be cell type-specific, varies with the RAS subtype, and depends on the kinetics and duration of RAS activation (Chen et al., 2003). Reported studies on this crosstalk are summarized in Table 3.

Table 3: Crosstalk of RAS and RhoA in transformation

Crosstalk promotes /favors transformation	Ras isoform	Remarks (key findings)	References
Yes	HRAS	RAS increased RhoA activity, through the RAF/MAPK pathway, by downregulating p190GAP. Active RhoA reduces p21 Cip expression.	(Chen et al., 2003)
Yes	Unspecified	Sustained RAS signaling downregulated Rac activity which in turn increased RhoA activity, leading to EMT	(Zondag et al., 2000)
Yes	HRAS	RhoA activities were required for the downregulation of p21 Cip1, which enable HRAS transformation.	(Olson et al., 1998)
Yes	HRAS	Activated RhoA cooperated with activated RAF to induce transformation. Dominant-negative mutant RhoA 19N can reverse HRAS transformation. (Interestingly, the coexpression of RhoA 19N with HRAS V12 can restore stress fiber formation in transformed cells; RhoA19N is known to cause stress fiber disruption).	(Qiu et al., 1995)
Yes	HRAS	Active RhoA-GTP was selected for by sustained RAF/MAPK signaling, which was required for proliferation of RAS transformed cells. RAS transformation caused RhoA to be uncoupled from stress fiber regulation.	(Sahai et al., 2001)
Yes	HRAS	Constitutively activated RhoA and HRAS synergistically induced transformation. Dominant negative RhoA T19N expression reduced RAS transformation.	(Khosravi-Far et al., 1995)
Yes	HRAS	Oncogenic HRAS signaling in cell deprived of p53 synergistically enhanced RhoA activity, through the p190GAP inactivation.	(Xia and Land, 2007)

Continued

Crosstalk promotes /favors transformation	Ras isoform	Remarks (key findings)	References
Yes	HRAS	Oncogenic HRAS transformation via a RAF independent pathway phenocopy RhoA 63L transformed NIH3T3. This transformation by the oncogenic RAS can be inhibited by dominant negative RhoA T19N mutant.	(Khosravi-Far et al., 1996)
Yes	HRAS	TGF-β-ALK5 activation of RhoA was essential for the HRAS mediated transformation.	(Fleming et al., 2009)
Yes	HRAS	RhoA signaling was required to downregulate p27 which facilitated RAS transformation.	(Vidal et al., 2002)
Yes	Unspecified	Co-expression of activated Rho1 (RhoA) enhances activated RAS mediated eye growth (*in vivo* drosophila eye model).	(Brumby et al., 2011)
No	HRAS	HRAS transformed fibroblast lack stress fiber and cell adhesion. Inactivation of the RhoA-Rock pathway may contribute to RAS transformation.	(Izawa et al., 1998)
No	KRAS	Oncogenic KRAS downregulated RhoA activity, resulting in reduced actin filament and stress fiber.	(Dreissigacker et al., 2006)
No	KRAS	RhoA expression was downregulated in ki-ras transformed NIH3T3; Transformed NIH3T3 displayed loss of stress fibers; Enforced Tropomysoin expression reverted transformed phenotype through Rho upregulation.	(Shah et al., 2001)
No	HRAS	RAS transformation downregulated Rho activities through Gankyrin. Increased Gankyrin in RAS transformed cells increases RhoA and RhoGDI interaction, leading to inactivation of RhoA.	(Man et al., 2010)

None of these studies was able to establish either the direct association or the functional influences of the crosstalk between RAS and RhoA. Furthermore, most of these studies, except for the study by Brumby and co-workers in 2011, were performed in cell culture *in vitro* system. Most of these earlier studies were performed in fibroblastic cell type and most of them utilized the HRAS isoform in their works. Nevertheless, these studies might still contribute to the eventual understanding of this crosstalk.

Recently, our laboratory has demonstrated that RhoA activates MEK/Erk pathway during zebrafish embryogenesis although the nature of interaction (direct or indirect) remains to be elucidated (Zhu et al., 2008). MEK/ERK signaling, one of the key downstream pathways of RAS could provide links between the interplay of RAS and RhoA.

There were two interesting studies that might provide another indirect link between the RAS and Rho crosstalk. The first study (Motti et al., 2007) showed that p27 expression level was reduced significantly in the presence of HRAS G12V. Study two (Besson et al., 2004) demonstrated that p27 can act as a negative inhibitor of the RhoA activation. It does so by binding to RhoA and thereby preventing its interaction with its GEF protein. Bringing together the two studies, it could imply that RAS down-regulates p27 expression, which in turn could not prevent RhoA activation. Consequently, it could result in an increased activation of RhoA.

1.2 Liver cancer

The liver is the largest interior organ of the human body. It performs many vital functions essential for life such as nutrients storage, metabolism, digestion, detoxification and etc. Liver cancer is one of the most common and deadliest cancers worldwide. Primary forms of liver cancers include mainly hepatocellular carcinoma (HCC) and cholangiocarcinoma, which develop from the hepatocytes and the bile duct cells, respectively.

1.2.1 Hepatocellular carcinomas

HCC is the predominant form of primary liver cancer. It is one of the most common solid tumors worldwide. It is the third-leading cause of death due to cancer worldwide with high incidences in Asia and Africa (Parkin et al., 2005). Its incidence rate in the West is also on the rise possibly due to the increase in hepatitis C virus infections (Gomaa et al., 2008). The major risk factor for developing HCC is the cirrhosis of the liver. Other major risk factors, many of which may be factors promoting cirrhosis are (1) chronic Hepatitis B and Hepatitis C viral infection, (2) alcoholism, (3) diabetes, (4) non-alcoholic fatty liver disease and (5) exposure to aflatoxins (Gomaa et al., 2008). Curative therapies are limited to only one-third of the diagnosed HCC patients (Llovet et al., 2003) as many patients were diagnosed in the later stages of the disease.

Sorafenib, an oral multi-kinase inhibitor that targets RAF/MEK/ERK and VGEF pathways, is the only molecular target therapy approved for use in advance HCC patients.

Sorafenib has been shown to increase overall survival significantly compared to placebo control in phase III clinical trial (Llovet et al., 2008). The usefulness and application of Sorafenib, a RAF/MAPK inhibitor, in HCC patients suggested the important role of RAS/RAF/MAPK signaling in mediating liver tumor progression.

Molecular analysis reported genetic and epigenetic alterations in HCC to involve the dysregulation of many oncogene or tumor suppressor genes, including p53, β-catenin, MET, hepatocyte growth factor, E-cadherin, Cox2, MYC, and DLC-1 (Farazi and DePinho, 2006; Hoshida et al., 2010). Studies reporting the presence of activating mutations of the *RAS* gene in human HCC are uncommon (Wong and Ng, 2008). Nevertheless, overexpression of the *RAS* gene have been reported in human HCC (Nonomura et al., 1987). The significance of the *RAS* genes in HCC can be inferred by the fact that physiological inhibitors of the RAS/RAF/MEK/Erk pathway, such as the RAF-1 kinase inhibitory protein (RKIP) and Spred-1, have been frequently down-regulated in human HCC (Wong and Ng, 2008). Another piece of evidence might come from the observation that the RAS-associated domain family (RASSF1) was frequently epigenetically silenced in HCC (Schagdarsurengin et al., 2003). RASSF1 is a downstream effector of the active RAS, which is responsible for the pro-apoptotic effect of the RAS signaling.

1.3 Zebrafish as a model in cancer biology

1.3.1 Zebrafish as an experimental biological model

The zebrafish, a tiny freshwater teleost, has become widely popular as a powerful tool for dissecting gene function during vertebrate embryogenesis in the recent few decades (Deiters and Yoder, 2006). Its popularity can be attributed to its small size (three to four centimeters), high fecundity, rapid external development and optical clarity during development. Its small size greatly reduces the cost of setting up and maintaining a zebrafish husbandry as compared to the other well-established vertebrate model such as the mouse model. Under optimal conditions, a breeding pair can produce up to 200 embryos per week. A large number of embryos can be collected which makes it suitable for large scale genetic analyses. The embryos developed at a rapid pace and much faster than the other related fish model, medaka (Lawson and Wolfe, 2011). Gastrulation is completed within ten hours post-fertilization (hpf). The developing embryos are optically clear and can be monitored real-time by use of a simple light microscope (Beis and Stainier, 2006; Westerfield, 2000).

The zebrafish is also amenable to both forward and reverse genetics (Beis and Stainier, 2006). Potential forward genetics amenability was the initial catalyst for researchers to adopt the zebrafish as a vertebrate model (Lawson and Wolfe, 2011). This approach utilized mutagens to generate random mutations and subsequent identification of the gene(s) responsible for an observable biological phenotype. Currently, N-ethyl-N-nitrosourea (ENU) is the standard choice of most researchers because of its high mutagenic loads in premeiotic germ cells and ease of application. But the chemical mutagen method suffers from the difficulty in identifying the mutated gene involved in

eliciting the phenotype (Lawson and Wolfe, 2011). Retroviruses and transposon vectors were reported as alternatives to chemical mutagens because of their ease of identifying the targeted locus (Nagayoshi et al., 2008; Sivasubbu et al., 2006). They are not well adopted yet because of their low mutagenic rate, thus the need to generate a larger library of zebrafish for effective screening/analyses (Lawson and Wolfe, 2011). The forward genetics can also be used to screen for cancer-susceptibility genes during early development as many cellular processes affected in cancer are also active during development (Liu and Leach, 2011).

Reverse genetics investigates the phenotypic/morphological changes of a gene of interest through the use of knock-out, knock-down or knock-in methods in the zebrafish embryo. Currently, morpholino antisense oligos (nucleic acid analogs) is the method of choice for most zebrafish researchers to study the gene function during embryogenesis through a knock-down of the gene of interest. Reduced gene expression was achieved through the steric hindrance blocking of the mRNA which resulted in translation blocking or modified pre-mRNA splicing. It was first demonstrated to work in the zebrafish in 2000 (Nasevicius and Ekker, 2000). Targeting induced local lesions in genomes (TILLING) can be used to generate germline mutations in a targeted gene (Wienholds et al., 2002; Wienholds et al., 2003). Targeted gene inactivation by zinc finger nucleases was demonstrated in zebrafish, recently (Doyon et al., 2008; Meng et al., 2008). It works by the binding of a pair of zinc-finger nucleases to the targeted region and the subsequent introduction of a double strand break. Repair of the double strand break by non-homologous end joining is occasionally imperfect, thus the introduction of insertion or deletions in the targeted gene (Lawson and Wolfe, 2011). Recent advancement in genome

modification has witnessed the introduction of the transcription activator–like effector (TALE) nuclease (TALENs) as a tool to create targeted mutations in the human genome (Miller et al., 2011). The TALENS function in a similar manner compared to the ZFN but have the advantage of being more predictable and specific in binding to targeted DNA (Boch and Bonas, 2010; Huang et al., 2011). In 2011, two studies demonstrated the usefulness of engineered TALENs in modification of targeted genes in the zebrafish genome (Huang et al., 2011; Sander et al., 2011).

1.3.2 Transgenesis in zebrafish

Transgenesis is an important tool for assessing gene functions in various biological processes (Kwan et al., 2007). Transgenic animals are created through the introduction of a foreign DNA into the organism. The function and regulation of the introduced gene can later be studied in these animals. Transgenesis in zebrafish can be broadly classified into transient or stable transgenic approaches (Kikuta and Kawakami, 2009).

In the transient approach, gene function and regulation of the transgene is studied immediately after its introduction. This approach is rapid and convenient but it suffers from differential and mosaic expression due to the mosaic segregation of the injected DNA during the cleavage stage (Westerfield et al., 1992).

Stable transgenesis refers to the germline transmission of the exogenously introduced transgene in the organism. Offsprings from the transgenic animal usually

follow an identical pattern of expression. It is because of the stable integration of the transgene into the genome. Stable transgenic zebrafish are more laborious to generate because of infrequent germline incorporation. Therefore, a large number of embryos need to be injected before a stable transgenic line can be obtained. The rate of germline transmission in zebrafish can be greatly enhanced through the use of transposase-based or enzyme-mediated approach such as the Tol2Kit (Kwan et al., 2007), Sce-I mediated transgenesis (Rembold et al., 2006) and the Tc1/mariner family transposable element Sleeping beauty (Davidson et al., 2003). Recently, Emelyanov and co-workers in 2006 demonstrated that the maize Activator (Ac) / Dissociation (Ds) system is capable of mediating the transposase-mediated transposition of exogenous DNA into the zebrafish genome (Emelyanov et al., 2006). Briefly, they cloned EGFP gene under the control of *keratin 8* promoter in between the 5' and 3' Ds-cis sequence. The plasmid was co-injected together with the truncated Ac transposase mRNA. The translated Ac transposase mediated the transposition of the EGFP into the zebrafish genome. It was also shown to yield remarkable germline transmission rates in their study. Thus, the Ac/Ds transposase system can be used as an invaluable tool for the generation of transgenic zebrafish. To date, the majority of findings on tumorigenesis using zebrafish came from transgenic zebrafish expressing mammalian/zebrafish oncogene (Feitsma and Cuppen, 2008). A summary of use of the transgenic zebrafish in tumor studies is presented in Table 4.

Table 4: Tumorigenesis in transgenic zebrafish

Gene of interest	Strategy/Target organ	Phenotype	Source
Xmrk	Tet-on inducible/Liver	HCC	(Li et al., 2011)
HrasV12	Transgenic/ Melanocytes	Melanomas	(Santoriello et al., 2010)
NRAS Q61K /p53-/-	Transgenic/ Melanocytes	Melanomas	(Dovey et al., 2009)
Constitutively active AKT2 / p53-/-	Transient expression/ Mesenchymal progenitors	Liposarcomas	(Gutierrez et al., 2011)
Brca2 Q658X/ p53-/-	ENU mutagenesis/ Global expression	Various tumors	(Shive et al., 2010)
TEL-JAK2	Transient expression/ Myeloid precursors	Acute myeloid leukemia	(Onnebo et al., 2005)
TEL-AML1	Constitutively expressed / Global expression	B-cell acute lymphoblastic leukemia	(Sabaawy et al., 2006)
c-Myc	Constitutively expressed/ Rag2 promoter	T-cell acute lymphoblastic leukemia	(Langenau et al., 2003)
c-Myc	Inducible/ Rag 2 promoter	T-cell acute lymphoblastic leukemia	(Feng et al., 2007)
Myst3/NCOA2	Transgenic/ Spi promoter	Acute myeloid leukemia	(Zhuravleva et al., 2008)
Kras G12V	Transgenic/ Global expression	Embryonal rhabdomyosarcoma	(Langenau et al., 2007)
Kras G12D	Inducible / Global expression	Rhabdomyosarcoma and various cancer	(Le et al., 2007)
BRAF V600E / p53-/-	Transgenic/ Melanocyte	melanomas	(Patton et al., 2005)
Hras G12V	Transgenic/ Melanocyte	Melanomas	(Michailidou et al., 2009)
Kras G12V	Transgenic/ Pancreas	Pancreatic cancer	(Park et al., 2008)
MYCN	Transgenic/ Pancreas	Neuroendocrine carcinoma.	(Yang et al., 2004)

1.3.2.1 Conditional transgenic system

Constitutively overexpressed gene products can be detrimental to the fitness of the transgenic animal when its expression can cause infertility or premature lethality. Thus, it can hinder the generation and maintenance of the animal. Conditional expression of the transgene allows the animals to develop healthily and only express the transgene when required. The different conditional systems employed in the zebrafish can be simply classified into two main categories, the binary system and the inducible system.

Binary systems such as the Cre-loxP and GAL4-UAS systems are alternative conditional expression systems to the inducible systems described below. The transgene in the transgenic animals (effector line) remains silent until it is crossed with another transgenic animal (activator line) carrying an activator gene. Only double transgenic animals will express the transgene of interest. The Cre-*loxP* system relies on the Cre-recombinase to excise the sequences (reporter-stop codon cassette) flanked by the two *loxP* site (same orientation), resulting in a single *loxP* site. This allows the sequence downstream of the *loxP* site to be transcribed and expressed. Two studies in 2007 reported the use of Cre-*loxP* system combined with the heat-shock inducible system to generate transgenic zebrafish (Feng et al., 2007; Le et al., 2007). The Cre-recombinase can also be introduced through the microinjection of Cre-mRNA into one-cell embryos, thus eliminating the need of crossing and maintaining of both activator and effector lines. Pioneering works by Scheer and Campos-Ortega successfully utilized the GAL4-UAS system for transgenesis in zebrafish by demonstrating the GAL4-dependent transactivation of the transgene under the UAS promoter. (Scheer and Campos-Ortega, 1999). The disadvantage of most binary systems is the maintenance of at least two lines,

the effector and the activator lines. On the other hand, the binary system allows the creation of one effector line which can be crossed to several existing tissue-specific activator lines to achieve many double transgenic fish with different tissue-specific distribution of the transgene.

An inducible system can be achieved through the use of an inducible promoter. The inducer can be either in the form of heat treatment or chemical treatment, thus achieving temporal control of expression of transgenes. The inducible system also allows the control of spatiotemporal expression when combined with the use of tissue specific promoters.

The heat-shock promoter is frequently used as temporal control of transgene expression in transgenic zebrafish. On top of offering temporal control on the expression, it can also control the expression level and period by varying the temperature and length of heat treatment (Murtha and Keller, 2003). The main drawbacks of this approach are the low leaky expression of the heat-shock promoter and the global expression of the transgene without any spatial regulation (Blechinger et al., 2002; Halloran et al., 2000). Heat-shock inducible Cre-Lox-mediated transgenic zebrafish lines conditionally expressing human KRAS G12D were generated by Le and co-workers (Le et al., 2007). In this study, the heat-shock protein 70 (hsp70) promoter was used to drive the expression of the Cre-recombinase in double transgenic fish. Transactivation of the Cre gene was achieved after the application of heat treatment. The Cre-recombinase then mediated the excision of the reporter gene cassette, which resulted in the expression of human KRAS G12D. Heat-treated zebrafish embryos developed rhabdomyosarcoma, myeloproliferative disorder, intestinal hyperplasia, and malignant peripheral nerve sheath

tumor. A similar strategy was also employed by Feng and colleagues in 2007 to induce expression of mouse c-myc oncogene in the zebrafish (Feng et al., 2007). It was also reported that the transgenic fish developed T-cell acute lymphoblastic leukemia (T-ALL). All reported tumors in these two studies recapitulated the human disease both molecularly and pathologically.

Another commonly used inducible system is the Tet-system. It can be divided into two types, the Tet-off and Tet-on system. The Tet-system is built on the negative regulator, Tetracycline repressor (*tet*R), of the tetracycline-resistance operon of the *E.coli* (Gossen and Bujard, 1992). In the presence of tetracycline, the *tet*R does not bind its operator thus allowing the transcription of tetracycline resistance genes.

The Tet-off system was generated by fusing the *tet*R with the VP16 of HSV to form the Tet-controlled transcriptional activator (tTA). In the absence of tetracycline, tTA binds to the tetracycline operator-minimal promoter to stimulate transcriptional activity. In the presence of tetracycline, the tTA does not bind the tetracycline-operator and the transcription activity of downstream gene is halted (Gossen and Bujard, 1992).

The Tet-on system was created by mutagenesis of the tTA to yield the reverse Tet-controlled transcriptional activator (rtTA). rtTA only binds the tetracycline operators in the presence of tetracycline, and drives the transcription of downstream genes (Gossen et al., 1995). The rtTA2s-M2, an improved version of the rtTA, is more sensitive to doxycycline induction and thus requires lesser amount of the inducer to achieve similar induction. Tissue-specific promoters are often used to drive the expression of the rtTA, thus allowing spatial control of expression. In the presence of tetracycline, rtTA can bind

to Tetracycline response element (TRE) (TRE is makes up several tetracycline operators) and transactivating the expression of the downstream transgene. The investigator can effectively control the presence or absence of the inducer. The Tet-on system has been reported in many organisms such as fungi (Meyer et al., 2011), mouse (Vitale-Cross et al., 2004), and etc. The first Tet-on system in the zebrafish was employed by Huang and colleagues. They demonstrated a specific strong expression of green fluorescence protein (GFP) in the heart, in the presence of doxycycline, under the control of the Tet-on system (Huang et al., 2005). Doxcycline is a more stable derivative of tetracycline. This system was chosen for my study because the expression and induction is strong, specific and reversible. Also, it can be quantitatively controlled by regulating the dosage of inducer used. The reversibility of this system could allow us to study regression of the tumors upon withdrawal of the inducer.

The mifepristone-inducible LexPR system is a relatively new system employed and reported by Emelyanov and Parinov (2008) for zebrafish transgenesis. It works in a way similar to Tet-on. In short, tissue-specific promoters will drive the expression of the LexPR transactivator. In the presence of mifepristone, the LexPR transactivator will bind to the LexA operator and drive the expression of the downstream gene by the minimal 35S promoter fused to it.

1.3.3 Tumorigenesis in zebrafish

1.3.3.1 Chemical carcinogenesis in zebrafish

Zebrafish is emerging as one of the many promising animal models that are used as tools to study human diseases, particularly in cancer. These studies can be generally classified into four main types, namely chemical carcinogenesis, mutant lines, transgenic lines and xenotransplants (Stoletov and Klemke, 2008).

It has been known for more than a century that teleost fish can develop tumors spontaneously or in response to various chemical carcinogens. Chemical carcinogenesis was the first approach used to induce tumorigenesis in zebrafish in 1965 by Mearle Stanton (Beckwith et al., 2000; Stanton, 1965). Subsequently, many other chemical carcinogenesis studies were carried out and many of these tumors were reported to resemble various types of human tumors at the histological level (Amatruda et al., 2002; Feitsma and Cuppen, 2008; Stoletov and Klemke, 2008). It was also noted that zebrafish have a very low incidence of spontaneous cancers and high tumorigenic response after chemical insults. This makes them an ideal model for chemical carcinogenesis (Stern and Zon, 2003). The small size of the fish also enables all major organs to be examined with relatively few histology sections placed on a small number of slides, thus reducing the histology costs involved (Spitsbergen et al., 2000a; Spitsbergen et al., 2000b). Its small size facilitated the housing of a large number of fish during a study, which further contributed to its greater statistical power over other mammalian carcinogenesis studies (Stern and Zon, 2003).

Chemically-induced tumors also resemble human tumors molecularly. Studies by Lam and colleagues demonstrated that the gene signatures of chemical carcinogens-induced zebrafish liver tumors shared high degree of similarities at the molecular level (cell cycle, apoptosis and DNA repair genes) with human liver cancers (Lam and Gong, 2006; Lam et al., 2006). Another comparative transcriptome study by the Zon laboratory also identified two conserved gene signatures found in both zebrafish and human embryonal rhabdomyosarcoma (ERMS). One was associated with tumor-specific and tissue-restricted gene expression in rhabdomyosarcoma and a second comprised a novel RAS-induced gene signature (Langenau et al., 2007).

Taken together, zebrafish tumors share remarkable histological and molecular similarities with human tumors. Thus, these findings further validated the use of zebrafish as a model for the study of tumorigenesis and tumor progression.

1.3.3.2 Zebrafish liver cancer model

Zebrafish have a very low spontaneous cancer incidence rate in the wild. On the other hand, zebrafish develop various malignancies, in particular, cancers of the liver, when treated with different chemical carcinogens such as Nitroso-compounds, 7-12-dimethyl benzanthracene, N-Nitrosodimethylamine and N-methyl-N-nitro-N-nitrosoguanidine (Goessling et al., 2007; Mizgireuv et al., 2004; Spitsbergen et al., 2000a; Spitsbergen et al., 2000b). Chemically induced liver cancers in the zebrafish

resemble human liver cancer histologically, for example, the increase in cell proliferation, low degree of differentiation and atypical nuclear morphology (Spitsbergen et al., 2000a; Spitsbergen et al., 2000b).

The first study on liver cancer in transgenic zebrafish was reported by Rekha and co-workers (2008). It was demonstrated that ectopic expression of the hepatitis C virus core protein in the liver increased HCC progression by two-fold as compared to the control when exposed to thioacetamide, a hepatotoxin (Rekha et al., 2008). It should be noted that it was not mentioned whether the transgenic fish in this study developed HCC in the absence of the hepatotoxin, thioacetamide. Our collaborators have recently established a zebrafish HCC model driven by ectopic expression of Xmrk oncogene under the control of the Tet-on system (Li et al., 2011). This demonstrated that transgenic zebrafish is a good model for studying liver cancers.

1.3.3.3 Histological classification of liver lesions (tumors) in zebrafish

Hepatocellular lesions of zebrafish during tumorigenesis can be classified into different categories. In order of increasing severity, they are cellular alterations, hyperplasia, hepatocellular adenoma and hepatocellular carcinomas (from less to more serious order). It is primarily determined by gross observation and histological diagnosis of the diseased fish. The primary criteria for the diagnosis are summarized in the Table 5. Figure 1.8 further illustrates the differences between HCC and HCA, visually.

Table 5: Classification of features of liver lesion in zebrafish liver cancer studies

Lesion / Observation	Gross observation	Histological observations
Cellular alteration	No significant differences.	Cell larger than normal.
Hyperplasia	Enlarged liver.	Retained two-cell plate arrangement. Enlarged hepatocytes with slight compression on neighboring tissue can be observed.
Hepatocellular adenoma	Enlarged liver, varies in color from normal liver.	Hepatic plates are more than two-cell thick with loss of structure. Hepatocytes are of various sizes and can be seen compressing on neighboring tissue, retain sharp boundary. Increased mitosis can be observed.
Hepatocellular carcinoma	Enlarged liver.	Hepatic plate arrangement are lost and replaced with multiple irregular and thick cell plates. Hepatocytes may resemble normal cell with various nucleus size, absence of sharp boundary (Figure 1.8). Mitosis and invasion may be present.

(Source: Dr Jan Spitsbergen, Oregon State University)

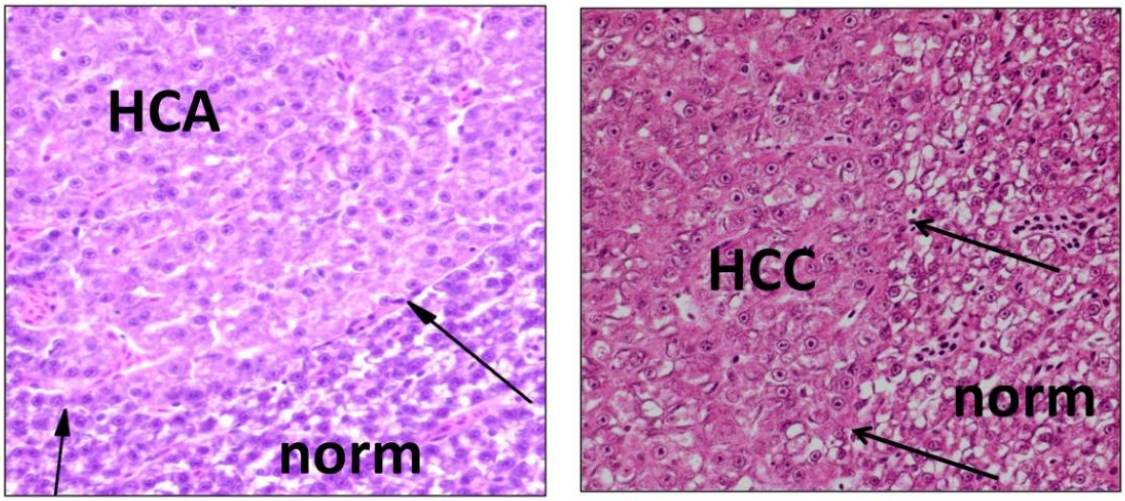

Figure 1.8: Differences between HCA and HCC. Arrows highlight the boundaries of the lesions. The boundary is lost in the HCC (left) as compared to the sharp boundary observed in the HCA sample (right). (Modified from sources: Dr Jan Spitsbergen, Oregon State University, USA)

1.4 Objectives

RAS is a master regulator of many cellular processes. It acts primarily as a signal transducer that links cell surface receptors to intracellular pathways (Pylayeva-Gupta et al., 2011). Aberrant RAS signaling, through the acquisition of activating mutations, are well known for its ability to promote tumorigenesis and is found in up to 30% of all human cancers. Activating mutations are frequently found on the codon 12, 13 and 61 of the RAS protein, with codon 12 making up the majority in HRAS (55%) and KRAS (85%) (Pylayeva-Gupta et al., 2011). Activating mutation diminished the ability of the RAS GTPase to hydrolyse the bound GTP to GDP, thus rendering it constitutively active. While there are three RAS isoforms, KRAS is found to be the most frequently mutated isoform in the human cancers with up to 85% of the cancers found with KRAS mutations (Karreth and Tuveson, 2009). It was suggested that the substitution of glycine 12 with valine in the KRAS was more potent than the substitution with glutamic acid (Pylayeva-Gupta et al., 2011). Mutations in KRAS genes are more frequently observed in the cancer of the organs forming the digestive system, with the pancreas (~60%) highly targeted. Approximately five percent of human liver cancers were found with activating mutation of the KRAS gene.

HCC is one of the most deadly primary liver cancers. It is always associated with poor prognosis and poor survival as most HCC were diagnosed in the later stage of the disease. It is ranked third in the number of deaths due to cancer, with incidence rates rising both in the East and the West. The progression and development of HCC is a complex process, which usually involves repeated cycle of necrosis-liver regeneration (hepatocyte proliferation) ultimately resulting in cirrhosis (Frau et al., 2010).

Molecularly, several altered/aberrant signaling pathways were identified and implicated in the development and progression of HCC. These pathways include receptor tyrosine kinases signaling, VEGF mediated angiogenic signaling, hepatocyte growth factor/c-MET signaling, mitogen activated protein kinase (MAPK) signaling, PI3K/AKT/mTOR signaling, WNT/β-catenin pathway, c-myc amplification, iNOS/IKK/NF-kB signaling (Frau et al., 2010; Whittaker et al., 2010). Many of these signaling pathways either utilize RAS as the signal transducer (receptor tyrosine kinase: EGFR or IGFR) or the effectors of active RAS signaling such as the RAF/MAPK and the PI3K/AKT pathways. This suggests the importance of RAS signaling in mediating liver transformation. Currently, only one animal model of RAS-driven HCC exists, where transgenic mice expressing HRAS G12V together with the loss of β-catenin signaling in the liver developed HCC (Harada et al., 2004). Therefore, this shows that there is a lack of animal models for RAS driven HCC.

The zebrafish is quickly growing in popularity as an alternative animal model for the study of human cancers in recent years (Amatruda et al., 2002; Beis and Stainier, 2006; Feitsma and Cuppen, 2008; Lam and Gong, 2006). Its popularity can be attributed to its low cost of setting and maintenance of the zebrafish husbandry, rapid development, high fecundity, amenability to reverse and forward genetics, low incidence of spontaneous tumor, ease of application of small chemical molecule and its small size. Most importantly, carcinogen-treated zebrafish developed liver tumor that resembled human liver cancers both molecularly and histologically (Lam and Gong, 2006; Lam et al., 2006; Spitsbergen et al., 2000a; Spitsbergen et al., 2000b). Thus, these make zebrafish a good model for the study of Kras-driven HCC.

RhoA, a member of the RAS superfamily, has been implicated in many human cancers. The expression levels and activities of RhoA were found to be elevated in many human tumors, for example in liver cancer (Fukui et al., 2006; Gomez del Pulgar et al., 2005; Li et al., 2006; Wang et al., 2007). This suggests the importance of RhoA in the development of liver malignancies. Interestingly, unlike the RAS protein, no activating mutations of RhoA have been reported and thus it was thought that the elevated level and activity of RhoA is sufficient to drive tumorigenesis. This might also suggest that the activating mutant of RhoA does not yield any significant tumorigenic properties (Karlsson et al., 2009) to the development of the neoplasia. Moreover, *in vitro* studies utilizing overexpression of RhoA or its constitutively active mutants (G14V or Q61L) only exhibited little or weak transforming activities (Narumiya et al., 2009). However, a study by Xue and co-workers in 2008 demonstrated the development of HCC in mice with the xenograft of liver progenitor cells ($p53^{-/-}$) transfected with RhoA G14V and Myc. This demonstrated that in a weakly transforming background of MYC and $p53^{-/-}$, the activation of RhoA was able to drive the formation of HCC.

RAS and Rho GTPases are key molecular switches that regulate cell dynamics, cell growth and tissue development through distinct signaling pathways. While much has been learnt about their individual functions and crosstalk in *in vitro* studies, the physiological/pathophysiological consequences of their signaling crosstalk *in vivo* remains largely unknown. In addition, the roles of RhoA in RAS-mediated transformation and their crosstalk *in vitro* still remain controversial. Many *in vitro* studies have reported an elevated level of RhoA and/or RhoA activities in oncogenic RAS-transformed cells or a requirement of RhoA signaling for RAS-mediated transformation

(Chen et al., 2003; Karaguni et al., 2002; Olson et al., 1998; Sahai et al., 2001; Xia and Land, 2007; Zondag et al., 2000). On the other hand, there are also studies that reported the contradictory results: the down-regulation or null requirement of RhoA/RhoA effectors activity in oncogenic RAS-transformed cells (Dreissigacker et al., 2006; Gupta et al., 2000; Izawa et al., 1998; Pawlak and Helfman, 2002). RAS transformed cells lack stress fibers and cell adhesion (key features of Rho activation), which demonstrated an inactivation of Rho-ROCK pathway in RAS transformed cells (Izawa et al., 1998). To date, the molecular mechanism of crosstalk between RhoA and RAS is still not well-defined. Moreover, it appears to be cell type-specific, varies with the RAS subtype, and depends on the kinetics and duration of RAS activation (Chen et al., 2003), which adds to the complexity.

The objectives of this study are as follows: (1) the generation of a zebrafish liver cancer model to study Kras-mediated liver tumorigenesis, with views to develop it into a platform for studying GTPase signaling, (2) to address the crosstalk of Kras and RhoA in liver development and tumorigenesis, and (3) to determine if the overexpression of RhoA can lead to liver tumor development.

In the next chapter, I will discuss the essential materials and methods/strategies that were employed in this study.

Chapter 2 Materials and Methods

2.1 General molecular techniques

2.1.1 Preparation of competent cells

The desired strains of *E.coli*, namely DH5α or XL-1 blue, were used for the preparation of competent cells. A streak plate was carried out on an antibiotic-free LB plate with glycerol-stock of the bacteria and incubated overnight at 37 ^{o}C. An overnight starter culture (~ two ml) was created by inoculating an isolated colony of the bacteria into antibiotic-free LB broth, under aseptic conditions. Approximately 100 µl of the starter culture was inoculated in 50 ml of antibiotic-free LB broth and incubated at 37 ^{o}C with strong agitation (~ 250 rpm). Growth of the culture was monitored periodically with the absorbance measurement at 600 nm with a spectrophotometer. The incubation was halted when the absorbance reached 0.4 to 0.6 at 600 nm. The bacteria were harvested by centrifugation at 4000 rpm for 30 minutes at 4 ^{o}C. The clear supernatant was removed and the pellet resuspended in 17 ml of CCMB buffer. The suspension was incubated on ice for 20 minutes. The suspension was then subjected to centrifugation at 4000 rpm for ten minutes at 4 ^{o}C. The supernatant was removed and the pellet resuspended in four ml of CCMB. The suspension was stored in aliquots of 100 µl in the -80 ^{o}C.

2.1.2 Transformation

Approximately 10 to 50 ng of plasmid or ligation reaction mixture in less than 10% of the total final volume were added to the competent cell suspension. The suspension was mixed by gentle tapping and incubated on ice for 30 minutes. The tube

was transferred to a pre-heated 42 ^{o}C heat block and incubated for one and half minutes. The tube was then transferred back on ice for at least one minute. One ml of antibiotic-free LB broth was added to the suspension. The tube was then incubated at 37 ^{o}C with strong agitation for one hour. The bacteria suspension was pellet down with centrifugation at 14000 rpm for 30 seconds. The supernatant was removed and the pellet resuspended in 100 µl of antibiotic-free LB broth. The suspension was plated onto LB agar containing the appropriate selection markers, antibiotic and/or x-gal. The LB agar plate was incubated at 37 ^{o}C overnight. An isolated colony was selected for future use.

2.1.3 Plasmid DNA preparation

XL-1 blue or DH5α laboratory strains of *E.coli* were used. Axygen miniprep kit, USA was used following the manufacturer's instruction for the purification of the plasmid DNA. Briefly, four ml of culture was harvested by centrifugation at maximum speed for one minute. The supernatant was decanted and the pellet was resuspended in 250 µl of buffer S1 by vortexing. 250 µl of buffer S2 (lysis buffer) was added to the suspension and mixed by inverting the tubes several times. 350 µl of buffer S3 was added to the mix and mixed by gentle inverting. The suspension was cleared by centrifugation at maximum speed for ten minutes. The cleared supernatant was applied to the mini-prep column. The column was washed by wash buffer W1 and W2. Pre-heated water (~ 60 ^{o}C) was applied to the dried column and incubated at room temperature for ten minutes. The solution containing the DNA was collected by centrifugation at maximum speed for one

minute. The concentration of the plasmid DNA was estimated by nanodrop spectrophotometer.

2.1.4 Polymerase chain reaction (PCR)

Typically, PCR were carried out on a Bio-rad thermal cycler. A typical PCR reaction consisted of 5 mM Tris-HCl (pH 9.0 at 25 ^{o}C), 1.5 mM $(NH_4)_2SO_4$ and 0.01% Triton® X-100, 1mM dNTPs (Promega, USA), 1.5 to 3.0 mM $MgCl_2$, 200 nM of forward primer (1st base, Singapore), 200 nM of reverse primer (1st base, Singapore) and approximately 50 ng to 100ng of template DNA. The cycling parameters were as followed: one cycle of five minutes at 95 ^{o}C, 20 to 30 cycles of 95 ^{o}C for 15 seconds; 50 to 68 ^{o}C for 15 to 30 seconds (temperature used dependent on the melting temperature of primer pair); 72 ^{o}C for one minute per kilo base of template, and one cycle of 72 ^{o}C for ten minutes. All PCR products were analyzed by agarose gel electrophoresis. The products were visualized by staining the DNA with Sybr-safe dye (Invitrogen, USA) and the use of an UV transilluminator. The documentation of the gel was performed by Bio-rad GelDoc XR system.

2.1.5 DNA sequencing and sequence analysis

Sequencing reaction was performed with the BigDye® terminator v3.1 kit (Applied Biosystems, USA). Typically, a five µl reaction was performed. Two µl of BigDye was added to three µl of solution containing 100 ng to 300 ng of DNA and 1 µM of primer. The sample was subjected to thermal cycling of 95 ^{o}C for 30 seconds and 68 ^{o}C for two minutes. The product was purified by sodium acetate/ethanol precipitation. 30 µl of 95% ethanol was added to the five µl reaction. The mixture was transferred to a fresh microfuge tube containing one µl of 3 M sodium Acetate, pH 5.2, and incubated on ice for 30 minutes. The precipitated DNA was spun down by centrifugation at 14,000 rpm for 20 minutes. The pellet was washed with 70% ethanol and dried on a 55 ^{o}C heat-block. The pellet was sent to the sequencing facilities, DSB, NUS for the further analysis. Sequencing results were analyzed by software like BLAST (http://blast.ncbi.nlm.nih.gov/Blast.cgi) and ClustalW2 (http://www.ebi.ac.uk/Tools/msa/clustalw2).

2.1.6 DNA purification from agarose gel or PCR or restriction digestion

QIAquick Gel extraction kit (Qiagen, USA) was used for DNA purification. DNA fragment, separated on a 1.0 to 1.5% agarose gel/1ppm Sybr safe DNA gel stain, was excised carefully with a scalpel. Three volumes of Buffer QG were added to one volume (by weight 100 mg -100 µl) of gel and the mixture was heated at 60 ^{o}C to dissolve the gel. One gel volume of isopropanol was added to the sample and mixed. The mixture was

applied to the QIAquick column and centrifuged to enable binding of DNA to the column. The column was washed with buffer QG and Buffer PE, and DNA eluted with pre-heated (65 ^{o}C) water.

For PCR/RE reactions clean-up, five volumes of Buffer PB were added to one volume of the reaction mix and applied to the QIAquick column. The column was washed with Buffer PE and dried by centrifugation. The bound DNA was eluted with pre-heated (65 ^{o}C) water.

2.1.7 Restriction endonuclease (RE) digestion/reaction

All restriction endonucleases used in this study were from New England Biolabs, USA, unless otherwise stated. Reactions were set-up and incubated according to the manufacturer's recommendations. Double digestions or sequential digestions were also performed according to manufacturer's recommendation. Restriction endonuclease reactions were used primarily to generate "sticky" ends for cloning purposes or the identification of "positive" clones.

2.1.8 DNA ligation reaction

DNA ligation was performed using the DNA ligation kit from New England BioLabs, USA. Typically, a ten µl reaction was prepared according to the manufacturer's

recommendation. The reactions were incubated overnight at 4 ^{o}C. The molecular ratio of vector to DNA fragment (insert) was kept at 1:3 to 1:10. Half of the reaction mix was used for transformation with chemically treated competent cells.

2.1.9 *In vitro* mRNA synthesis for microinjection (Ac mRNA)

The pAc SP6 plasmid was a kind gift from Dr Parinov, TLL. The plasmid was linearised with BamHI restriction endonuclease and gel-purified. The linearised DNA fragment was used as a template for mRNA synthesis using the mMESSAGE mMACHINE™ SP6 Kit (Ambion, Applied Biosystems, USA). One µg of linearised DNA was set-up in a 20 µl reaction according to the manufacturer's protocol, and incubated at 37 ^{o}C for two hours. The mRNA was purified by Lithium chloride precipitation. The mRNA was quantified by nanodrop spectrophotometer and stored in aliquot at -80 ^{o}C.

2.2 Tet-on eGFP-Kras G12V transgenic line

The Tet-on liver-specific oncogenic Kras transgenic was generated by Dr Liu Xingjun. It was later characterized by me as part of my PhD thesis. Briefly, restriction enzymes linearized plasmids, namely the *TRE2*-eGFP-Kras G12V cassette and the *lfabp* promoter-rtTAs-M2 cassette, were co-injected into the one-cell stage embryo. The

injected embryos were screened for the integration of the plasmids in their genome. Selected larvae were grown up to adulthood. The adult fish were rescreened by out-crossing with wild-type fish. It was done to identify the founder generation when the genetic materials had successfully integrated in the germline. One founder fish was identified. The F1 progeny of this founder fish was raised up to adulthood. Characterization and experiments were performed using the progeny from the F1 generation. The strategy employed is illustrated in Figure 2.1.

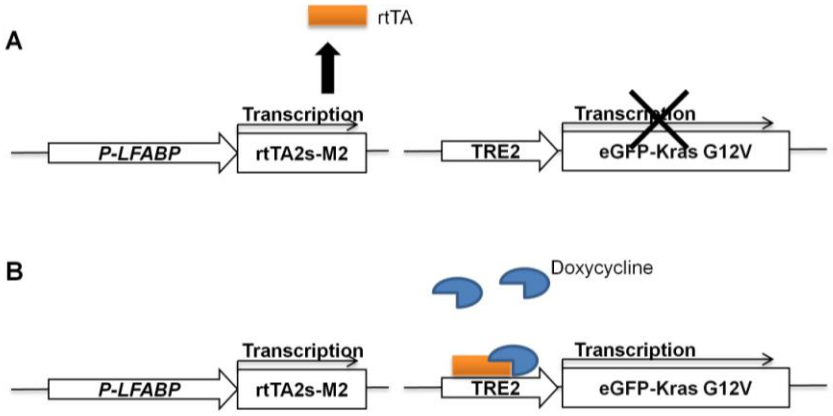

Figure 2.1: Schematic diagram of the Tet-on system employed. (A) The rtTA is expressed in a liver specific manner directed by the *lfabp* promoter. In the absence of doxycycline, the rtTA does not bind the *TRE2*. Therefore there is no expression of the eGFP-Kras G12V in the liver. (B) In the presence of the doxycycline, the rtTA binds to the *TRE2* and transactivate the expression of the eGFP-Kras G12V in a liver specific manner.

2.3 Generation of RhoA transgenic lines

The Ac/Ds transposase system was utilized for the creation of the RhoA transgenic lines. Five primary plasmids were used for the generation of the secondary plasmid, pDS-LF-rtTA2s-M2-*TRE2*-mCherry-RhoA plasmids. The five primary plasmids were pDS-vector and pDs(cry:C-LOP:Ch) vector (a kind gift from Dr Parinov, TLL), pLF-rtTA2s-M2 vector (a kind gift from Dr Zhen HuiQing, NUS), pCS 2+ -RhoA (wt or G12V or T19N) vectors (kind gifts from Dr Jane Zhu, NUS), p*TRE2* vector (Clontech Taraka, USA), The LF of the pLF-rtTA2s-M2 refers to the *lfabp* promoter. DNA fragments were subcloned directly using appropriate REs or PCR/RE digestion to generate appropriate "sticky" ends. RE sites were introduced or deleted using site-directed mutagenesis kit (Stratagene, USA). Briefly, the RhoA fragment was subcloned into p*TRE2* vector by PCR/RE/ligation to yield p*TRE2*-RhoA vector. mCherry fragment was then subcloned from the pDs(cry:C-LOP:Ch) vector into the p*TRE2*-RhoA vector by PCR/RE/ligation to yield p*TRE2*-mCherry-RhoA. Subsequently, the *TRE2*-mCherry-RhoA fragment was subcloned into pDS vector by RE/ligation to yield pDS-*TRE2*-mCherry-RhoA vector. Site-directed mutagenesis was performed on the pLF-rtTA2s-M2 vector to add an additional *XhoI* restriction site. The LF-rtTA2s-M2 fragment was subcloned into the pDS-*TRE2*-mCherry-RhoA vector to yield the pDS-LF-rtTA2s-M2-*TRE2*-mCherry-RhoA vector. The pDS-LF-rtTA2s-M2-*TRE2*-mCherry-RhoA (Figure 2.2) vector was subsequently used for the transgenesis by microinjection. (RhoA refers to wild-type RhoA or its mutants).

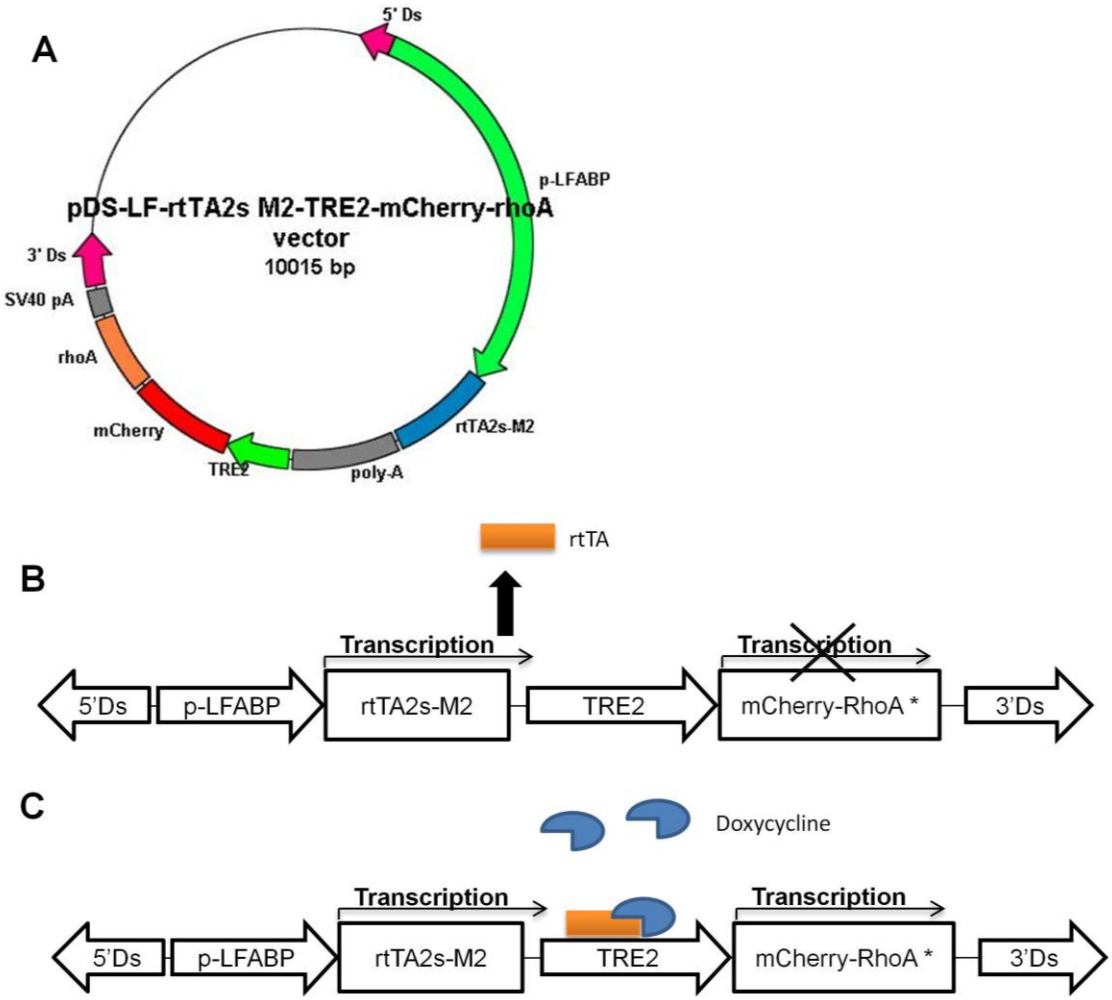

Figure 2.2: Schematic representation of the plasmid and the Tet-on system employed in the generation of RhoA transgenic lines. (A) Systematic representation of the pLF-rtTAs M2-*TRE2*-mCherry-RhoA used in this study. (B) The rtTA protein is driven by the liver-specific promoter, *lfabp* promoter. In the absence of doxycycline, the rtTA does not bind the TRE and thus no transactivation of the mCherry-RhoA gene. (C) In the presence of doxycycline, the rtTA binds the TRE and transactivate the mCherry-RhoA gene. RhoA denotes: RhoA, constitutively active RhoA G14V or dominant negative RhoA T19N.

Table 6: List of primers used for the construction of pDS-LF-rtTA2s-M2-*TRE2*-mCherry-RhoA

Name of Primers	Sequence (5'-3')	Target/Remarks
mCherryfwdBamHI	CCG GAT CCC GCC ACC ATG GTG AGC AAG GGC GAG	mCherry
mCherryrevBamHI	CCG GAT CCC TTG TAC AGC TCG TCC ATG CC	mCherry
RhoAfwdBamHI	CCG GAT CCA TGG CAG CAA TTC GCA AGA AGC	RhoA
RhoArevNotI	CCG CGG CCG CTC ACA GCA GAC AGC ATT TGT TGC	RhoA
LF-SDM	ACT ATA GGG CGA ACT CGA GCT CCA CCG CG	To insert *XhoI* into pLF-rtTA vector
LF-SDM	CGC GGT GGA GCT CGA GTT CGC CCT ATA GT	To insert *XhoI* into pLF-rtTA vector

Micro-injection was performed using the micro-injector from World Precision Instrument, USA. Embryos were collected and aligned on an agarose-coated petri-dish. A total of 2.3 nl, containing 25 to 30 pg of plasmid DNA, 200 to 300 pg of transposase mRNA and 0.01% phenol red, was microinjected directly into the cell of the embryo at the one-cell stage. The surviving embryos were screened at 1 dpf for mCherry expression. mCherry positive larvae were raised separately from the mCherry negative larvae. Founder fish screening was carried out by out-crossing the adult fish with wild-type fish. The resulting progeny was analyzed for mCherry expression under a fluorescence microscope to determine the presence of germ-line integration of the transgene. Four founders were identified in the Tg(*lfabp*-rtTAs-M2; *TRE2*-mCherry-

RhoA) line. One founder each was identified in the Tg(*lfabp*-rtTAs-M2; *TRE2*-mCherry-RhoA G14V) and Tg(*lfabp*-rtTAs-M2; *TRE2*-mCherry-RhoA T19N), respectively. The process of creation and screening are summarized in the Table 7. Progeny from one of the four founders from the Tg(*lfabp*-rtTAs-M2; *TRE2*-mCherry-RhoA) line was chosen to be used for the rest of this study because of its higher expression. The F1 generation fish from the founder were raised to maturity and the rest of the study was conducted using the generations after F2.

Table 7: Summary of transgenesis of RhoA transgenic lines

Genotype	**Total number of fish that survived more than 3mths**	**No. of fish screened**	**No. of founders identified**	**Transgenesis percentage**
RhoA	144	61	4	6.56%
RhoA G14V	48	15	1	6.67%
RhoA T19N	44	15	1	6.67%

2.3.1 Induction of transgene expression

Typically, the induction of transgene in the embryos was performed with doxycycline 20 μg/ml at 2 dpf. Sorting of larvae according to genotypes were carried out at 4-5 dpf using an inverted fluorescence microscope from Zeiss, Germany. The larvae

were sorted to various genotypes based on the presence of different reporter gene(s) expressed in their liver after induction. The reporter genes used are eGFP and mCherry. eGFP and mCherry fluorescence proteins are used to label oncogenic Kras G12V transgene and various RhoA (wt/mutants) transgenes, respectively. Table 8 provides a summary of the transgenic lines created and used in this study.

Table 8: Summary of the transgenic lines created and used

Name	Transgene	Biological effects
Tg(*lfabp*-rtTA2s-M2; *TRE2*-eGFP-Kras G12V)	eGFP-Kras G12V	Constitutively active mutant of Kras, Insensitive to GAP activities
Tg(*lfabp*-rtTAs-M2; *TRE2*-mCherry-RhoA)	mCherry-RhoA	Wild-type RhoA
Tg(*lfabp*-rtTAs-M2; *TRE2*-mCherry-RhoA T19N)	mCherry-RhoA T19N	Dominant-negative mutant of RhoA; Prevent activation of other RhoA; Bind GEF and sequester them from activating other RhoA
Tg(*lfabp*-rtTAs-M2; *TRE2*-mCherry-RhoA G14V)	mCherry-RhoA G14V	Constitutively active mutant of RhoA Insensitive to GAP activities

Footnote: All transgenic lines express the transgene in a liver-specific manner under the influence of the Tet-on system.

The induction of the transgene into the respective adult transgenic fish was achieved with the application of 10 μg/ml of doxycycline unless otherwise stated. Change of water was carried out every other day with the fresh application of doxycycline during induction. All tanks were maintained in the dark throughout the treatment. The density of the zebrafish was kept at five fish to one liter of water. Aeration was provided by the use of an air-pump. The zebrafish were fed brine-shrimp twice daily. The large scale

inductions were carried out to determine the oncogenicity of the transgene(s) in the adult liver. The flow chart in Figure 2.3 summarized the experimental set-up. Eight different combinatory genotypes were studied. Each genotype was divided the treatment and control group with 40 fish in each group. The treatment group was subjected to doxycycline induction at 10 μg/ml and the control group was not treated (zero μg/ml). The water was changed every other day and dosed with doxycycline where applicable. Death events were (1) dead and rotten, (2) fresh dead and (3) near death fish. The fresh dead fish were fixed immediately for histological analysis whiles the near dead were sacrificed and fixed for histological analysis. Not all dead/sacrificed fish were examined histologically because of the constraint in resources.

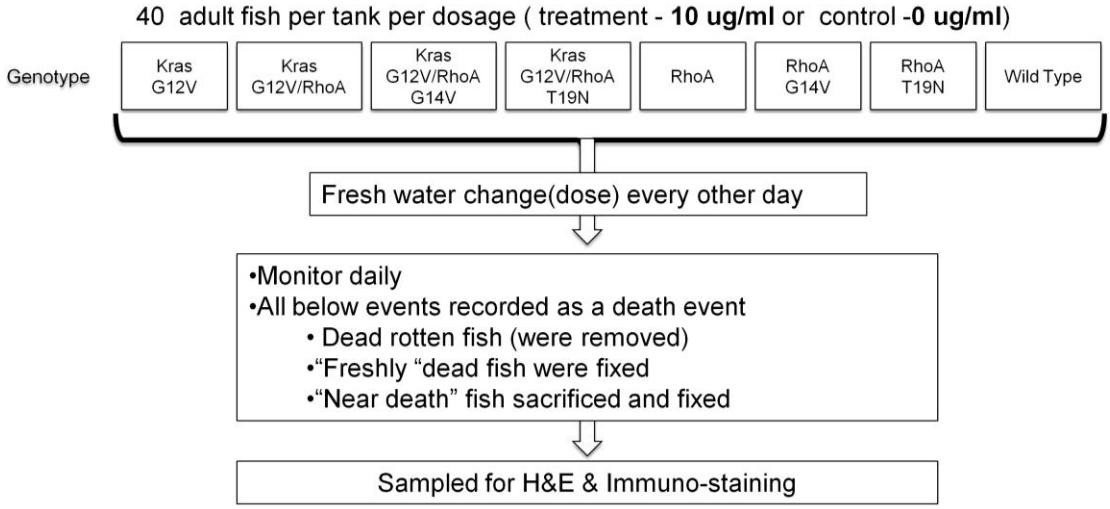

Figure 2.3: Flow chart of induction treatment. Eight different genotypes were studied. Each genotype was separated in two groups, 40 fish each. One group was subjected to doxycycline induction at 10 μg/ml while the other was used as control without doxycycline.

2.4 Maintenance of zebrafish

2.4.1 Crossing of selected transgenic/wild-type line

Wild-type and transgenic zebrafish were raised and maintained under standard laboratory conditions (Salas-Vidal et al., 2005). For the collection of embryos, a two tank system (inner tank with mesh which sits in a plastic tank) was used. Breeding pairs of female zebrafish and male zebrafish were placed in the inner tank separated by a plastic divider. The spawning tanks were kept in the photo-period room (14 hours of dark, 10 hours of light) to stimulate spawning. The plastic dividers were removed in the morning to enable spawning. Embryos were collected and cleaned by the use of a strainer. Embryos were then transferred to petri-dishes with egg water (60 μg/ml; Red Sea Salt, USA) and raised at 28 ^{o}C. The development stages are presented in this thesis as days post-fertilization (dpf). Feeding started at four dpf for the larvae with powdered fish flakes and egg yolk solution. Brine shrimp were given from six dpf. The larvae were raised in a stand-alone tank until 14 to 20 dpf before they were transferred to the system.

2.5 Western analysis with zebrafish larvae

2.5.1 Protein extraction from zebrafish larvae and adult liver

Five dpf larvae were harvested for Western analysis. Approximately 50 larvae from each genotype were collected in 1.5 ml tubes. Excess water was removed by careful pipetting. The larvae was either lysed immediately or stored in -80 ^{o}C for future analysis. Larvae were lysed in RIPA buffer [50 mM Tris-HCl, 150 mM NaCl, 0.75 mM EDTA,

1% sodium deoxycholate, 1% Triton X-100, 0.2% NaF, 0.1% SDS, 25 mM β-glycerol phosphate, 5 mM Na Orthvanadate, 1X protease inhibitor cocktail (Roche, USA), pH 7.3]. Approximately 2.5-3.0 µl of RIPA lysis buffer was added per larva. The larvae were grinded using a pellet pestle for at least two minutes. The resulting mixtures were incubated on ice for at least 30 minutes before centrifugation at 14000 rpm for 20 minutes at 4 ^{o}C. The supernatant was collected. Lysate protein concentration was estimated with BCA protein assay (Piercenet, USA), according to manufacturer's instructions.

Adult fish were sacrificed and dissected. The livers were carefully extracted, transferred into clean tube and weighed. The liver tissue was snap-freezed in liquid nitrogen immediately. It was either stored in -80 ^{o}C or processed immediately for protein extraction. The liver tissue was lysed in T-per (Piercenet, USA) supplemented with proteinase inhibitor, with 25 -30 µl used per mg of liver tissue. The livers were grinded using a pellet pestle for at least two minutes. The resulting mixtures were incubated in the cold with strong agitation for two hours before centrifugation at 14000 rpm for 20 minutes at 4 ^{o}C. The supernatant was carefully collected without the top oil layer. The total protein concentration was estimated with BCA protein assay (Piercenet, USA).

2.5.2 Protein concentration estimation

For BCA protein assay, the lysate was diluted ten times with the lysis buffer. 200 µl of the pre-prepared BCA reagent was added to a well containing 25 µl of the diluted

sample (in a 96-wells plate). The plate was incubated at 37 ^{o}C for 30 minutes. It was cooled to room temperature before analysis by a microplate reader (Bio-rad, USA) at 562 nm. The concentration was estimated to a BSA standard curve in the assay. The samples were denatured at 90 ^{o}C for three minutes in Laemmli buffer (50 mM Tris/ HCl pH 6.8, 1% (v/v) 2-mercaptoethanol, 2% SDS, 0.1% Bromphenolblue, 10% Glycerol).

2.5.3 SDS-PAGE and Western blotting

The lysate was resolved on an 8% or 10% or 12% polyacylamide gel using the mini protean II electrophoresis apparatus (Bio-rad, USA). The resolving gel contains 8 or 10 or 12% acrylamide, 0.375 nm TRIS-HCl pH8.8, 0.001% SDS, 0.001% APS, 0.001% TEMED. The stacking gel contains 5% acrylamide, 0.125 mM Tris-HCl pH 6.8, 0.001% SDS, 0.001% APS and 0.001% TEMED. Electrophoresis was performed at 50 mA/gel for 1 hour at room temperature in SDS-running buffer (18.6 mM Tris, 144 mM glycine and 0.075% SDS). A wet transfer was performed in an ice-cold transfer buffer (25 mM Tris, 192 mM glycine, 0.01% SDS and 20% methanol) at 100 V for 90 minutes.

2.5.4 Detection of the protein of interest

After transferring, the PVDF membrane was blocked in blocking solution (5% BSA in TBST) for one hour at room temperature. The blot was probed with the

appropriate primary antibody (Table 9) diluted in blocking solution at 4 ^{o}C, overnight with gentle agitation. Blot was washed three times with TBST, for five minutes each. After that, the blot was incubated in diluted HRP-conjugated secondary antibodies (Sigma, USA) for one hour at room temperature with gentle shaking. The blot was washed three times with TBST, for five minutes each. Detection was carried out with enhanced chemiluminescence (ECL) substrates (Piercenet, USA) and X-ray film (Kodak, USA and Fuji, Japan). For re-probing of membrane with another primary antibody, the blot was stripped with stripping buffer (25mM Glycine-HCl, pH2.0, 1% SDS). The membrane was washed in two changes of stripping buffer, for 15 minutes each. After which, the blot was washed with TBST six times, for five minutes each. Blot was re-block with blocking buffer for one hour at room temperature with gentle shaking before the appropriate antibody was applied.

Table 9: Antibodies used in Western analysis and immunostaining

Name	Source	Applications/dilutions
Anti-p-ERK1/2	Sigma, USA	Western/ 1:1000 Immunostaining/ 1:1000
Anti-ERK1/2	BD Transduction, USA	Western/ 1:1000
Anti-p-AKT2	Genscript, USA	Western/ 1:1000
Anti-AKT2	Genscript, USA	Western/ 1:1000
Anti-p-p21	Santa Cruz, USA	Western/ 1:1000
Anti-p21	Santa Cruz, USA	Western/ 1:1000
Anti-β-actin	Sigma, USA	Western/ 1:1000
Anti- Cox IV	Cell Signaling Technology, USA	Western/ 1:1000
Anti-GAPDH	Cell Signaling Technology, USA	Western/ 1:1000
Anti-PCNA	Santa Cruz, USA	Immunostaining/ 1:75
Anti-pH3	Millipore, USA	Immunostaining/ 1:200
Anti-mouse Horse radish peroxidase	Sigma, USA	Western/ 1:2500
Anti-rabbit Horse radish peroxidase	Sigma, USA	Western/ 1:2500
Anti-rabbit Alexa 647	Invitrogen, USA	Immunostaining/ 1:200

2.6 Active Ras pull-down assay

2.6.1 Preparation of Glutathione-GST-RBD conjugates

BL21 *E.coli* harboring GST-RBD (Ras binding domain) or GST bacterial expression vectors were inoculated into five ml of LB broth containing ampicillin and grown overnight at 37 ^{o}C with strong agitation. One ml of the starter culture was inoculated into 200 ml of LB ampicillin and incubated at 37 ^{o}C with strong agitation until the O.D. of the culture reached 0.5 to 0.6 at 600 nm. The expression of the GST protein or the GST-RBD was induced by addition of 0.1 M IPTG followed by incubation at room temperature with strong agitation for 20 hours. The culture was harvested by centrifugation at 4000 rpm for 30 mins at 4 ^{o}C. 50 ml and 100 ml of culture were collected as bacterial pellet for the GST-RBD and GST, respectively. Lysis and capturing of the GST-RBD or GST was performed on ice with ice-cold buffer. Five ml of lysis buffer [1x PBS, 1% Trition-X100, DTT (0.15 g/ml) and protease inhibitor (one tablet per 100 ml; Roche, USA)] was added per pellet and resuspended. The resuspended solution was transferred to 15 ml falcon tube and subjected to sonication at 20% amplitude for three minutes (Pulse: three second on and nine second off). The cell debris was removed by centrifugation for 30 minutes at 5500 rpm at 4 ^{o}C. Supernatant was then transferred to a fresh 15 ml falcon tube. 150 µl of glutathione agarose bead (GE healthcare life science, USA) was added and the mixture incubated at 4 ^{o}C with gentle rotation for one hour. The supernatant was removed by centrifugation and the pellet was washed thrice with 1X PBS with 0.1% triton-X100, followed by two washes with 1X PBS. The beads were resuspended in 150 µl of 1X PBS. The concentration of purified beads was estimated by

running SDS-PAGE with known concentrations of BSA (10 μg, 20 μg, 30 μg and 100 μg).

2.6.2 Pull-down of active Ras

Total larval lysate was obtained as described in Section 2.5.1. The protein concentration was adjusted with RIPA buffer to achieve equal concentration among the different samples. 25 μg of the purified GST-RBD or GST was added per reaction. The suspension was incubated at 4 ^{o}C with gentle rotation for one hour. The beads were collected by centrifugation at 200 rpm for one second. The beads were washed three times with 750 μl of RIPA buffer. The beads were resuspended in 2X Laemmli buffer and heated at 90 ^{o}C for five minutes. The mixture was cooled on ice and pulse-centrifuged. The supernatant was resolved on a SDS-PAGE and analysed by Western, probing for eGFP-Kras protein with anti-Kras and anti-eGFP antibody.

2.7 Cryostat sectioning

Embryos of selected stages were fixed in 4% paraformaldehyde at 4 ^{o}C overnight. Fixed embryos were washed three times with 1X PBST for five minutes each. Washed embryos were embedded in 1.5-2.0% agarose/5% sucrose. Agarose embedded embryos were stored in excess amount of 30% sucrose solution at 4 ^{o}C, overnight or until the

agarose blocks sink to bottom of the container, for equilibrations. Agarose blocks were mounted onto metal stands using OCT (Lecia, USA) for cryostat sectioning. Sections of 10 µm were cut using a cryostat (Lecia, USA). Sections were mounted onto positively charged slides (Fisher scientific, USA). Slides were dried on a 40 ^{o}C hotplate for 2-3 hours prior to staining/storage at -80 ^{o}C.

2.7.1 Immunofluorescence of cryostat sections

Slides were washed in 1X PBS for five minutes. The sections on the slide were blocked and permeablised with 5% goat serum/PBS/0.3% Triton-X 100 for two hours at room temperature. The blocking solution was removed by carefully blotting with filter paper. Primary antibodies (Table 9) in blocking solution were applied and slides placed in a humid chamber. Incubation in primary antibodies was performed at 4 ^{o}C overnight. The slides were washed in 1X PBS for three times, for five minutes each. Secondary antibodies (fluochrome conjugated) were applied and incubated at room temperature for two hours. Slides were washed twice in 1X PBS for five minutes each, and counter-stained with DAPI. The slides were mounted with fluorsave (Calbicom, USA). Images were captured with Zeiss LSM 510 Meta microscopy or Lecia TCS SP5x. For slides that did not require immunostaining, they were stained with DAPI and mounted for imaging directly.

2.8 Confocal imaging of larvae for volumetric analysis

Six dpf larvae were fixed in 4% PFA at 4 ^{o}C overnight with gentle agitation. Fixed larvae were washed three times in 1X PBST, for five minutes each. Larvae were cleared in 50% glycerol in PBS through a progressive increment of glycerol from 10% to 50%. Larvae were stored overnight in 50% glycerol/PBS/2.5% DABCO at 4 ^{o}C before use. Larvae were mounted in aqueous mounting media (50% glycerol, 1X PBS, 7.5% gelatin, 2.5% DABCO) for documentation. The larvae were arranged on glass bottom petri-dishes with the left side of the larvae facing the glass bottom. Images (Z-stack) were documented by Lecia MP 5x microscopy. Image processing was subsequently performed with IMARIS (Bitplane, USA), which enabled the estimation of the liver volume of the larvae. Briefly, the z-stack images were converted to suitable Imaris format. The z-stack images were viewed in the surpass model and the surfaces were created using the fluorescence signals. The volume occupied by the 3D model (based on the fluorescence signal) was estimated by the Imaris.

2.9 Histological analysis

Adult fish were anaesthetized in 0.5% phenoxyethanol and sacrificed. The fish were cut open at the belly and the skin on the left side of the fish removed. Bouin's fixative (saturated picric acid: formalin (37%): acetic acid, 15:5:1) was pumped into the fish body through the mouth with the use of a syringe. The swim bladders were deflated and the whole fish were fixed in Bouin's fixative for four days at room temperature. The

fixed samples were washed with ddH_2O. The fixed samples were then washed in changes of 70% ethanol (EtOH) for twice a day for four days. The samples were dehydrated through a series of ethanol in the following sequence: 70% EtOH for one hour; 90% EtOH for two hours; 95% EtOH for one hour; 100% EtOH for two hours; 100% EtOH for one hour; 100% EtOH for one hour; 50% EtOH/50% Histoclear for 30 mins; Histoclear-I for 1.5 hours; Histoclear-II for overnight; Paraffin-I for two hours; Paraffin-II for four hours; Paraffin-III for overnight. The samples were embedded in paraffin. Five μm thick sections were cut from the block using a microtome and mounted onto a positively charged glass slide (Fisher Scientific, USA). Sectioning of paraffin blocks and H&E stained slides were partially prepared by service from Histology unit, Biopolis shared facilities.

2.9.1 Immuno-histochemistry of paraffin section

2.9.1.1 De-wax of paraffin section

Sections were deparaffined and rehydrated by running it through the following sequence: Histoclear – ten minutes; Histoclear – ten minutes; 100% EtOH – five minutes; 100% EtOH – three minutes; 90% EtOH – three minutes; 70% EtOH – three minutes; 50% EtOH – three minutes; ddH_2O – three minutes; ddH_2O – three minutes. Deparaffined slides were stained with Heamatoxylin and Eosin (H&E) or immuno-histochemically stained.

2.9.1.2 Immuno-histochemistry of paraffin section

Deparaffined and rehydrated slides were subjected to heat based antigen retrieval. Briefly, rehydrated sections were soaked in antigen unmasking solution (10mM Sodium Citrate Buffer pH 6.0, 0.5% Tween 20 or Tris-EDTA pH9.0, 0.5% Tween 20) and heated up to a boil (high power) and maintained at sub-boiling temperature for 10 to 15 minutes (medium high power) in a microwave (Sanyo, Japan).The sections were allowed to cool on the bench for 30 minutes. The slides were rinsed once with TBS. Endogenous peroxidases were blocked using 0.5% hydrogen peroxide in TBS or DAKO endogenous blocking solution at room temperature for 15 minutes. The slides were rinsed thrice with 1X TBST. The tissue sections were blocked in blocking buffer (10% goat serum in TBS/1% BSA) for one hour at room temperature. Primary antibody (Table 9) diluted in 1% BSA/TBS were applied and the slides were incubated at 4 ^{o}C overnight. The slides were washed three times with 1X TBST for five minutes each. HRP polymer (Dako, Denmark) was applied and the slides were incubated at room temperature for 30 minutes. Slides were washed twice with 1X TBST and once with 1X TBS for five minutes each. DAB staining buffer was applied and incubated at room temperature. Color development was monitored carefully under a microscope. The reaction was stopped by rinsing the slides with water. Hematoxylin counter stain was applied according to manufacturer's recommendation (Sigma, USA). Tissue sections were dehydrated and mount permanently. Documentation of the colorimetric staining was performed using the Zeiss Axioskop2 microscope.

For immuno-fluorescence study, the peroxidase blocking step was omitted and the HRP polymer was replaced with fluorochrome conjugated secondary antibodies. The

section was mounted with fluorsave. Documentation of the staining was performed using the Zeiss Meta 510 confocal scanning microscope.

2.9.2 Slides/histological diagnosis

The H&E stained slides were diagnosed by Dr. Jan Spitsbergen of Oregon State University, U.S.A, based on criteria stated in Table 5.

2.10 Statistical test

T-test was used for testing of differences in mean between two populations/samples. Fisher exact test was used for analysis of the comparisons of liver lesions caused by the various genotypes. Log rank test was employed for the analysis of the Kaplan-Meier plot with Graphpad Prism 5, USA.

Chapter 3 Results

3.1 Characterization of Tg(*lfabp*-rtTA2s-M2; *TRE2*-eGFP-Kras G12V)

3.1.1 Controlled liver-specific expression of eGFP-Kras G12V

The founder fish, Tg(*lfabp*-rtTA2s-M2; *TRE2*-eGFP-Kras G12V), harboring the eGFP-Kras G12V transgene was created by Dr Liu Xingjun as described in Section 2.2. I aimed to investigate whether the eGFP-Kras G12V transgene is exclusively expressed in the liver after induction. The F1 fish were out-crossed with wild-type fish. Embryos were collected, treated with doxycycline at 2 days post-fertilization (dpf) and they were allowed to develop until 6 dpf. The enhanced green fluorescent protein (eGFP) was used as a reporter for oncogenic Kras expression, which can be detected with fluorescence microscopy. After induction by doxycycline, the eGFP expression was observed exclusively in the liver of the larvae (Figure 3.1).

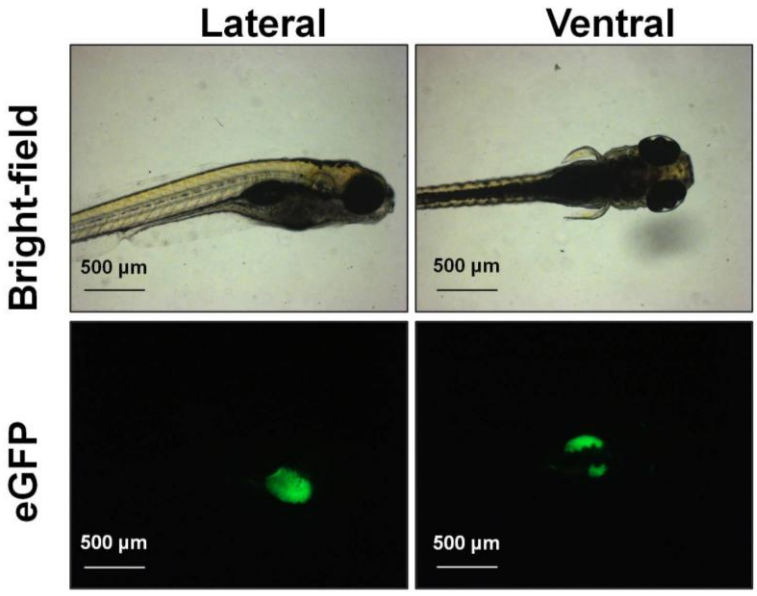

Figure 3.1: eGFP expression in transgenic larva after induction. Application of doxycycline induced the expression of eGFP-Kras G12V transgene in the liver of the 6 dpf larva, specifically.

3.1.2 Ectopically expressed eGFP-Kras G12V resided at the plasma membrane predominantly

In order to determine the cellular distribution of eGFP-Kras G12V, eGFP positive transgenic larvae were cryostat-sectioned for confocal fluorescence microscopy analysis. I demonstrated that the eGFP-Kras G12V were enriched at the plasma membrane (Figure 3.2). It is known that the sub-cellular localization of RAS proteins can determine its interaction with different effectors, thus eliciting different signal outputs. RAS-GTP has been shown to translocate to the plasma membrane predominantly after stimulation by growth factors (Augsten et al., 2006).

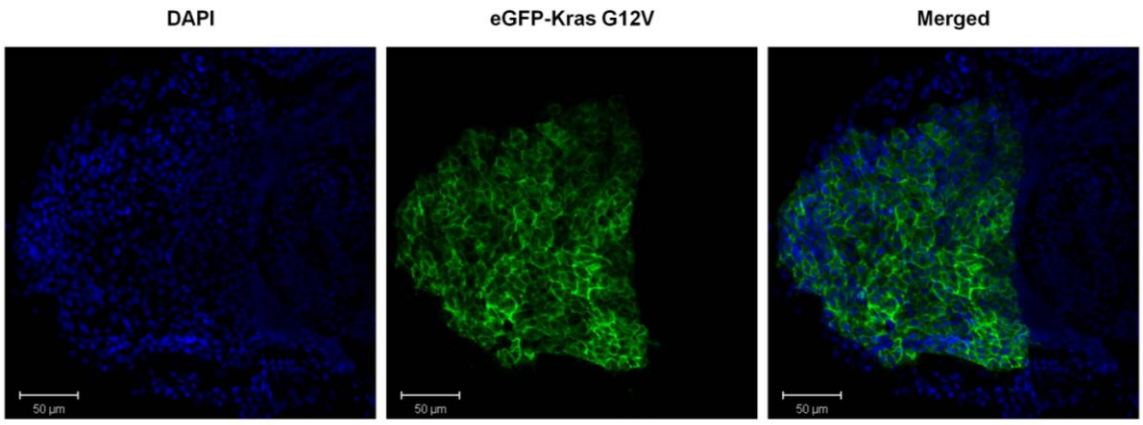

Figure 3.2: Plasma membrane bound eGFP-Kras G12V. Confocal images of cross-section of eGFP-positive transgenic 6 dpf larva. The ectopically expressed eGFP-Kras G12V proteins (green) were predominantly distributed to the plasma membrane. Section was counterstained with DAPI (blue) to illustrate the nucleus.

3.1.3 Oncogenic Kras G12V was expressed as an eGFP-tagged protein and retained its ability to interact with its effectors

I investigated whether the introduced oncogenic Kras protein is expressed as an eGFP-fusion protein and whether it retains its ability to interact with its effectors. To do so, doxycycline-treated larvae were screened and separated into the GFP positive and GFP negative groups. The GFP negative group (wild-type siblings) was used as a control. Both groups of embryos were lysed and whole embryo lysate samples were collected. The samples were subjected to Western analysis with both anti-Kras and anti-eGFP antibodies. The result here demonstrated that the Kras was expressed as a fusion protein with molecular weight of approximately 50kDa (Kras ~ 21kDa; eGFP ~27 KDa; eGFP-Kras ~ 48kDa), and was detectable with both anti-Kras and anti-eGFP antibodies (Figure 3.3A).

Active RAS-GTP binding assays (RBD-assay) were performed to ascertain that the eGFP-Kras G12V still retained its ability to interact with its effectors. The RAS binding domain (RBD) of Ral GDP dissociation stimulator (RalGDS) was used as a probe to "pull down" active GTP-bound Kras as described in Section 2.6. The RBD recognized the differences in the conformation of GST-RAS and GDP-RAS and had high affinity to GTP-bound RAS (active). The results in Figure 3.3B illustrated that the ectopically expressed GFP-Kras G12V was pulled-down by the RBD and detected by both the anti-Kras and anti-eGFP antibodies. Bacterial synthesized GST was used as a control to ensure that no non-specific binding to GST protein occurred. The results demonstrated that the ectopically expressed oncogenic Kras protein was active and able to interact with its effector proteins.

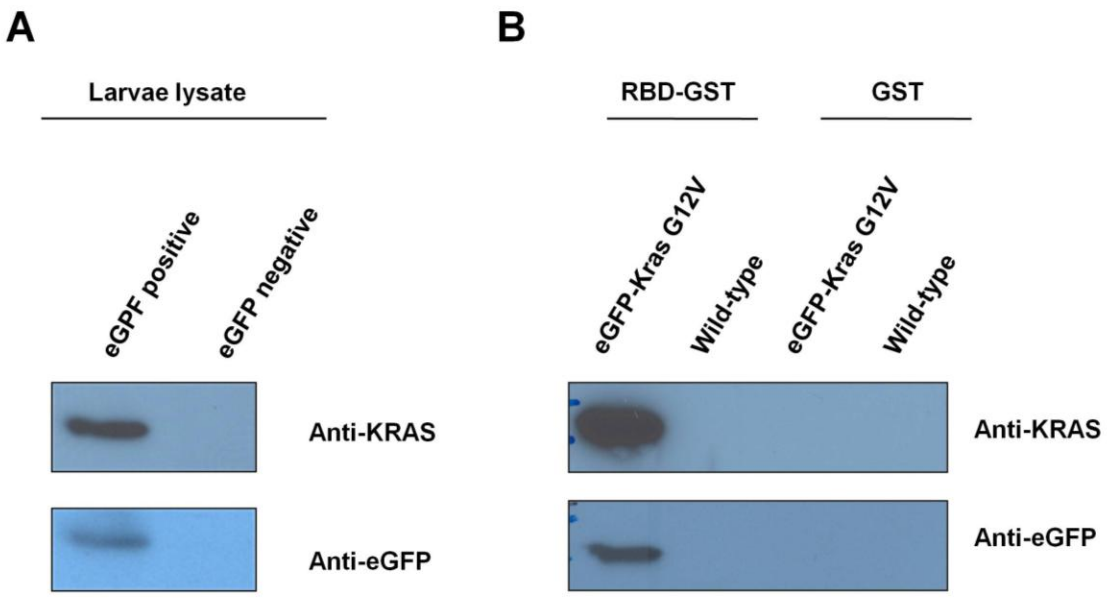

Figure 3.3: Oncogenic Kras G12V protein was expressed as an eGFP-tagged protein and retained its ability to interact with its effector. (A) Western blots of whole embryo lysates of eGFP positive and eGFP negative 5 dpf larvae. Both showed a band corresponding to approximately 50 kDa when probed with anti-Kras antibody and anti-eGFP antibody, respectively, in the eGFP positive larval lysate (B) RBD pull-down assay followed by Western analysis indicates that the ectopically expressed eGFP-Kras G12V protein (~50 kDa) is GTP-bound and active. Blots were probed with anti-eGFP (rabbit) and developed; stripped and re-probed with anti-Kras (mouse) for the second development of blots.

3.1.4 Oncogenic Kras expression caused enlargement of liver during development

It was observed that the liver-specific expression of eGFP-Kras G12V caused an enlargement of the organ during early development. To examine this Kras G12V-mediated liver enlargement, volumetric analyses were performed. The Tg(*lfabp*-rtTA2s-M2; *TRE2*-eGFP-Kras G12V) was crossed to the Tg(*lfabp*:dsRED; elaA:eGFP) named Lipan line (Korzh et al., 2008). The Lipan line constitutively expressed the dsRED

protein and eGFP in the liver and pancreas, respectively. Lipan line was used because of the need for a fluorescence reporter for the confocal imagining and volumetric quantification assay. The crossing of the two transgenic lines was performed to reduce the effect of genetic background and developmental speed/time. The embryos were induced with doxycycline at 2 dpf. The larvae were screened and selected for dsRED expression at 4 dpf and raised to 6 dpf. The dsRED positive larvae were screened for eGFP expression in the liver and separated into the eGFP positive and the eGFP negative group. The double transgenic (eGFP & dsRED) and single transgenic (dsRED) were used as a surrogate for the Tg(*lfabp*-rtTA2s-M2; *TRE2*-eGFP-Kras G12V) and wild-type age-matched larvae, respectively. The specimen were prepared and imaged as described previously in Section 2.8. The result in Figure 3.4A demonstrated that ectopic expression of eGFP-Kras G12V caused a significant enlargement of the liver during early development.

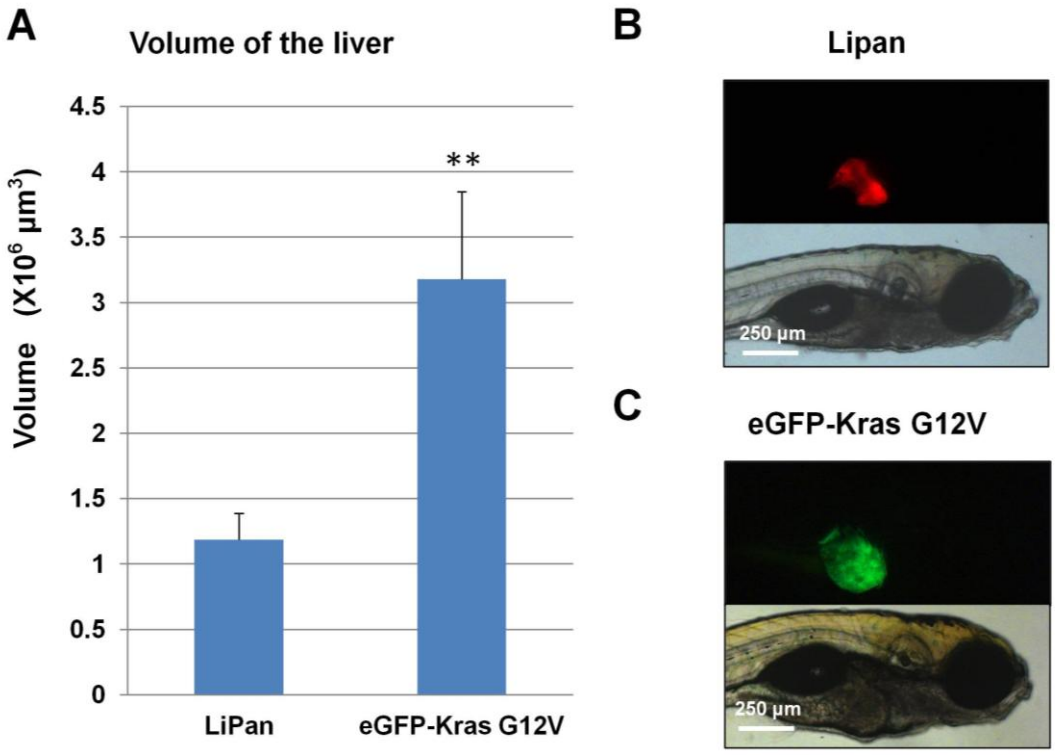

Figure 3.4: Oncogenic Kras expression in the liver caused an enlargement of the organ. (A) Volumetric analyses of the liver in the Lipan line vs Tg(*lfabp*-rtTA2s-M2; *TRE2*-eGFP-Kras G12V). Liver-specific expression of eGFP-Kras G12V caused significant increase in the organ volume (size) as compared to the control. (** denotes: p-value <0.01; n=12). Error bars represent standard deviation. (B) Fluorescence (top panel) and bright-field images (bottom panel) of the Lipan line. (C) Fluorescence (top panel) and bright-field images (bottom panel) of the eGFP-Kras G12V transgenic larvae. (Scale bar: 250 µm.)

3.1.5 Increased hepatocyte proliferation in eGFP-Kras G12V transgenic larvae

In order to determine if increased proliferation was the cause of enlargement of the liver, immunofluorescence staining with the proliferation marker, phospho-Histone3 (pH3) was carried out. Cryostat sections obtained from 6 dpf larvae from out-cross of Tg(*lfabp*-rtTA2s-M2; *TRE2*-eGFP-Kras G12V) with wild-type fish were used. The results established that there was significant increase in proliferation of the hepatocytes in

the eGFP-Kras G12V expressing larvae compared to their wild-type siblings, as indicated by the significantly increased pH3 staining (Figure 3.5 B).

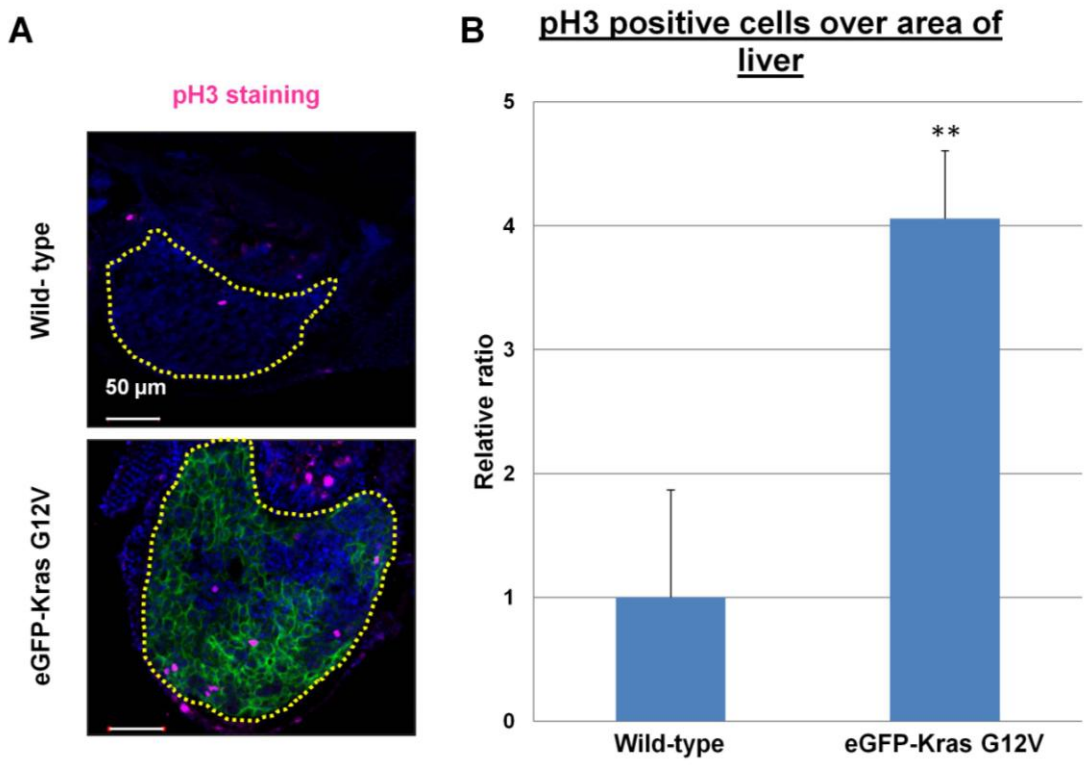

Figure 3.5: Increased proliferation of the hepatocytes in Tg(*lfabp*-rtTA2s-M2; *TRE2*-eGFP-Kras G12V) larvae. (A) More pH3 positive cells were observed in the liver of the Tg(*lfabp*-rtTA2s-M2; *TRE2*-eGFP-Kras G12V) compared to wild-type. The wild-type liver is highlighted with yellow dotted line. The liver of Tg(*lfabp*-rtTA2s-M2; *TRE2*-eGFP-Kras G12V) is labelled green and highlighted with yellow dotted line. pH3 positive cells were stained pink. (Scale bar: 50 µm.) (B) Proliferative index was scored based on number of pH3 stained cells over area occupied by the liver. The bar chart plotted relative ratio vs genotypes. The wild type is set as the reference value of one. Oncogenic Kras increased the hepatocyte proliferation significantly as compared to the wild-type. (n=4; p-value < 0.01). Error bar denotes standard deviation.

3.1.6 Increased activity of RAF/MEK/ERK and PI3K/AKT pathways in eGFP-Kras G12V expressing larvae

As shown earlier, the liver overgrowth is largely due to the increase in proliferation in the eGFP-Kras G12V-expressing hepatocytes. Herein, I investigated if the two well-studied signaling cascades downstream of Kras are responsible for the increase in the liver overgrowth. RAF/MEK/ERK and the PI3K/AKT were well studied for the role in cell proliferation and cell survival, respectively. Western analyses were carried out to investigate the involvement of these two pathways. As shown in Figure 3.6 A, the level of phospho-Erk (an indicator of MEK/ERK activation) was increased in the eGFP-Kras G12V transgenic larvae as compared to the wild-type control. The level of total Erk remained relatively unchanged. As shown in Figure 3.6 B, the level of phospho-AKT2 (an indicator of PI3K/AKT2 activation) and total AKT2 was increased in the eGFP-Kras G12V transgenic larvae as compared to the wild-type. Thus, these results suggested that the increased in RAF/MEK/Erk and PI3K/Akt2 activities, downstream of Ras signaling, were largely responsible for the increase in liver size.

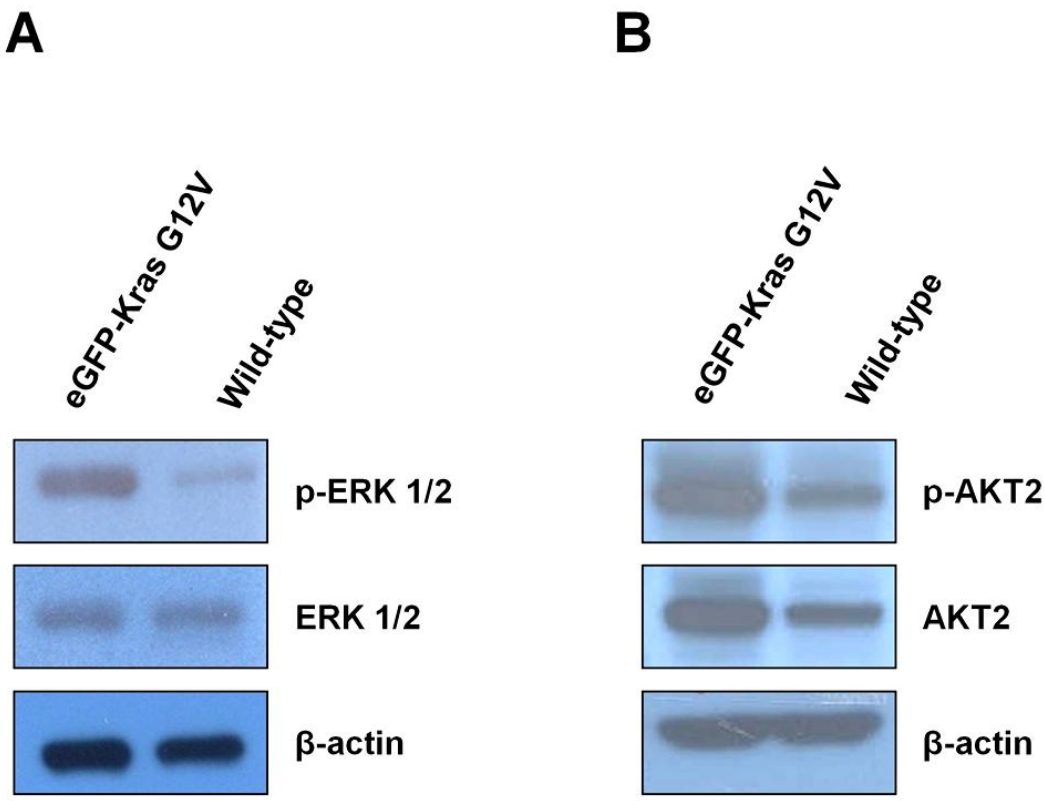

Figure 3.6: eGFP-Kras G12V expression increased activation of the RAF/MEK/Erk and PI3K/Akt2 signaling. Larvae from out-cross of Tg(*lfabp*-rtTA2s-M2; *TRE2*-eGFP-Kras G12V) with wild-type were used. Larvae were induced with doxycycline at 2 dpf, screened and harvested at 5 dpf for Western analysis. At least 50 larvae were pooled for each genotype (lane) per Western analysis. Immunoblots representative of at least three repeats. It was probed for phospho-Erk1/2, total Erk 1/2, phospho-Akt2 and total Akt2. (A) There was an increase in the amount of phospo-Erk1/2 in the eGFP-Kras G12V expressing larvae, while the total Erk 1/2 level remained relatively similar. (B) There was an increase in both the amount of phospho-Akt2 and Akt2 in the eGFP-Kras G12V larvae compared to the wild-type siblings. Anti-β-actin was used to demonstrate equal loading in both Figures 3.6 A and B.

3.1.7 Inactivation of p21 (Cip1) by phosphorylation

I examined the involvement of p21 (Cip1), a downstream target of AKT2, in mediating the increase in proliferation. p21 (Cip1) is a potent cyclin-dependent kinase inhibitor and thus functions as a regulator of cell cycle progression. Western analysis was carried out with anti-phospho-p21 and anti-p21 antibodies with whole larvae lysates prepared as described in Section 2.5. As shown in Figure 3.7, there was an increase in the level of phospho-p21 in the Tg(*lfabp*-rtTA2s-M2; *TRE2*-eGFP-Kras G12V) larvae as compared to the wild-type siblings. The total amount of p21 remained unchanged in both samples. β-actin was used as a loading control.

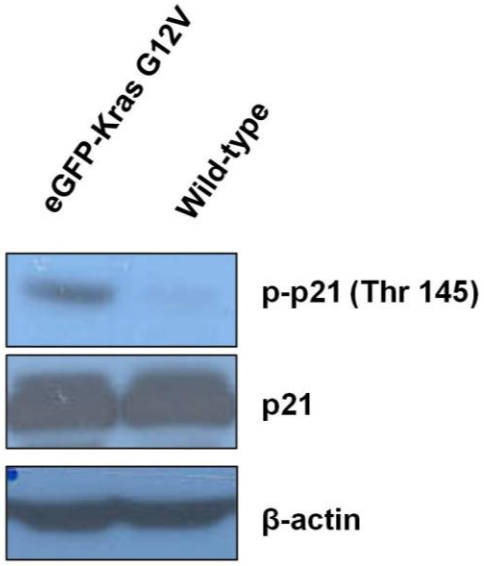

Figure 3.7: Akt2 inactivation of p21 (Cip1) as one of the possible mechanisms to promote cell growth. Larvae from out-cross of Tg(*lfabp*-rtTA2s-M2; *TRE2*-eGFP-Kras G12V) with wild-type were used. Larvae were induced with doxycycline at 2 dpf, screened and harvested at 5 dpf for Western analysis. At least 50 larvae were pooled for each genotype (lane) per Western analysis. Immunoblots representative of at least three repeats. It was probed with anti-phospho-p21 (Thr 145) and anti-p21. There was an increase in the level of phosphorylation of p21 in the eGFP-Kras G12V expressing larvae. β-actin and total p21 proteins were used to demonstrate equal loading.

3.2 Functional crosstalk between Kras and RhoA signaling

To study the functional crosstalk of Kras and RhoA in liver development and liver tumorigenesis, transgenic lines expressing RhoA (or its mutant) were required. The detailed strategy of RhoA transgenesis was described in the Section 2.3.

3.2.1 Expression of the mCherry-RhoA transgene was both liver-specific and inducible

I investigated whether the mCherry-tagged RhoA transgene was exclusively expressed in the liver after induction. The F1 fish were out-crossed with wild-type fish. Embryos were collected, treated with doxycycline at 2 dpf and were allowed to develop until 6 dpf. The mCherry was used as reporter for the RhoA expression, which can be detected with fluorescence microscopy. As shown in Figure 3.8A to C, the mCherry expression was observed in the liver of the transgenic larvae specifically after induction by doxycycline.

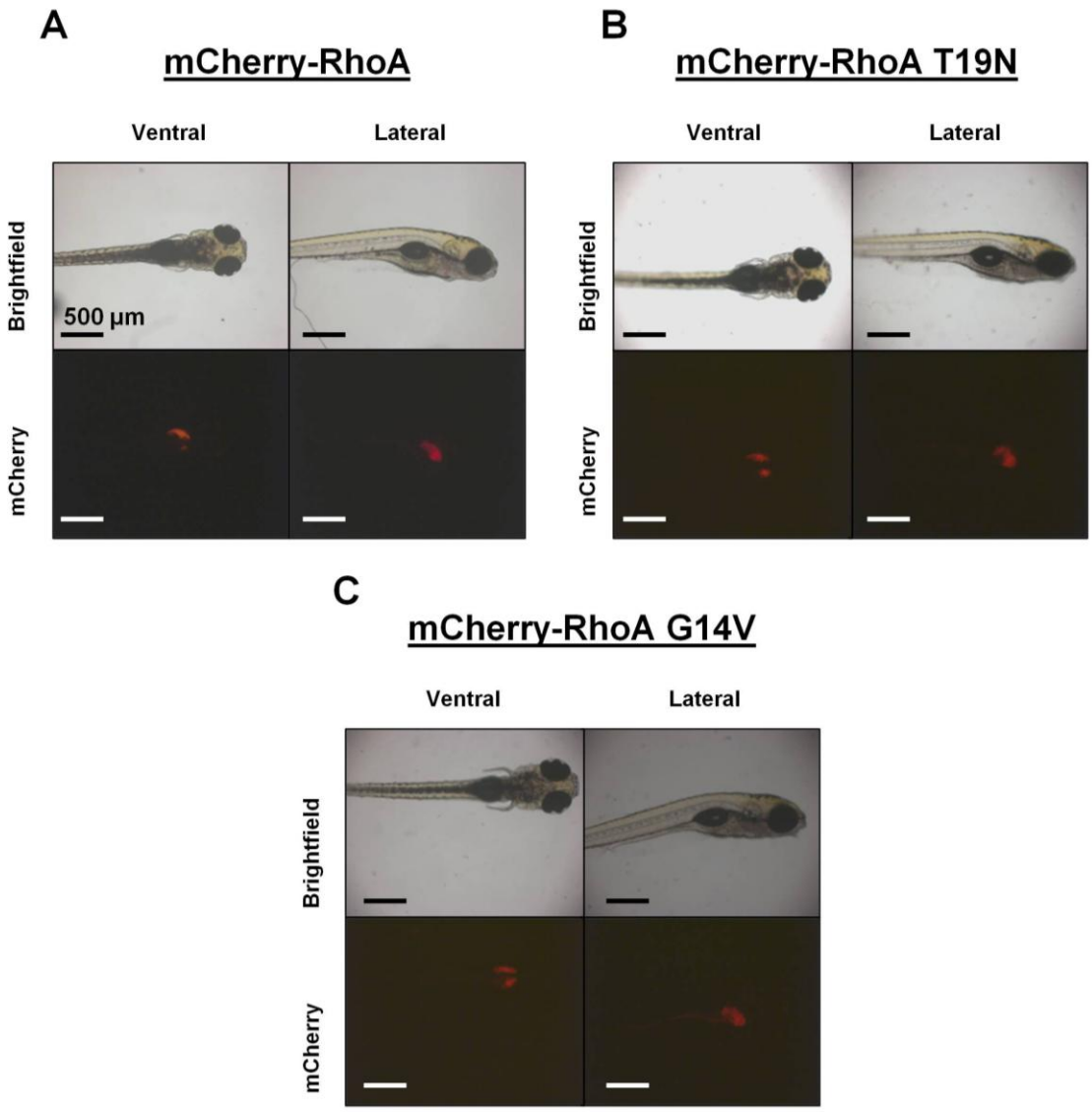

Figure 3.8: Liver specific expression of mCherry-RhoA (or its mutants) upon induction. Lateral and ventral views of the larvae were documented. Respective genotypes of the larva are labelled on top. mCherry signals were restricted to the liver of the respective transgenic larvae after induction by doxycycline. (Scale bar: 500 µm.)

3.2.2 Ectopically expressed mCherry –RhoA and its mutant were largely distributed in the cytosol

I aimed to determine the liver-specific expression and cellular distribution of the mCherry-tagged RhoA proteins. For this, I fixed and prepared 10 μm thick sections by cryostat sectioning as described in the Section 2.7. The sections were counterstained with DAPI and mounted for imaging. The images in Figure 3.9 showed that the ectopically expressed proteins (mCherry-RhoA, mCherry-RhoA T19N & mCherry-RhoA G14V) in the respective transgenic lines were restricted to the liver. The enlarged images further revealed that the mCherry-RhoA was distributed in the cytosol with numerous punctate-like structures (Figure 3.9A iii & iv). Punctate distribution of the mCherry-RhoA T19N and mCherry-RhoA G14V in the cytosol were observed in Figure 3.9B (iii) and Figure 3.9B (iii) respectively.

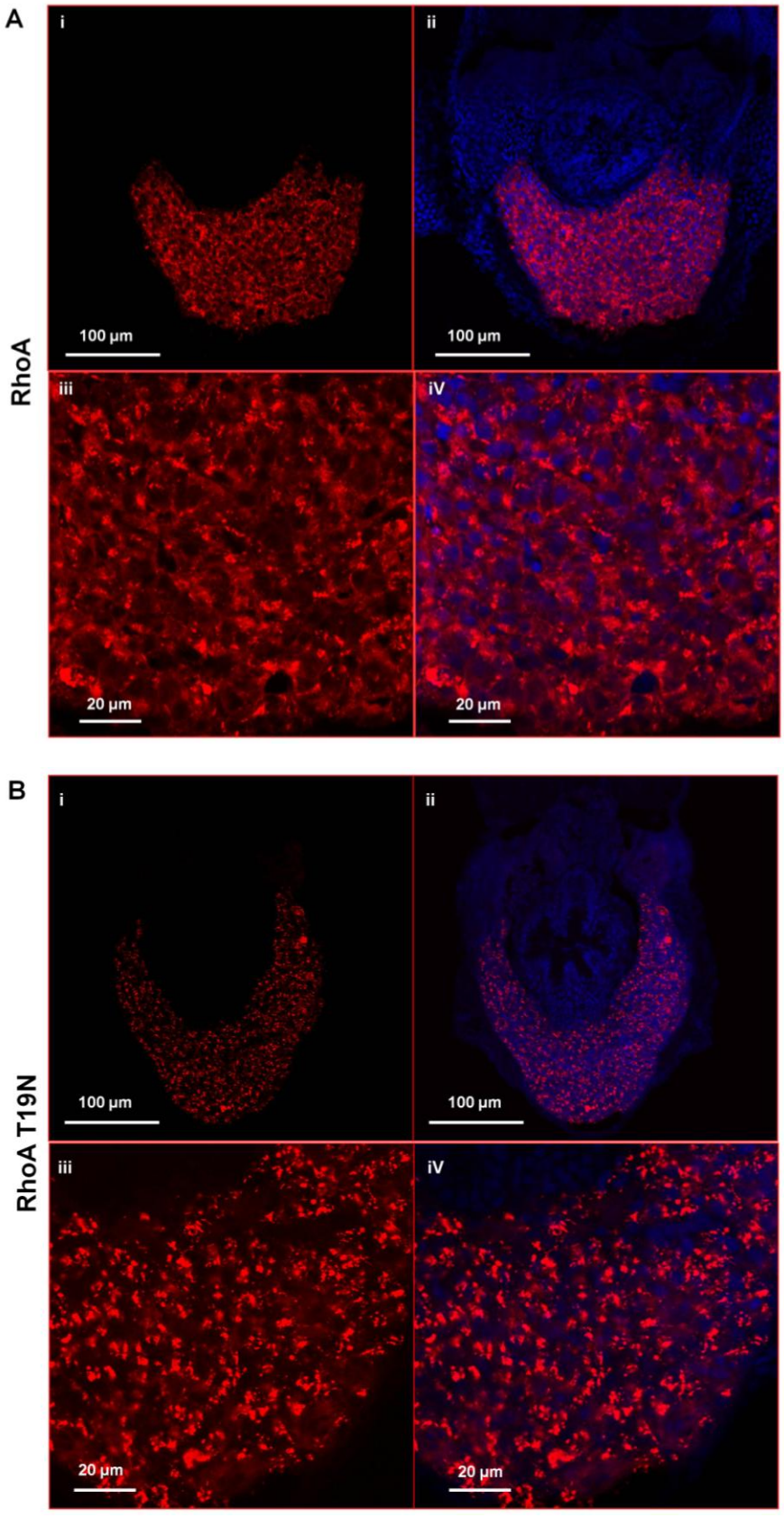
A
RhoA
i
ii
100 µm
100 µm
iii
iV
20 µm
20 µm
B
RhoA T19N
i
ii
100 µm
100 µm
iii
iV
20 µm
20 µm

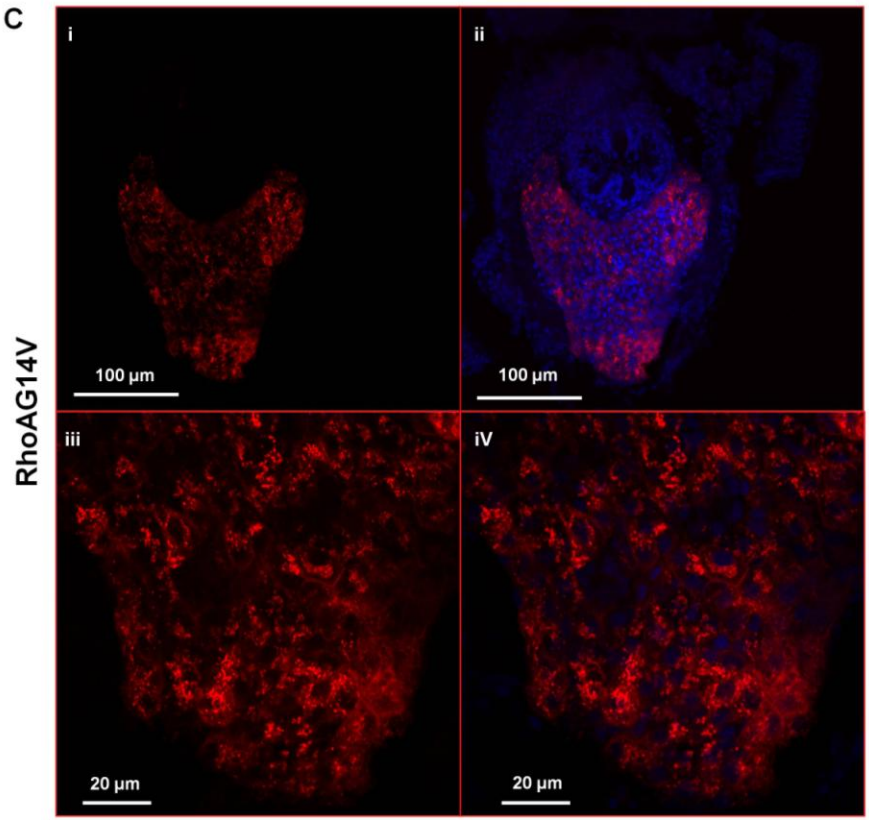

Figure 3.9: Distribution of the mCherry tagged RhoA (or its mutants) after induction. Confocal images of cross sections of 6 dpf transgenic larvae - (A) RhoA, (B) RhoA T19N and (C) RhoA G14V. Panels iii and iv showed an enlargement of the picture in panels i and ii, respectively. (Panel iii of A) mCherry-RhoA was distributed in the cytosol with some punctate distribution. (Panel iii of B and C) Punctate distributions of the mCherry-tagged proteins in the cytoplasm were observed in the cross-section of mCherry-RhoA T19N and mCherry-RhoA G14V transgenic larvae. The sections were counterstained with DAPI to highlight the nucleus.

3.2.3 RhoA and its mutants were expressed as a mCherry-tagged protein

Liver lysate were harvested from respective transgenic fish that were treated with 60 µg/ml of doxycycline for one week as described in Section 2.5.1. They were resolved with SDS-PAGE and probed with anti-RhoA and anti-GAPDH antibodies. The

immunoblot demonstrated bands at approximately 50 kDa that were reactive to anti-RhoA antibody (Figure 3.10). RhoA and mCherry proteins are approximately 21 kDa and 33 kDa, respectively. A fusion protein would be approximately 50 kDa in size. Here, I can deduce that the RhoA or its mutants were expressed as a mCherry-tagged protein.

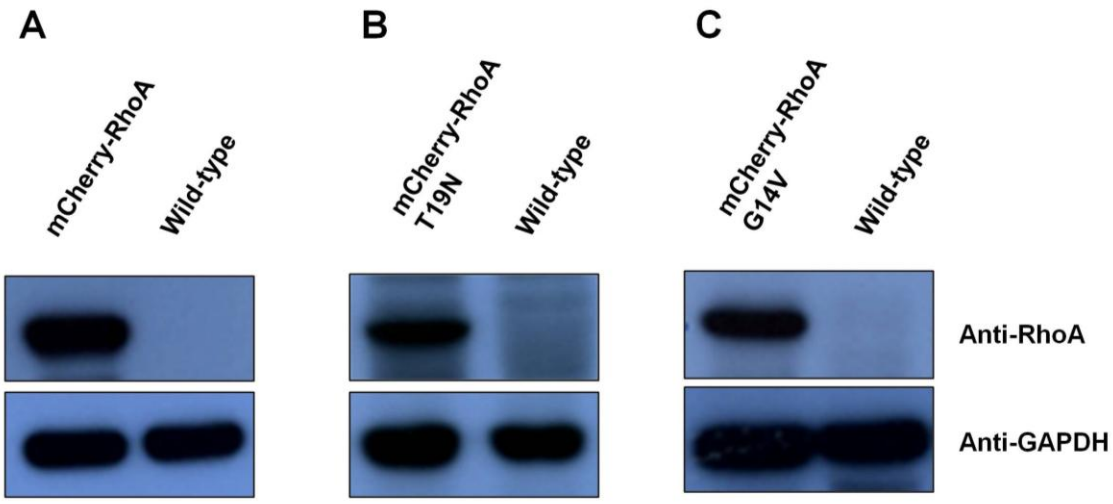

Figure 3.10 RhoA and its mutants were expressed as mCherry-tagged proteins. Immunoblots of the liver lysate analysed with Western probing for anti-RhoA antibody. Western demonstrated the detection of a band of 50 kDa in the respective RhoA transgenics, – (A) RhoA, (B) RhoA T19N and (C) RhoA G14V, but not in their respective wild-type control.

3.2.4 Generation of double transgenic lines and their functional characterization

After the initial characterization of the three RhoA transgenic lines, I set to investigate their crosstalk with oncogenic Kras, especially during liver development and liver tumorigenesis. These can be achieved by crossing of the various RhoA transgenic lines (Tg(*lfabp*-rtTAs-M2; *TRE2*-mCherry-RhoA), Tg(*lfabp*-rtTAs-M2; *TRE2*-mCherry-RhoA T19N) or Tg(*lfabp*-rtTAs-M2; *TRE2*-mCherry-RhoA G14V) with the Tg(*lfabp*-rtTA2s-M2; *TRE2*-eGFP-Kras G12V) line to generate the double transgenic lines, respectively. Figure 3.11 illustrates the crossing strategy that was employed to generate the double transgenic lines. Only double transgenic larvae were shown. The double transgenic provided an invaluable tool to study the crosstalk of Ras and RhoA in an *in vivo* vertebrate model. Crosstalk between RAS and RhoA in an *in vivo* model was under-appreciated as most studies were conducted in the *in vitro* cell model. For ease of labelling, the double transgenic will be labelled Kras G12V/RhoA for Tg(*lfabp*-rtTA2s-M2; *TRE2*-eGFP-Kras G12V ; *lfabp*-rtTAs-M2; *TRE2*-mCherry-RhoA), Kras G12V/RhoA G14V for Tg(*lfabp*-rtTA2s-M2; *TRE2*-eGFP-Kras G12V ; *lfabp*-rtTAs-M2; *TRE2*-mCherry-RhoA G14V) and Kras G12V/RhoA T19N for Tg(*lfabp*-rtTA2s-M2; *TRE2*-eGFP-Kras G12V ; *lfabp*-rtTAs-M2; *TRE2*-mCherry-RhoA T19N).

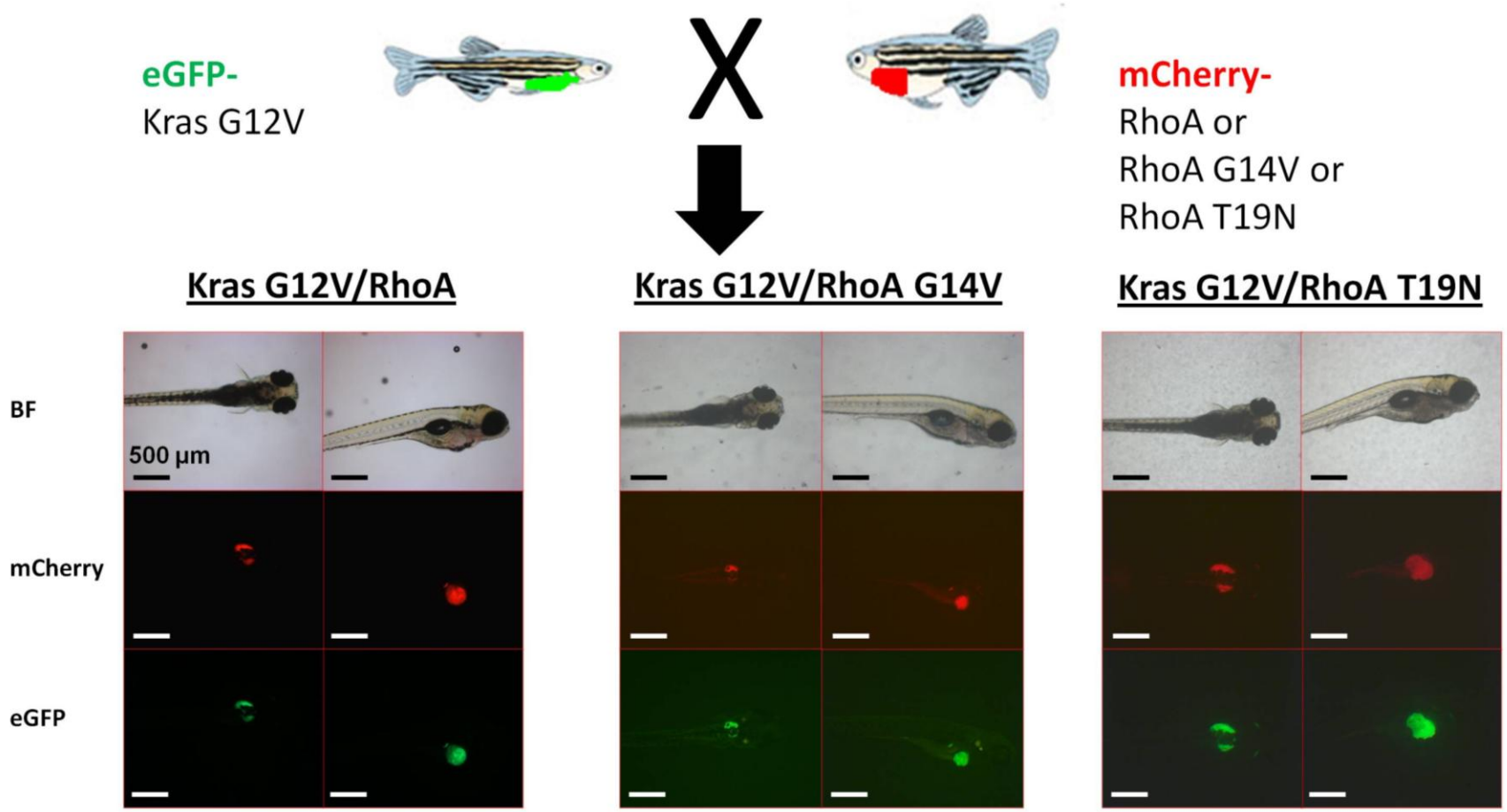

Figure 3.11: Schematic representation of simplified crossing of the Tg(*lfabp*-rtTAs-M2, *TRE2*-eGFP-Kras G12V) with the respective RhoA transgenic line. Double transgenic larvae were labelled with both mCherry and eGFP, and can be differentiated easily from their single transgenic or wild-type siblings. BF denotes bright-field. Simplified diagram for the purpose of illustrating the double transgenic larva from each cross. Scale bar is 500 µm for all images.

3.2.5 Effects of RhoA signaling on oncogenic Kras-mediated liver enlargement during development

As described earlier in Section 3.1.4 and 3.1.5, the ectopic expression of oncogenic Kras resulted in an enlargement of the liver during development, concomitant with elevated hepatocyte proliferation. Applying the same strategy of quantitative imaging, I investigated the effect of RhoA or its mutants on this oncogenic Kras-mediated phenotype. Crosses were set up according to the scheme in Figure 3.11 for the respective genotypes. The larvae were treated with doxycycline at 2 dpf and sacrificed at 6 dpf for imaging/documentation as described in the Section 2.8.

As shown in Figure 3.12 A, the dominant-negative mutant of RhoA T19N augmented the oncogenic Kras-mediated liver overgrowth significantly. The constitutively active RhoA G14V reduced the effect of Kras G12V mediated liver enlargement significantly, reducing it by up to 25% (Figure 3.12 B). No significant change in the liver volume of the double transgenic of Kras G12V/RhoA was observed as compared to the Kras G12V single transgenic (Figure 3.12 C).

In addition, I investigated if the changes in the liver overgrowth were caused by any alterations in proliferation. Phospho-histone 3 staining was performed as described in Section 2.7.1. In Figure 3.13, the co-expression of RhoA T19N with Kras G12V increased the hepatocyte proliferation while the co-expression of RhoA G14V reduced the proliferation rate. Taken together, the blocking of RhoA signaling could enhance Kras G12V-driven proliferation thus resulting in a larger liver phenotype. Conversely, the

activation of RhoA signaling, in the background of activated Kras signaling, could reduce oncogenic Kras-driven processes, resulting in a smaller liver phenotype.

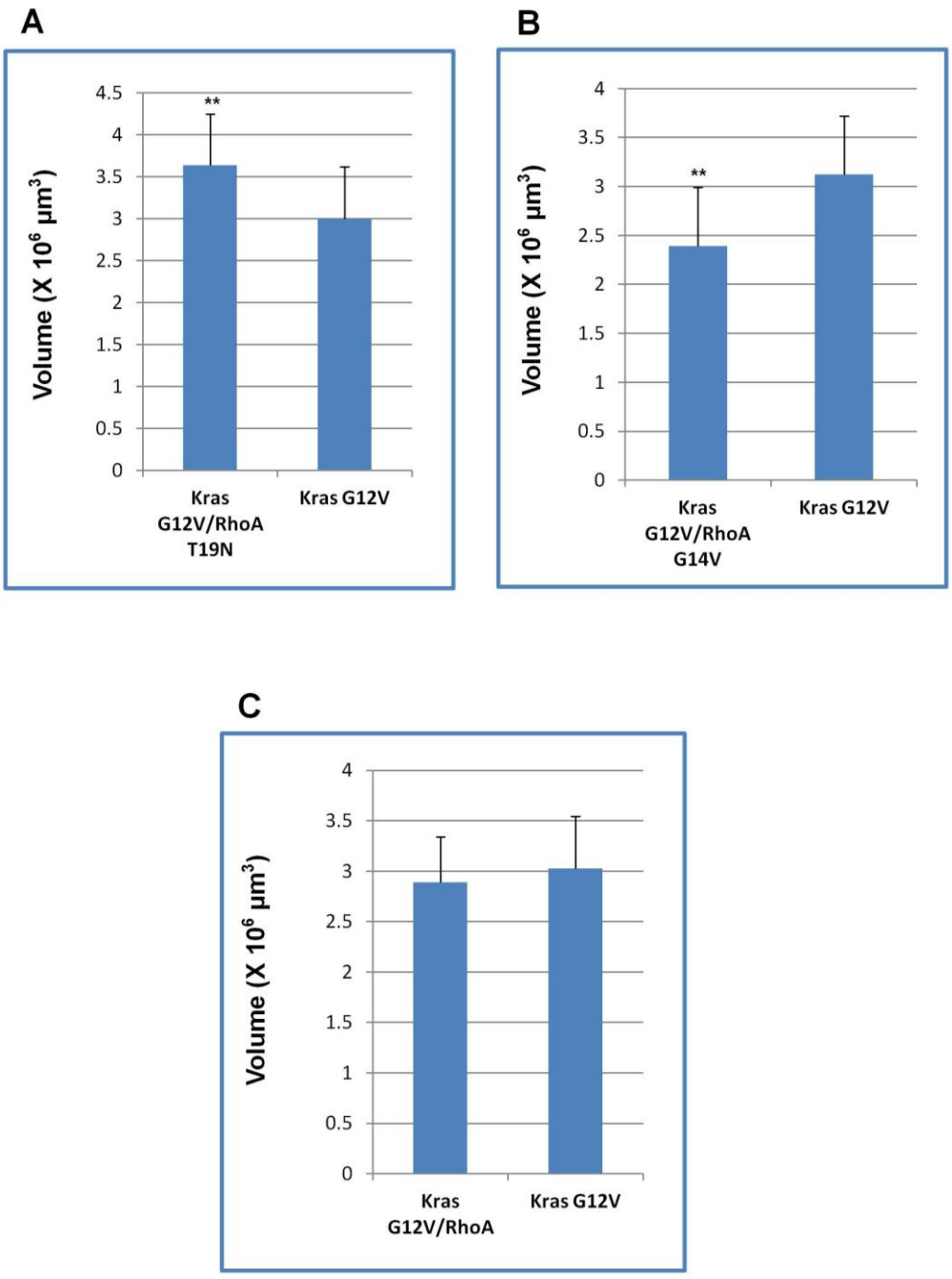

Figure 3.12: Volumetric analyses on the effect on RhoA signaling on Kras G12V mediated liver enlargement. The larvae were analyzed from the same family to account for the genetic background effects and variation in environment on growths. (A) RhoA T19N augmented the Kras G12V mediated liver enlargement significantly, (B) while the RhoA G12V reduced that, significantly. (C) No significant change in liver volume was observed in the double transgenic of Kras G12V/RhoA compared to the Kras G12V larvae. $n \geq 50$ in Figure 3.12 B and C. $n \geq 80$ in Figure 3.12 A (** denotes p-value < 0.01). Error bars denote standard deviation.

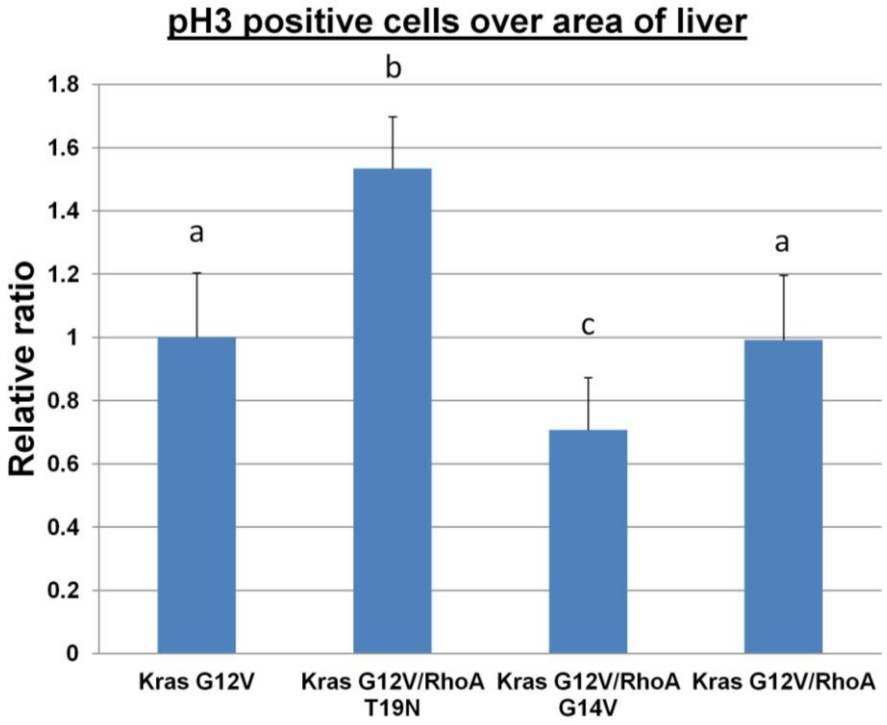

Figure 3.13: Effects of RhoA or its mutant on Kras G12V-induced hepatocyte proliferation. The proliferative index was scored based on phospho-histone3 staining on cryostat sections. It was defined as the number of pH3-positive cells over the area occupied by the liver. The bar chart plotted relative ratio vs genotypes. Kras G12V proliferative index was set as the reference value of one. Co-expression of RhoA T19N with Kras G12V caused a significant increase in the proliferation compared to Kras G12V. The co-expression of RhoA G14V with Kras G12V caused a reduction in the proliferation index compared to the Kras G12V. Co-expression of RhoA with oncogenic Kras did not affect the liver proliferation index significantly. (Different letters represent p-value < 0.05; n=5) Error bars represent standard deviation.

3.2.6 Impacts of RhoA signaling on oncogenic Kras-mediated AKT2 upregulation and activities

The induced expression of Kras G12V was demonstrated, earlier in Section 3.1.6, to upregulate Akt2 expression and activities. I investigated whether the Akt2 expression and activities were affected by the co-expression of RhoA, RhoA G14V or RhoA T19N. Consistent with the result presented in Figure 3.6 B, the induced expression of Kras G12V caused an increase in expression and activity of Akt2 compared to the wild-type siblings as shown in Figures 3.14 A to C. In Figure 3.14A, the dominant-negative RhoA T19N co-expression with Kras G12V caused an increase in the expression or activity of Akt2 as compared to the single transgenic larvae expressing Kras G12V only. In Figure 3.14 B, the co-expression of constitutively active RhoA G14V with Kras G12V caused a decrease in both the expression and activity of Akt2 compared to the transgenic larvae expressing Kras G12V alone. The co-expression of RhoA with oncogenic Kras did not cause changes in the expression or activities of Akt2 (Figure 3.14 C).

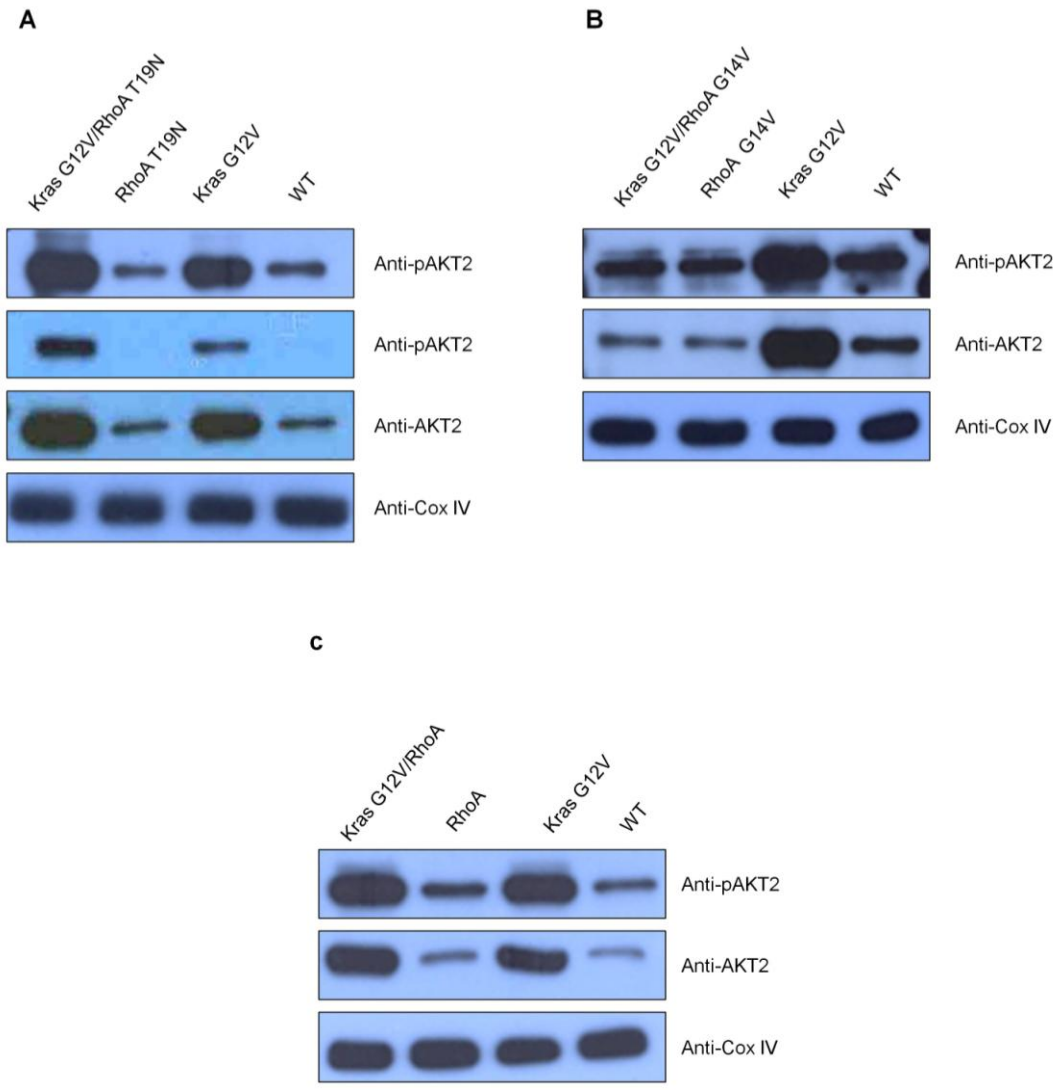

Figure 3.14: Co-expression of RhoA G14V with Kras G12V downregulated oncogenic Kras-induced Akt2 upregulation and activities. Whole larvae lysate of 5 dpf larvae were used. Larvae were induced with doxycycline at 2 dpf, screened and harvested at 5 dpf for Western analysis. At least 50 larvae were pooled for each genotype (lane) per Western analysis. Immunoblots were representative of at least three repeats. (A) Co-expression of RhoA T19N with Kras G12V caused an increase in Akt2 expression and activities. (B) Co-expression of RhoA G14V caused a significant reduction in oncogenic Kras induced AKT2 expression and activities. (C) Co-expression of RhoA did not affect the Kras G12V induced AKT2 expression and activities. Anti-Cox IV was used as loading control.

3.2.7 Oncogene-induced tumorigenesis/Survival study

I carried out the survival study to answer the following: (1) does the expression of Kras G12V cause the development of HCC, (2) does RhoA or its mutants cause HCC development and (3) impacts of RhoA signaling on the Kras G12V-driven liver tumorigenesis, if any. This study was carried out as described in Section 2.3.1.

From the Kaplan-Meier survival curve in Figure 3.15, I observed the following, (1) 100% of the wild-type fish survived the doxycycline induction treatment, (2) 100% of the single RhoA transgenic fish survived the doxycycline induction treatment, (3) induction of Kras G12V expression in the liver caused a significant decrease in survival (p-value < 0.01, log rank test) compared to the wild-type and three single RhoA transgenic fish, (4) co-expression of RhoA or RhoA G14V with Kras G12V did not cause significant changes to the survival rate compared to the single transgenic expressing Kras G12V alone, (5) co-expression of RhoA T19N with Kras G12V caused a significant increase (p-value < 0.01, log rank test) in death rate compared to the single transgenic Kras G12V and the double transgenic line expressing either RhoA or RhoA G14V with Kras G12V. All the eight groups in the no-doxycycline control treatment achieved 100% survival.

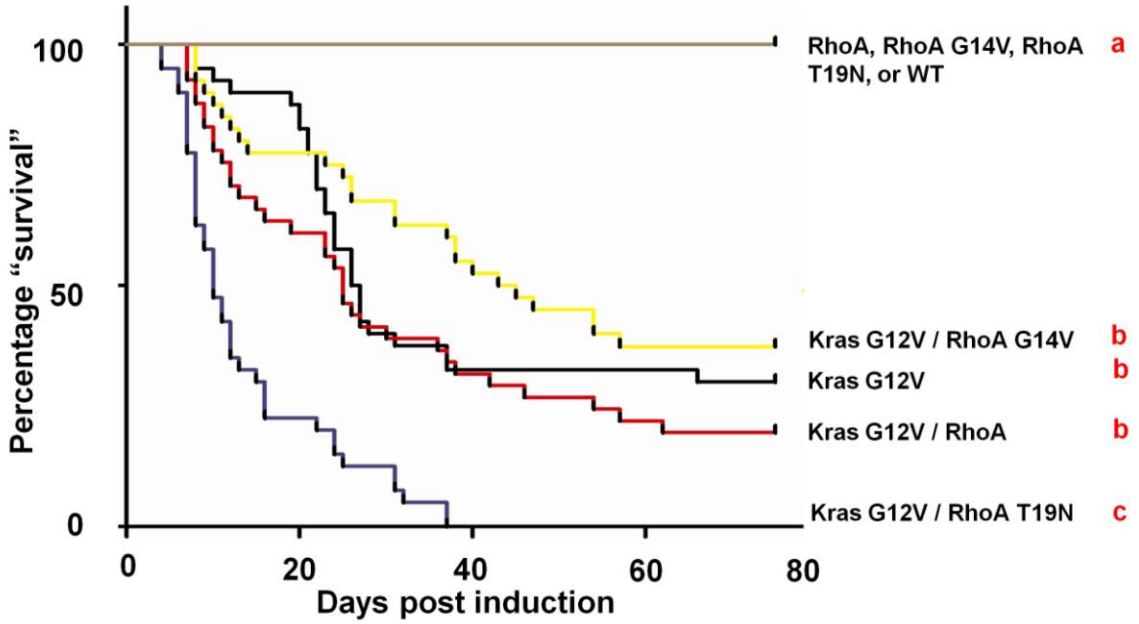

Figure 3.15: Survival curve of the induction treatment. The graph shows days post induction plotted against percentage survival. The dosage of doxycycline used was 10 µg/ml and the treatment was halted at 75 days. No death was observed in the wild-type and three single transgenic of RhoA, RhoA G12, and RhoA T19N after 75 days of treatment. The expression of Kras G12V (black line) in the liver caused a significant decline in survival as compared to the wild-type and the three single transgenic RhoA transgenic fish (grey line). The double transgenics of Kras G12V/RhoA T19N (blue line) accelerated death significantly compared to the single Kras G12V (black line); double transgenic Kras G12V/RhoA (red line) and Kras G12V/ RhoA G14V (yellow line). No significant changes were observed in the Kras G12V vs the double transgenic of Kras G12V/RhoA and Kras G12V/RhoA G14V, respectively. No death event was recorded for the zero µg/ml control group. Different letters in red represent p-value < 0.01.

3.2.8 Over-expression of RhoA or its mutants did not cause liver malignancy

Dysregulation of RhoA, a master regulator of many biological processes, has always been implicated in the development and progression of tumorigenesis (Vega and

Ridley, 2008). Over-expression and over-activation of RhoA, over-expression of GEF and suppression of GAP have been reported in many human cancers (Gomez del Pulgar et al., 2005). One of the objectives in this study was to investigate the transforming properties of RhoA by the over-expression of RhoA or its mutants in the liver. From the survival curves described above, the induction of RhoA, RhoA G14V and RhoA T19N expression did not result in any death event. The single transgenic fish of RhoA, RhoA G14V and RhoA T19N were sampled, sacrificed, fixed and processed for histological analyses. The results in Figure 3.16 demonstrated that the induction of ectopic expression of RhoA or its mutants caused neither liver enlargement nor any liver lesion formation that is characteristic of HCC.

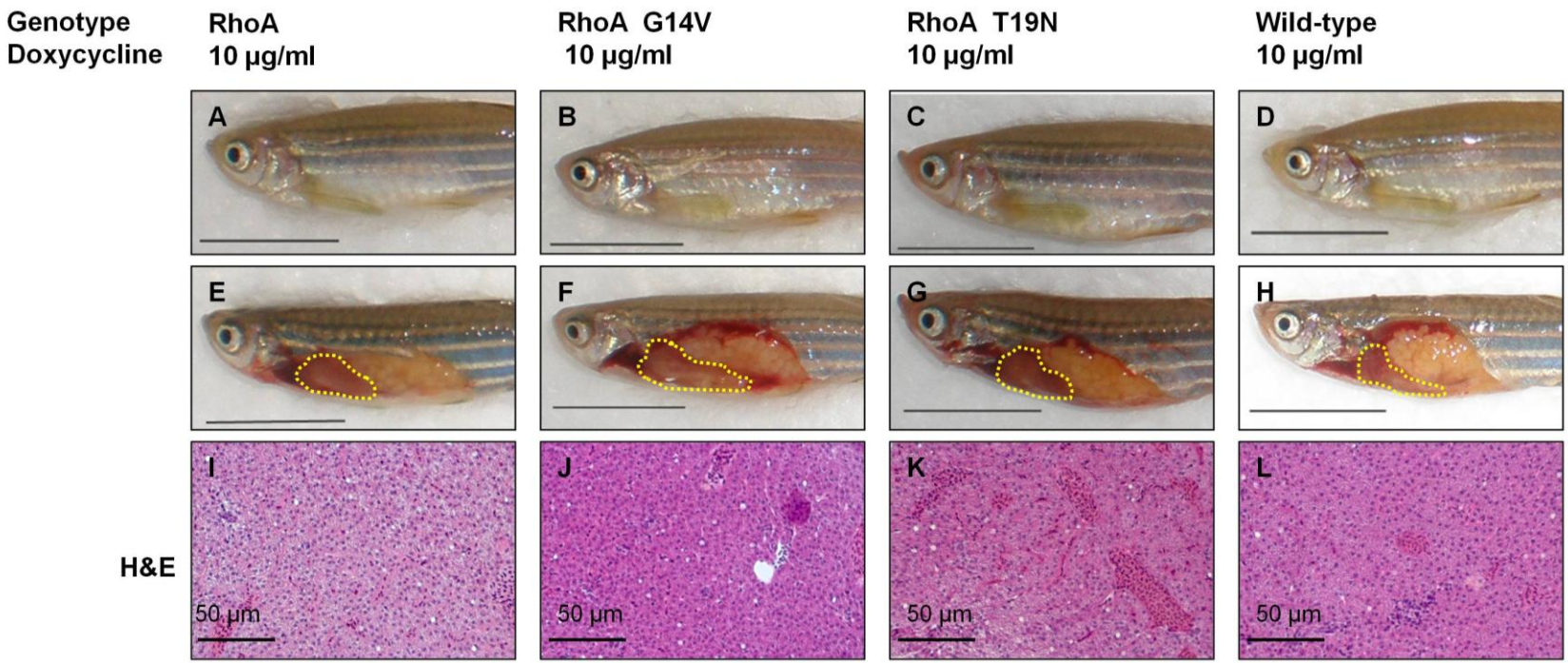

Figure 3.16: Over-expression of RhoA or its mutants did not induce the formation of liver malignancy. The genotypes of the fish and the treatment dosages of doxycycline were labelled with the treatment dosages of doxycycline at the top. (A-D) Gross observations of the various fish. (E-H) The fish were dissected to show the size of the liver. The livers are highlighted with the dotted yellow line. There was no obvious enlargement of the liver in transgenic fish compared to the wild-type control. (I-L) H&E stained paraffin sections. No significant lesion was observed in the single transgenic fish. The scale bar for Figures 3.16 A to H is one cm. The scale bar for Figures 3.16 I to L is 50µm.

3.2.9 Liver-specific expression of Kras G12V caused HCC development

Next, I investigated whether the liver-specific ectopic expression of oncogenic Kras G12V can result in the formation of malignancies in the zebrafish, which resulted in the significant increase in death rate. As shown in Figure 3.17 G, the ectopic expression of eGFP-Kras G12V was able to induce the development of HCC. It was possibly driven by the increased proliferation of the hepatocytes as demonstrated by the increased PCNA staining (Figure 3.17 J) as compared to the controls (Figure 3.17 K and L). The increased proliferation of the hepatocytes also contributed to liver overgrowth as shown in Figure 3.17 D. Wild type fish were used as the control which demonstrated that the exposure to doxycycline did not cause the development of malignancies. Tg(*lfabp*-rtTA2s-M2; *TRE2*-eGFP-Kras G12V) siblings in the no-doxycycline treatment control group were also used as the control to demonstrate that the induced expression of the eGFP-Kras G12V is necessary for the development of HCC.

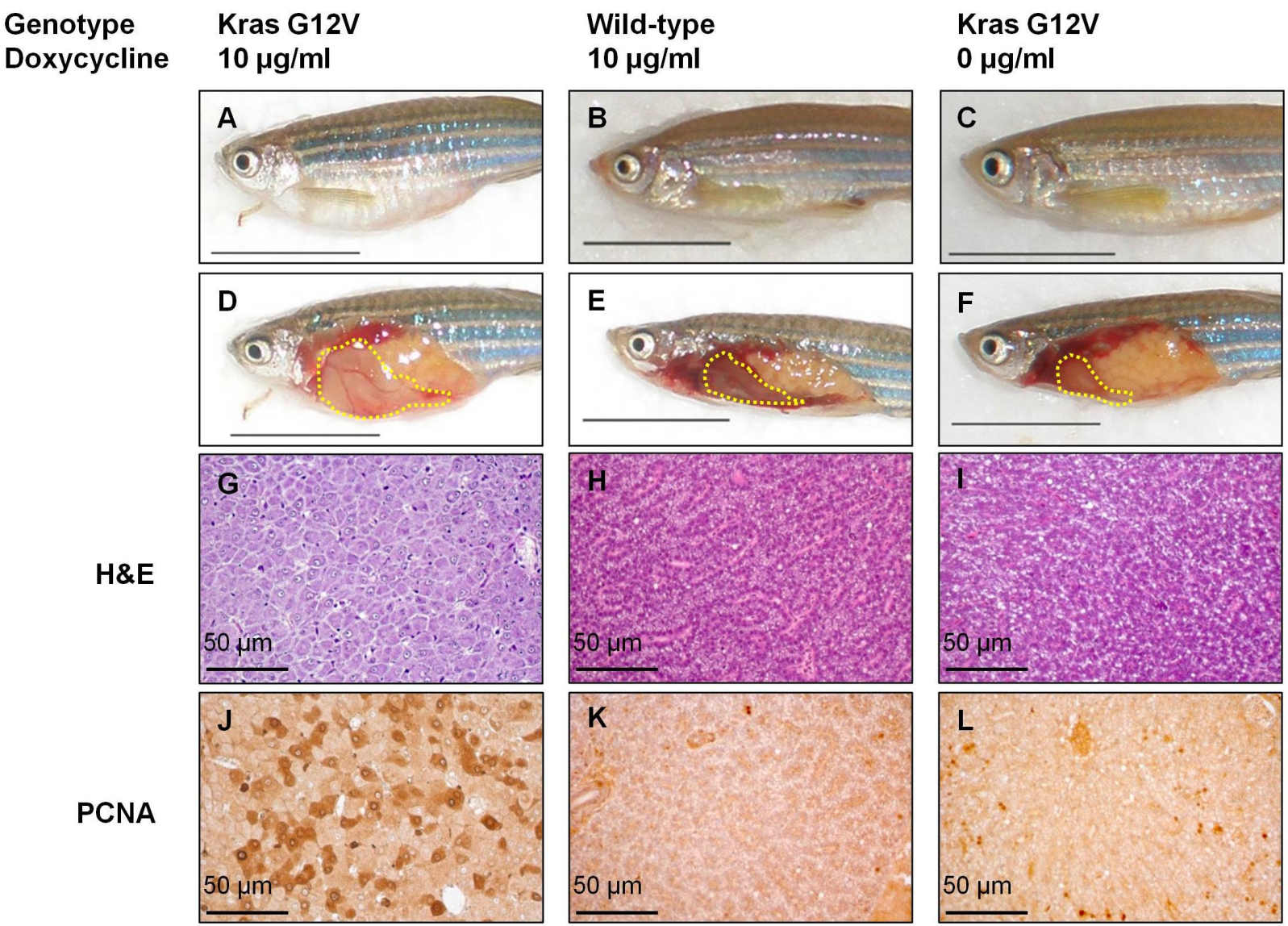
Genotype
Doxycycline
Kras G12V
10 µg/ml
Wild-type
10 µg/ml
Kras G12V
0 µg/ml
A
B
C
D
E
F
G
H
I
J
K
L
H&E
PCNA
50 µm
50 µm
50 µm
50 µm
50 µm
50 µm

Figure 3.17: Formation of hepatocellular carcinomas (HCC) upon the induction of the eGFP-Kras G12V transgene in the Tg(*lfabp*-rtTA2s-M2; *TRE2*-eGFP-Kras G12V) adult fish. The genotypes of the fish and treatment dosages of doxycycline are labelled with the treatment dosages of doxycycline at the top. eGFP-Kras G12V denotes the Tg(*lfabp*-rtTA2s-M2; *TRE2*-eGFP-Kras G12V) line. (A-C) Gross observations of the various fish. (D-F) The fish were dissected to illustrate the size of the liver. The livers are highlighted with the dotted yellow line. There was obvious enlargement of the liver in Figure 3.17 D as compared to Figures 3.17 E & F. (G-I) H&E staining of the paraffin sections. Figure 3.17 G illustrate the development of lesions that are characteristic of HCC, while the Figures 3.17 H & I showed no significant lesions. (J-L) Immunohistochemical (IHC) staining of the paraffin section with proliferation marker, PCNA (brown). Figures 3.8J showed a significant increase in the staining as compared to the Figures 3.17 K & L. The scale bar for Figures 3.17 A to F is one cm. The scale bar for Figures 3.17 G to L is 50μm.

3.2.10 Erk activation was upregulated in the oncogenic Kras-driven HCC

From the observation of the increased proliferation of the hepatocytes in the treated Tg(*lfabp*-rtTA2s-M2; *TRE2*-eGFP-Kras G12V), I investigated whether proliferation-related Erk signaling was upregulated in oncogenic Kras-mediated HCC. Immunofluorescence staining was performed as described in Section 2.9.1. As demonstrated in Figure 3.18, there was an increase in the MEK/Erk activation as indicated by the increase in phospho-Erk1/2 staining in the HCC samples as compared to the wild-type controls. The phospho-Erk1/2 staining was mainly observed in the nucleus of the hepatocytes. It was also observed that the upregulation of the MEK/Erk signaling was stronger at the periphery of the organ as compared to its centre in the HCC sample.

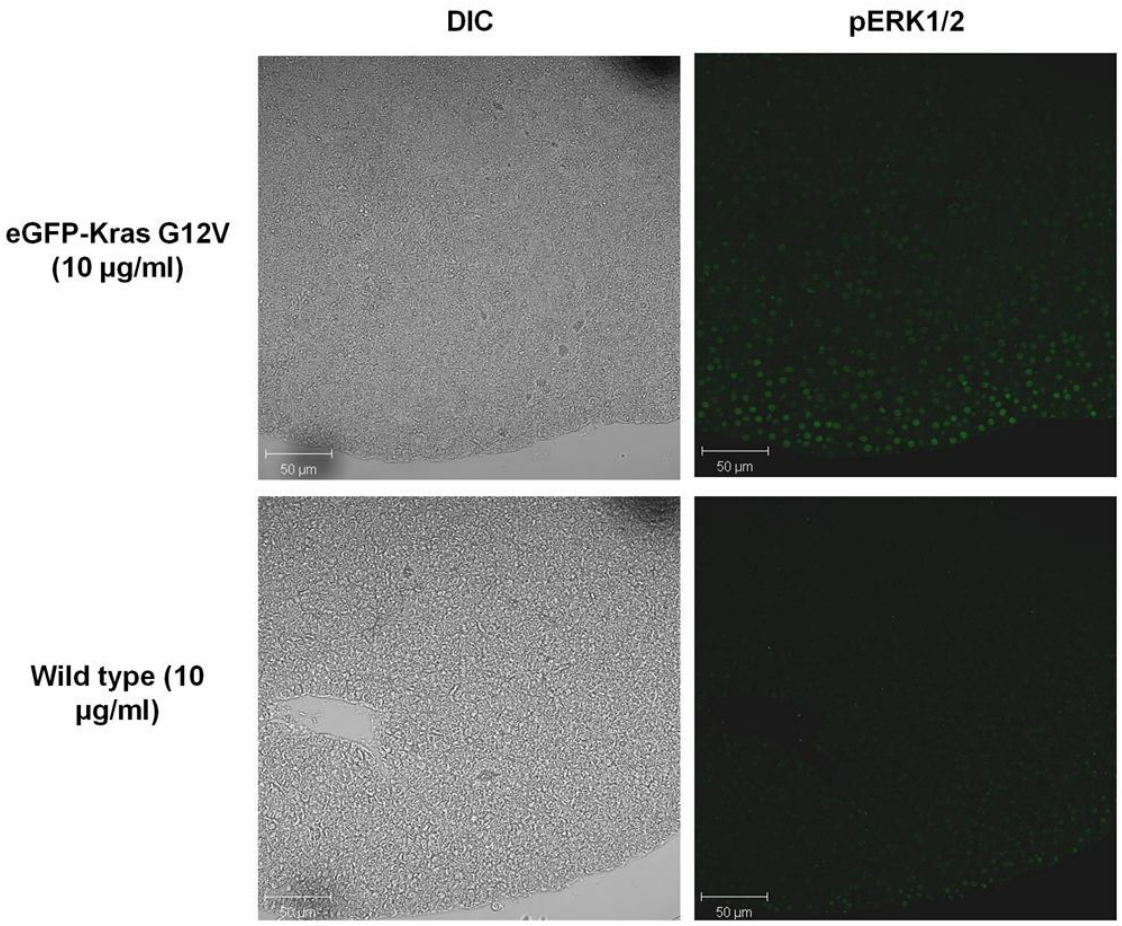

Figure 3.18: Increased Raf/MEK/Erk signaling in the Tg(lfabp-rtTA2s-M2; *TRE2*-eGFP-Kras G12V) as compared to the wild type control. The genotypes of the fish are labelled on the left side and the treatment dosages of doxycycline are in parentheses. eGFP-Kras G12V denotes the Tg(*lfabp*-rtTA2s-M2; *TRE2*-eGFP-Kras G12V) line. The paraffin sections were with anti-pErk1/2 (green). The stainings of the phosho-Erk1/2 were mainly observed in the nucleus. DIC images were used to illustrate the liver. The scale bar is 50 µm.

3.2.11 Alteration in RhoA signaling affected the rate of developing liver malignancies but not the outcome of oncogenic Kras-mediated transformation

I sought to determine whether the death of the fish was due to the development of liver lesions/malignancies or related complications in the double transgenic lines. Fresh dead fish or sick-sacrificed fish were fixed and processed for H&E and IHC staining. Due to practical reasons, sampling was performed and not all fixed specimens were analyzed.

In Figure 3.19, the oncogenic Kras expressing transgenic lines were observed with enlarged liver (Figure 3.19 E to H) and diagnosed with HCC (Figure 3.19 I to L) associated with increased proliferation. Table 10 summarizes the findings (diagnosis) of the four transgenic lines (illustrated in Figure 3.19) that showed significant increase in death rate compared to the wild-type control in the induction treatment group (Section 3.2.7, Figure 3.15). All the fish sampled in these four groups developed various liver lesions, described in Table 5, which could be the underlying cause(s) of death. All of the double transgenic Kras G12V/RhoA T19N sampled fish were diagnosed with HCC. They also have higher proliferation rate (Figure 3.19 N) compared to the other three genotypes analysed (Figure 3.19 M, O and P), as determined by the PCNA staining. 90% of the single Kras G12V transgenic line developed HCC. 70% and 50% of the double transgenic Kras G12V/RhoA G14V and double transgenic Kras G12V/RhoA developed HCC, respectively. Samples that were not diagnosed with HCC were either diagnosed with hepatocellular adenoma or hyperplasia. The three double transgenic lines did not develop more or less severe lesions when compared to the single Kras G12V transgenic line significantly.

Moreover, I demonstrated that without the induced expression of the transgene by doxycycline, the transgenic fish did not develop HCC or significant liver lesion spontaneously (Figure 3.20).

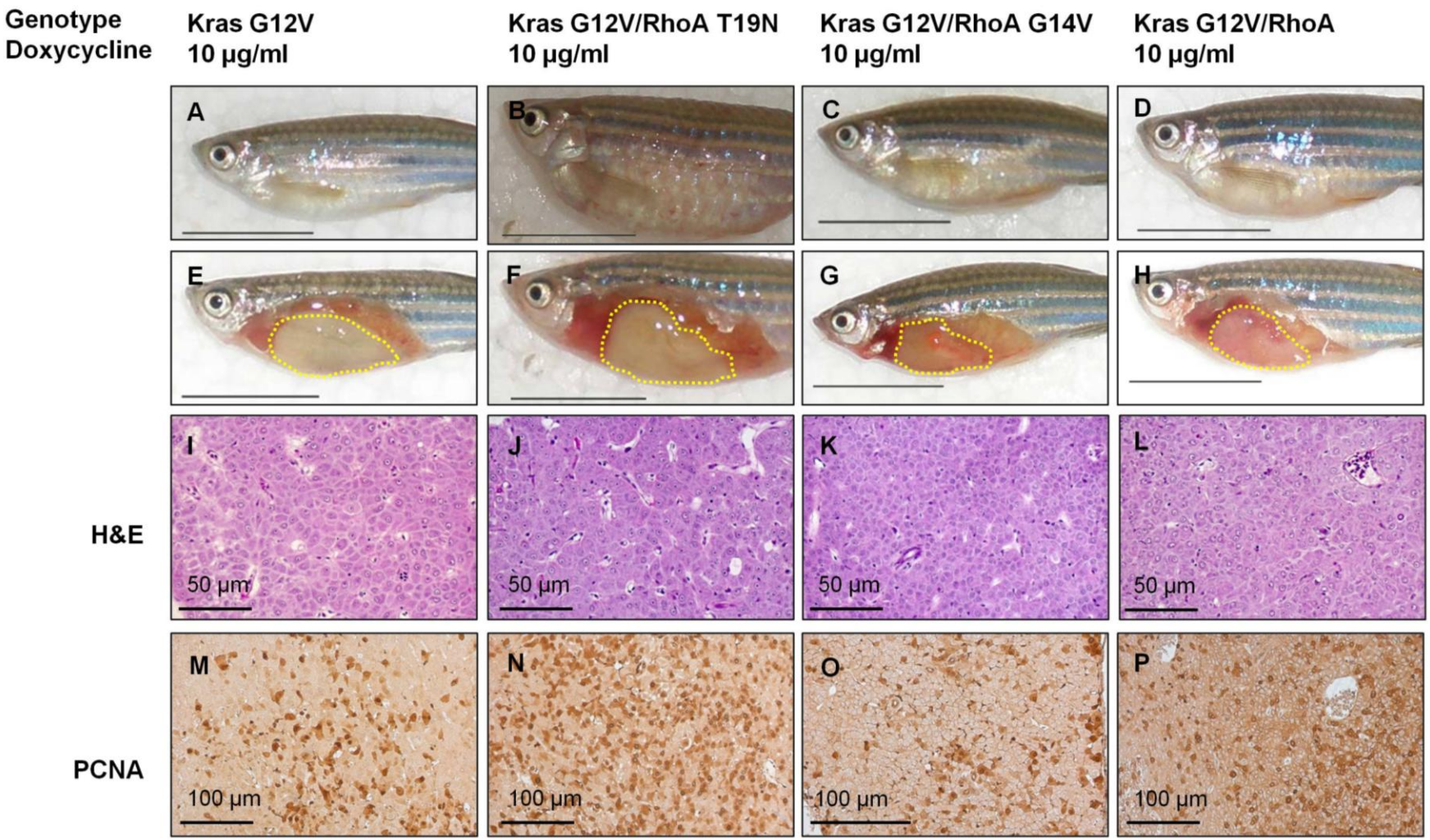
Genotype
Doxycycline
Kras G12V
10 µg/ml
Kras G12V/RhoA T19N
10 µg/ml
Kras G12V/RhoA G14V
10 µg/ml
Kras G12V/RhoA
10 µg/ml
A
B
C
D
E
F
G
H
I
J
K
L
H&E
50 µm
50 µm
50 µm
50 µm
M
N
O
P
PCNA
100 µm
100 µm
100 µm
100 µm

Figure 3.19: Induction of liver tumors in transgenic zebrafish. The genotypes and dosage of doxycycline are labelled on top of the images. The fish with the most severe phenotypes are represented in this Figure. (A-D) Gross observations from the left of the respective fish. (E-H) Fish showing abdominal internal organs, with the liver highlighted in the yellow dotted lines. All fish had enlarged liver compared to the wild-type (Figure 3.17E). (I-L) H&E staining of the Bouin's-fixed paraffin sections which displayed characteristic features of HCC. (M-P) IHC staining performed with PCNA to demonstrate the increased proliferation in the HCC samples. More PCNA positive were observed in the Kras G12V/RhoA T19N (Figure 3.19 N) compared to the other three genotypes. Slides were counterstained with hematoxylin. The scale bars for A to H are one cm, I to L are 50 μm and M to P are 100 μm.

Table 10: Summary of diagnosis on selected transgenic fish treated with 10μg/ml doxycycline

Genotype	**Died fish/ total number of fish at 75 dpt**	**Number of fish sampled**	**Number of sample diagnosed with liver lesion**	**Distribution of lesion**		**Lesion comparison with Kras G12V transgenic (Fisher's exact test)**
				HCC	**HCA/HP**	
Kras G12V	28/40 (70%)	10	10 (100%)	9 (90%)	1 (10%)	Not applicable
Kras G12V/RhoA	33/41 (80.5%)	6	6 (100%)	3 (50%)	3 (50%)	Not significant
Kras G12V/RhoA G14V	26/40 (65%)	10	10 (100%)	7 (70%)	3 (30%)	Not significant
Kras G12V/RhoA T19N	40/40 (100%)	10	10 (100%)	10 (100%)	0	Not significant

Diagnosis based on the most severe phenotypes observed. (Not significant: p-value >0.05)

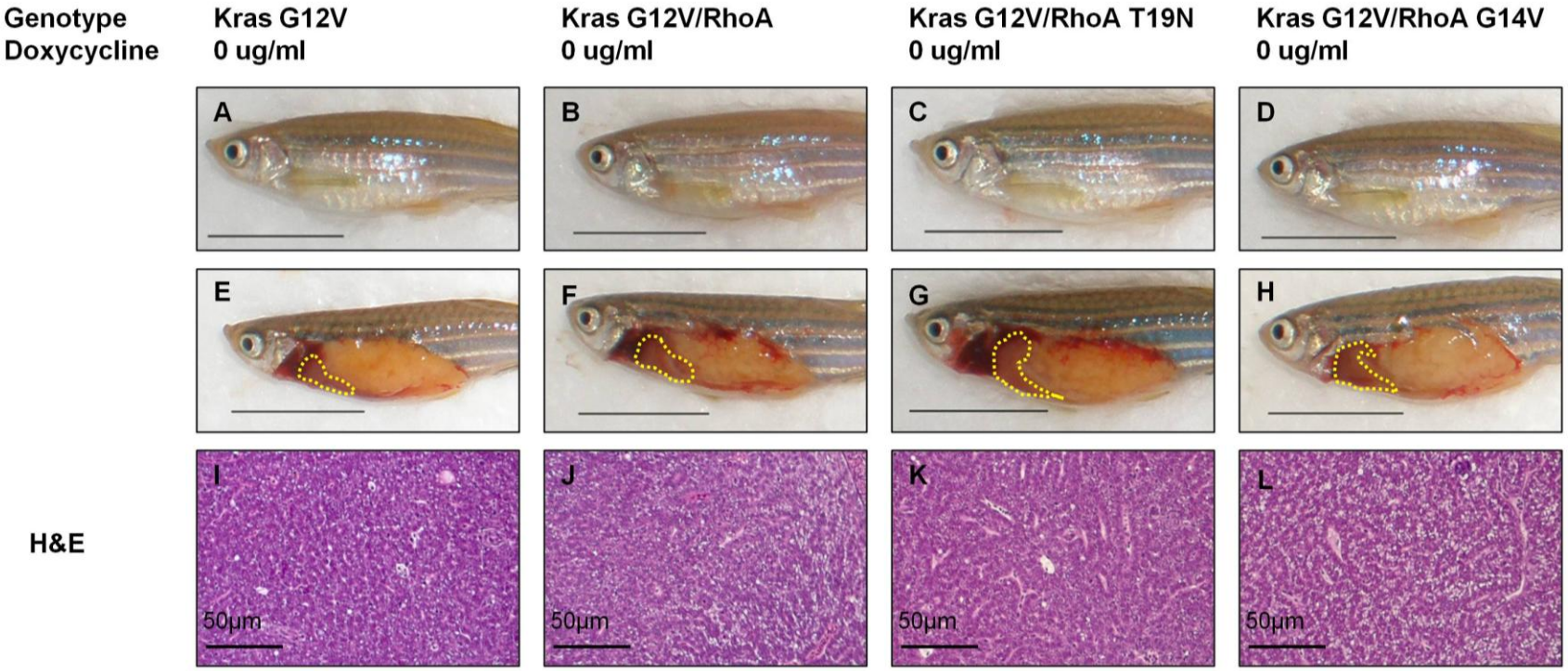

Figure 3.20: Non doxycycline-treated transgenic fish did not develop HCC. The genotypes and dosage of doxycycline are labelled on top of the images. No doxycycline was added in this batch (A-D) Gross observations of the left side of the respective fish. (E-H) Fish showing abdominal internal organs, with the liver highlighted with yellow dotted lines. No significant change in the liver size was observed. (I-L) H&E staining of Bouin's fixed paraffin sections. No significant lesions were observed in the H&E stained slides. The scale bars from A to H and I to L are one cm and 50 μm, respectively.

Chapter 4 Discussion and Conclusion

4.1 Modeling HCC in zebrafish

Since the identification of RAS as an oncogene nearly three decades ago, numerous efforts and researches have been carried out in attempt to elucidate the role of RAS and its associated signaling cascades in human malignancies. Pioneering work on RAS in the *in vitro* cell-based systems defined the transforming ability of RAS and the importance of its downstream effectors signaling cascade in mediating such transformation, in particularly the RAF/MAPK and PI3K/AKT pathways (Cox and Der, 2010; Malumbres and Barbacid, 2003).

In recent years, genetically modified mouse models have been instrumental in unraveling how deregulated RAS signaling leads to tumorigenesis (Karreth and Tuveson, 2009). There is an obvious lack of mouse models in modeling human liver cancers with the RAS oncogene. To date, there is only one study describing the effect of oncogenic HRas in mediating HCC formation only in the presence of a β-catenin mutation (Harada et al., 2004). This could be partly attributed to the lower percentage of human liver cancers being associated to the mutation of the *RAS* gene. Up to 60% of pancreatic cancers were attributed to the mutation of the KRAS while only 5% of human liver cancers were found with the activating mutation in the KRAS (Pylayeva-Gupta et al., 2011). Coupled with the increasing relevance of the zebrafish as an alternative animal model for the modeling of human liver cancers (Lam and Gong, 2006; Lam et al., 2006), we generated the first *in vivo* liver cancer (HCC) model driven by inducible Tet-on ectopic expression of oncogenic Kras G12V in the zebrafish [Tg(*lfabp*-rtTA2s-M2; *TRE2*-eGFP-Kras G12V)].

4.1.1 Characterization of the Tg(*lfabp*-rtTA2s-M2; *TRE2*-eGFP-Kras G12V)

The inducible Tet-on system was employed for this study because it provides two main advantages. Firstly, inducible systems reduce the problem of maintenance of the animal as the constitutive expression of the oncogenic Kras could result in early lethality. It was reported that transgenic mice expressing high levels of oncogenic HRAS in the liver suffered from enlarged liver at birth and died shortly thereafter (Sandgren et al., 1989). Secondly, it allows me, the investigator, to control the spatial and temporal expression of the transgene through the use of tissue-specific promoters. As described in Figure 3.1, the expression of eGFP was observed exclusively in the liver only after induction by doxycycline. Although the leaky expression of the Tet-on system has been reported by in the zebrafish (Huang et al., 2005), neither leaky expression in the absence of doxycycline nor mis-targeted expression in the presence of doxycycline was observed in our transgenic line, Tg(*lfabp*-rtTA2s-M2; *TRE2*-eGFP-Kras G12V). With the eGFP reporter, the transgenic fish could be separated from their wild-type siblings by simple visual inspection with a fluorescence dissecting microscope.

Western blot analysis of the whole larvae lysates (Figure 3.3 A) revealed that the oncogenic Kras G12V was expressed as an eGFP-tagged protein in the transgenic line. Thus, the eGFP expression can be used as an indicator for the expression of the oncogenic Kras G12V. I further demonstrated that the ectopically expressed eGFP-Kras G12V protein was predominantly localized to the plasma membrane (Figure 3.2). KRAS, like the HRAS and NRAS, had to be plasma membrane-bound for effective signaling to take place, in particularly for growth and transformation related processes (Hancock, 2003). Plasma membrane bound oncogenic KRAS-induced transformation, while

mitochondrial membrane-bound oncogenic KRAS cause apoptosis through a BCL-XL dependent manner (Bivona et al., 2006). Non-plasma membrane bound HRAS is less effective in the activation of the RAF, PI3K and JNK than plasma membrane bound HRAS, and resulted in loss of 25 to 90% of its transforming ability in NIH3T3 focus assays (Chiu et al., 2002; Hancock, 2003; Hancock et al., 1990).

The ectopically expressed oncogenic Kras was enriched in an active-RAS RDB pull-down assay (Figure 3.3 B). These indicated that the ectopically expressed Kras G12V can be loaded with GTP, activated and retains the ability to bind and interact with its effector.

Further evidence documenting the activities of the ectopically expressed oncogenic Kras were provided as illustrated in Figure 3.6. The activities of downstream RAF/MAPK and PI3K/Akt2 signaling cascade were measured by probing for the phosphorylated species of Erk1/2 and AKT2, respectively. Both Erk1/2 and Akt2 were activated through activating phosphorylation by their respective upstream kinase. Activities of both the Erk1/2 and Akt2 were increased in eGFP-Kras G12V expressing larvae compared to their wild-type siblings. This faithfully recapitulates the effects of aberrant RAS signaling observed in previous *in vitro* and *in vivo* studies.

MAPK signaling was found to be both sufficient and necessary to induce cellular transformation in mouse cell lines (Leevers et al., 1994; Stokoe et al., 1994; White et al., 1995). Activated Erk1/2 has been known to activate transcription factors, driving expression of growth-related proteins. The importance of MAPK signaling in human

cancers can be inferred through the oncogenic mutations found in receptor tyrosine kinases, RAS and RAF, and its upstream regulators (Karreth and Tuveson, 2009).

Like the MAPK pathway, hyperactivation of AKT had also been frequently found in many human cancers, which was not surprising as AKT regulates many different cellular processes including cell proliferation, cell survival, cell size, angiogenesis and invasion (Altomare and Testa, 2005). Interestingly, in the case of Akt2, the protein level was also elevated in Figure 3.6 B. AKT2 expression level is reported to be up-regulated in many human cancers and the increased expression is correlated to higher pathological grades, such as hepatocellular carcinoma, colon cancers, squamous cell carcinomas, gliomas and etc (Mure et al., 2010; O'Shaughnessy et al., 2007; Roy et al., 2002; Xu et al., 2004).

There are three isoforms of AKT found in human, namely AKT1, AKT2 and AKT3. I only probed for the activity of Akt2 and not all three isoforms in this study because of the following reasons. Firstly, there was a lack of useful antibodies available for research in zebrafish as many commercially available antibodies only works for the higher vertebrate species like mouse, rat and human. Secondly, to date, Akt2 (Q802Y3) is the only one of the three isoforms that was characterized and studied in zebrafish. Our laboratory has demonstrated that the Kras/PI3K/Akt2 signaling is important for the zebrafish hematopoiesis and angiogenesis during early development (Liu et al., 2008). It was also shown that Akt2 is important for modulating glucose availability/homeostasis, by regulating glut1 gene expression, during early zebrafish development (Jensen et al., 2010). Thirdly, until now, the Akt1 and Akt3 proteins remain relatively uncharacterized in zebrafish. Akt1 was only predicted to exist based on predication (source: Uniprot).

Akt3 is found at the protein level and two paralogs were present, namely *akt3a* and *akt3b*. Akt3 is the only isoform in the zebrafish to be found with paralogous gene. Lastly, there was no data available to illustrate the isoform selectivity (of activation) by the RAS/PI3K signaling cascade (Gonzalez and McGraw, 2009).

4.1.2 Kras G12V caused liver overgrowth in developing larvae

By means of bioimaging and image processing, I demonstrated that the ectopic expression of eGFP-Kras G12V was able to cause liver overgrowth during development compared to the control (Figure 3.4). This liver enlargement can be attributed to the increased hepatocyte proliferation as shown by an increased staining by anti phospho-histone 3 antibody, a mitotic marker (Figure 3.5). This increased proliferation was the result of oncogenic Kras signaling. As discussed earlier, cell proliferation related downstream signaling cascades of Kras activation, MAPK/Erk and PI3K/Akt pathways, were found to be upregulated in the eGFP-Kras G12V expressing transgenic larvae. In addition, increased amount of p21 (Cip) (a potent cell cycle progression inhibitor) was found to be inactivated by phosphorylation at Thr145 (Figure 3.7). AKT-mediated inhibitory phosphorylation at threonine 145 has been reported to be a negative regulator of its function and disrupted its inhibitory interaction with proliferating cell nuclear antigen (PCNA) (Li et al., 2002; Rossig et al., 2001; Zhang et al., 2007), thus promoting proliferation and cell survival. Phosphorylation of p21 (Cip) at Thr 145 by AKT caused the protein to residue in the cytosol, thus preventing its inhibitory interaction with the

cyclin-dependent kinase (CDK) or PCNA (Zhou et al., 2001). Taken together, the ectopically expressed oncogenic Kras activated the RAF/MAPK and PI3K/AKT signaling cascade causing an increase in hepatocyte proliferation, resulting in liver overgrowth.

4.1.3 HCC development caused by expression of oncogenic Kras

The liver-specific expression of oncogenic Kras in the adult zebrafish drove the formation of HCC in the transgenic fish (Figure 3.17). The transgenic fish that developed HCC displayed enlarged livers and increased proliferation (PCNA staining in Figures 3.17 J-L) as compared to the controls. Immunofluorescence staining with anti-phospho-Erk1/2 demonstrated that the activity of Erk1/2 was increased in the oncogenic Kras driven HCC (Figure 3.18). The phospho-Erk1/2 was largely localized in the nucleus, which concur with current knowledge that the activated Erk1/2 needs to translocate into the nucleus for activating transcription factor for mitogenic responses (Mebratu and Tesfaigzi, 2009). Impaired nucleus translocation of activated Erk1/2 (cytosolic retention) not only reduced cell proliferation and survival signals, but at the same time also activated Death-associated protein kinase to promote apoptosis (Mebratu and Tesfaigzi, 2009).

4.1.4 Summary of the Tg(*lfabp*-rtTA2s-M2; *TRE2*-eGFP-Kras G12V)

I demonstrated that the transgenic zebrafish, Tg(*lfabp*-rtTA2s-M2; *TRE2*-eGFP-Kras G12V) line, is a robust and unique model for modeling human liver cancer. The induction of oncogenic Kras expression led to the development of HCC. This correlates well with the phenotypic change of liver enlargement during early development. Thus, this model, in the larval stage, is very suitable for high throughput small-chemical compound screening. Potential drug candidates could be screened for their efficacy in inhibiting oncogenic Kras-mediated responses/phenotypes and signaling cascades, for example, in reducing the size of the liver enlargement. The screening performed on the larvae has an added advantage compared to the *in vitro* cell-based screening, as chemical compounds with embryonic developmental toxicity can be picked out earlier. Thus, it can reduce the attrition rate during the long and expensive drug development process.

4.2 Crosstalk of Kras and RhoA in mediating liver development and hepato-tumorigenesis

RAS and Rho GTPases are master regulators of numerous biological events, with many overlapping processes, for example, proliferation and survival. Their crosstalk in regulating tumorigenesis has been intensively investigated over the last two decades, but remains largely limited to cell-based studies. The only exception was a study carried out in the drosophila model by Brumby and co-workers (2011) for the study of crosstalk of

RAS and Rho. Despite the many reported studies, the role of RhoA in RAS-mediated tumorigenesis remains highly contentious. To date, there is no reported study of this crosstalk in a vertebrate *in vivo* model organism and this remains highly underappreciated.

4.2.1 Generation of RhoA transgenic lines

To study the crosstalk of Kras and RhoA in regulating liver tumorigenesis, transgenic lines expressing RhoA, constitutively active RhoA G14V or dominant-negative RhoA T19N were generated, respectively. The maize Ac/Ds transposase system was employed for transgenesis because of the reported high efficacy in zebrafish transgenesis (Emelyanov et al., 2006). One single plasmid vector (Figure 2.2 A) harboring both the transactivator and the response element was used instead of two separate plasmid vectors each with either the transactivator or the response element. This is to ensure a more stable transmission of both the transactivator and the response element to the future progeny of the transgenic fish. I consistently achieved germline transmission rates of 6.67% for all three RhoA transgenic lines. It is much lower than the 60% reported when the Ac/Ds transposase system was applied to the zebrafish (Emelyanov et al., 2006). It could be attributed to the higher DNA load (larger DNA insert) in my system compared to their studies.

I successfully generated three transgenic lines that express mCherry-RhoA, mCherry-RhoA G14V and mCherry RhoA T19N, respectively. As demonstrated in

Figures 3.8 and 3.9, the transgenic larvae expressed mCherry in a liver-restricted manner upon induction by doxycycline. The confocal images of cryostat sections of the respective transgenic larvae further demonstrated that the punctuate distribution of the ectopically expressed mCherry RhoA, mCherry RhoA T19N and mCherry RhoA G14V proteins. Similar punctuate distribution of the RhoA proteins were also observed/reported in many other studies (Covian-Nares et al., 2004; Hehnly et al., 2009; Kulkarni et al., 2002; Woodside et al., 2003). It was further ascertained by Western analysis that the three variants of the RhoA transgene were expressed as mCherry-fusion proteins (Figure 3.10), thus the usefulness of mCherry as a reporter for the transgenes expression.

4.2.2 Impact of RhoA signaling on Kras G12V induced liver overgrowth in developing larvae

I generated double transgenic lines, by crossing the Tg(*lfabp*-rtTA2s-M2; *TRE2*-eGFP-Kras G12V) with the respective RhoA transgenic lines, to study the impact of RhoA signaling on oncogenic Kras transformation of the liver (Figure 3.11).

Like many earlier studies on the function of RhoA, constitutively active and dominant-negative mutants of RhoA were employed in this study in addition to RhoA. RhoA shares high sequence identity with the two closely related proteins, RhoB and RhoC. The motifs and domains for their interaction with regulators and effectors are rather conserved, which could result in their extensive overlapping interactions with RhoGEFs, RhoGAPs and/or target proteins (Wheeler and Ridley, 2004). As such, it raises

the possibility of functional interference by non-specific activation or inhibition of closely related members. For example, the use of dominant-negative RhoA T19N could result in the inhibition of all three Rho members. Likewise, the use of RhoA G14V could result in the activation of all three Rho effectors (Wang and Zheng, 2007). Nevertheless, in view of the lack of feasible knockout technology and mutagenesis methods to silence or activate RhoA in zebrafish, respectively, the use of dominant-negative and constitutively active mutants of RhoA still remain an attractive and viable option to study RhoA function in liver tumorigenesis. The use of the ectopic expression of activating and inhibitory mutants has an added advantage in the zebrafish. RhoA has five paralogous genes present in the zebrafish genome. The ectopic expression of mutants is less likely to be affected by the presence of paralogous genes, unlike the case of morpholinos studies, which may affect the results.

Leveraging on the knowledge that the ectopic expression of oncogenic Kras caused liver overgrowth in the developing larvae and the methods devised to measure liver size quantitatively in the larvae, the impact of the co-expression of RhoA or its mutants with Kras G12V were investigated during early development. Here, I reported that the co-expression of RhoA T19N (together with Kras G12V) augmented Kras-mediated liver overgrowth significantly (Figure 3.12 A) coupled with the increased hepatocyte proliferation (Figure 3.13), while the co-expression of RhoA G14V with Kras G12V caused a significant reduction in the liver overgrowth by oncogenic Kras (Figure 3.12 B) together with a significant decrease in hepatocyte proliferation (Figure 3.13). However, the co-expression of RhoA with Kras G12V did not affect the liver overgrowth

and proliferation rate, significantly (Figures 3.12 C and 3.13) and served as an internal control for the effects of RhoA on oncogenic Kras signaling.

These observed effects of RhoA on proliferation have also been reported by other researchers. The inactivation of RhoA activities by the dominant-negative T19N mutant was associated with a higher rate of proliferation of hematopoietic progenitor cells, via decreased p21 Cip expression and increased cyclin-D1 level (Ghiaur et al., 2006). The proliferation restrain imposed on osteoblasts which were grown on calcium phosphate apatite surface, through increased RhoA activities, can be reversed by the inhibition of RhoA/ROCK signaling (Yang et al., 2011). Moreover, the abilities of RhoA signaling to retard proliferation were also reported in two other studies. Activation of RhoA by vasopressin (vasoactive peptide hormone) downregulated cyclin-D1 expression, which resulted in the inhibition of oncogenic KRAS-driven proliferation (Forti and Armelin, 2007). In the other study, it was demonstrated that the ectopic expression of RhoA G14V inhibited proliferation by slowing down the G1 to S phase cell cycle transition and hindering the completion of cytokinesis. It was also shown by the authors that the active RhoA could impair MAPK pathway activation and the downregulation of cell cycle and cytokinesis-related proteins like the epithelial cell transforming sequence 2 and cyclinB1 (Morin et al., 2009).

Here, I conclude that the inhibition of RhoA signaling could potentiate oncogenic Kras-mediated proliferative effects in the liver; while the activation of RhoA signaling had an inhibitive effect on oncogenic Kras-mediated hepatocyte proliferation.

My findings on this crosstalk of RAS and Rho in regulating liver growth did not concur well with the findings of the majority of studies where RhoA activation favors RAS transformation, as summarized in Table 3. However, it is worthwhile to note that all of these studies, which demonstrated the requirement of active RhoA in RAS transformation, utilized the HRAS isoforms instead of the KRAS isoform investigated in this study. Furthermore, all except one of those studies used the fibroblast cell type instead of epithelial cell type which the hepatocyte belonged to. It was reported that the fibroblast cell type responded differently from the epithelial cell type when activated RAS is introduced. It was even suggested by the authors that the fibroblast is an inappropriate model for RAS-induced transformation (Skinner et al., 2004). Interestingly, two out of the four studies that supported our findings employed the KRAS mutants in their experimental setup, and one of these two studies utilized an epithelial cell type for their investigation (Dreissigacker et al., 2006; Shah et al., 2001). It was suggested that this crosstalk of RAS and Rho depends on the cell-types, the RAS isoforms, and the duration of RAS activation (Chen et al., 2003). All the studies summarized in Table 3 were conducted in an *in vitro* cell based setting except for the Drosophila study. Therefore, it is of paramount importance that I addressed this crosstalk between Kras and RhoA in an *in vivo* animal model.

In this study, I have also identified the Akt2 pathway as a possible target for regulation by RhoA signaling. I have established that the ectopic expression of Kras G12V could lead to an increase in Akt2 expression and activities. The co-expression of RhoA G14V with Kras G12V led to a decrease in both the expression and overall activities of Akt2 compared to the single transgenic of Kras G12V (Figure 3.14 B). This

result coincides with the previous data that the co-expression of RhoA G14V with Kras G12V caused a reduction in hepatocyte proliferation and liver size. Constitutively active RhoA was reported to inhibit AKT activation through the Rho kinase-dependent pathway (Ming et al., 2002). The decreased activities of Akt2 could also be an indirect effect of active RhoA on the expression level of Akt2. RhoA has been known to modulate the expression of various proteins, such as epithelial nitric oxide synthase, p21 and p27 (Chen et al., 2003; Ming et al., 2002; Olson et al., 1998; Vidal et al., 2002). RhoA has also been shown to be able to regulate the activities of various transcription factors, for example, GATA4, AP-1, NF-κB, and serum-response factor (Chang et al., 1998; Charron et al., 2001; Hill et al., 1995; Perona et al., 1997). Therefore it is not surprising that the constitutively active RhoA was able to downregulate Akt2 expression induced by oncogenic Kras in my study.

In addition, I have also reported the increase in expression and activities of the Akt2 in the double transgenic - Kras G12V/RhoA T19N. Increased Akt activation by phosphorylation in response to the inactivation of RhoA signaling had been described in two separate studies. Inhibition of the ROCK, a key effector of RhoA signaling, by Y-27362 treatment led to an increase in Akt activation (Yang et al., 2011). The ectopic expression of RhoA T19N in murine prostate cancer cells caused an increase in the activity of Akt (Ghosh et al., 2002).

4.2.3 Impact of RhoA signaling on Kras G12V-induced liver tumors

To further investigate the effects of RhoA signaling on the Kras-induced HCC formation, induction treatment was carried out in the adult fish. The outcomes of this induction treatment were analyzed by a Kaplan-meier plot (Figure 3.15) and histopathological examination (Figures 3.16, 3.17, 3.19 and 3.20; Table 10).

All the fish in the control group (eight genotypes) without doxycycline treatment survived the 75 days treatment. Selected genotypes (corresponding to the genotypes that had significant death rate compared to the wild-type control in the doxycycline induced group) were processed, H&E stained and analysed. As demonstrated in Figure 3.20, the transgenic fish did not have enlarged liver and did not develop any significant liver lesion. These indicated that the expression of the Kras G12V transgene was necessary for the transformation to occur.

The wild-type control doxycycline-treated group did not differ in the survival rate from the wild-type control in the non-treated control group after 75 days of treatment. The survival rate of the wild-type controls in both treatments was at 100%. Histopathological examination of the liver in the doxycycline-treated wild-type controls revealed no significant liver lesions (Figures 3.16 and 3.17). Therefore, we can deduce that the exposure to doxycycline did not contribute to the development of any liver lesion.

All the single RhoA, RhoA G14V and RhoA T19N transgenic fish survived the doxycycline induction treatment (Figure 3.15). In addition, histopathological examination of the liver revealed that there was no significant lesion presented (Figure 3.16 I to K).

Thus, I deduced that the ectopic expression of RhoA or its mutants (RhoA G14V or RhoA T19N) did not result in the development of liver tumors.

The survival rate of the single Kras G12V transgenic fish was significantly lower (log-rank test: p-value < 0.01) than the wild-type control upon doxycycline induction. The gross observation and histopathological analysis demonstrated the presence of features typical of HCC (Figures 3.17 A, D & G; Figures 3.19A, E & I).

Consistent with the earlier findings in the liver proliferation and overgrowth in the larvae, the adult double transgenic of Kras G12V/RhoA T19N exhibited a significantly higher mortality rate compared to the single transgenic of Kras G12V (Figure 3.15). The proliferation rate was also elevated in the double transgenic Kras G12V/RhoA T19N compared to the single transgenic Kras G12V as indicated by the PCNA staining (Figure 3.19 N and M, respectively). Despite the increased death rate of the double transgenic Kras G12V/RhoA T19N compared to the single Kras G12V transgenic, it did not translate into a more severe phenotype (higher grade HCC or invasive). It could be because the zebrafish could have died before the HCC could develop further. It indicated that the blockage of RhoA signaling by dominant-negative RhoA T19N could potentiate and accelerate the rate of Kras G12V-mediated tumorigenesis.

The co-expression of RhoA with Kras G12V did not exhibit any significant differences in the survival rate compared to the single Kras G12V transgenic fish (Figure 3.15). It is consistent with the results presented earlier in Section 3.2.5, where the co-expression RhoA with Kras G12V did not affect the Kras-mediated liver overgrowth.

Interestingly, the co-expression of RhoA G14V with Kras G12V did not show any significant differences in its survival rate compared to the single Kras G12V. It must be noted that the survival curve of the double transgenic Kras G12V/RhoA G14V has a gentler gradient and a larger median value compared to the single Kras G12V but the differences between the two curves were not statistically significant as determined by the log rank test (p-value > 0.05). A larger sample size or a longer duration of treatment may be required for the differences to be statistically significant. These observations did not concur with previous findings in the larvae presented in Section 3.2.5. This could be attributed to the differences in the inherent molecular machineries present in the different life stages of the zebrafish, specifically the larvae and the adult fish.

It is worthwhile to note that no metastasis or invasion of the carcinoma was observed in all histological specimen analyzed. The transgenic fish might have succumbed to the Kras G12V-driven tumorigenesis before the disease can develop further. This could also be attributed to the inducer, doxycycline, used for this study. Doxycycline had been reported to downregulate several matrix metalloproteinases (MMPs) expression and inhibit their activities (Duivenvoorden et al., 2002; Saikali and Singh, 2003). MMPs play important roles in tumor invasion and metastasis. Many studies have reported that doxycycline can reduce the invasiveness of various cancer cells such as colorectal cancer, prostate cancer, oral squamous cell carcinoma, cervical cancer, breast cancer and ovarian cancer lines, via downregulation of the MMPs and/or inhibiting their activities (Duivenvoorden et al., 2002; Lokeshwar, 1999; Onoda et al., 2004; Roomi et al., 2010; Saikali and Singh, 2003; Shen et al., 2010).

In summary, I presented an *in vivo* zebrafish HCC model driven by oncogenic Kras for modeling human HCC. This oncogenic Kras-driven model faithfully recapitulates the activation of major downstream signaling cascades, for example the RAF/MAPK and PI3K/AKT pathways. Thus it can be used as tool for the identification of novel signaling pathway/effectors of RAS signaling. These could be essential for a more detailed understanding of RAS-driven hepato-oncogenicity. This transgenic line is unique in the sense that there is strong correlation of the liver overgrowth in the larval stage with the development of HCC in the adult stage. This uniqueness could be explored for small chemical compound screening to identify compounds that can suppress RAS signaling. I have also presented the zebrafish as an alternative *in vivo* model for studying small GTPase signaling and interplay. I have presented evidence that the inhibition of RhoA signaling accelerates/augments Kras-mediated liver overgrowth and tumorigenesis. This could caution the development and application of therapeutics directed at inhibiting RhoA signaling in Kras-driven tumors. With these, I presented the first vertebrate *in vivo* study of the crosstalk of Ras and Rho in regulating liver development and liver tumorigenesis. Herein, I propose the following models in Figure 4.1 A and B to illustrate the crosstalk of Ras and Rho during larval liver overgrowth and HCC development, respectively.

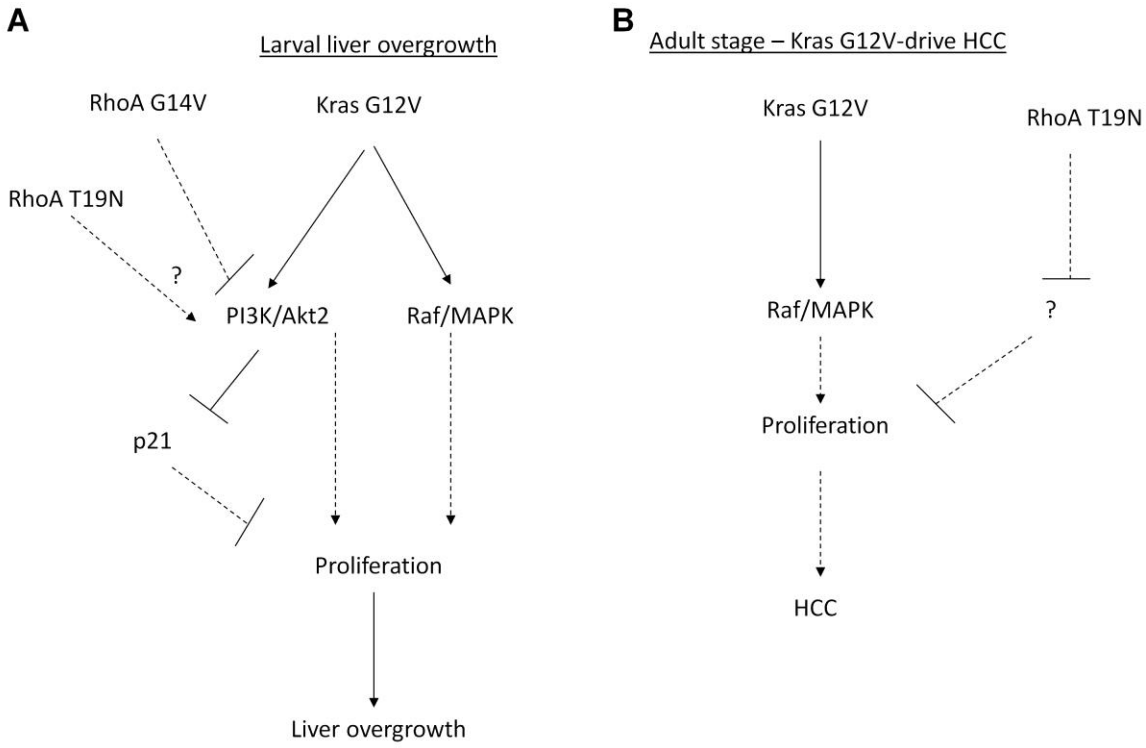

Figure 4.1: Proposed model of crosstalk between Ras and Rho in liver development and HCC formation. (A) Kras G12V caused liver overgrowth through the activation of the Raf/MAPK and PI3K/Akt2 pathways. RhoA G14V caused a reduction in liver enlargement possibly through the reduction in PI3K/Akt2 signaling. RhoA T19N enhanced liver enlargement probably through the increase in PI3K/Akt signaling output. (B) Kras G12V caused the formation of HCC in adult upon induction. It could be partly attributed to the increased Raf/MAPK signaling leading to increased proliferation. The co-expression of RhoA T19N accelerated Kras G12V-mediated HCC formation through the increased in proliferation via an uncharacterized pathway.

4.3 Limitations

One of the main problems encountered in this study was the lack of suitable antibodies that were reactive against the zebrafish proteins of interest. This largely limited the different pathways that I could study with our model.

Transgenesis is an attractive way of studying the effects of certain genes in various biological processes. Along with it comes the problem of managing the side-effect of having the transgene inserted into regions (coding region, promoter, DNA elements) where it could disrupt gene expression and thus functions. The knowledge on the number of insertions and the sites of integration could provide useful information by deciphering if there were chances of any by-product. To reduce the possibility of observations being just by-products, one could use more than one transgenic line for the same transgene of interest to verify the outcomes. However, this was not performed in this study because of the practical reasons like the limitation of resources.

Another drawback of this study is the use of the over-expression system. Ectopic expressions of protein, which exceed physiological levels, are often criticized for being a misrepresentation of the real events. However, it is currently one of the most feasible ways of studying the tumorigenesis effects of an oncogene. The advancement in this field such as the TALENs offered great potential to create targeted mutations at the gene of interest. But much work needs to be done to have a better understanding and control of the TALENs system. Until then, transgenesis by ectopic expression will remain as the choice of method in this type of study.

4.4 Future perspectives

Is there Akt isoform-specificity in oncogenic Kras signaling?

I demonstrated that the ectopic expression of oncogenic Kras in the liver resulted in the upregulation of Akt2 expression and activities, which contributed to increased liver

overgrowth. The introduction of RhoA G14V in the background of oncogenic Kras signaling reduced the Kras G12V-mediated liver overgrowth along with a decrease in both expression and activities of Akt2. Interestingly, one of my colleagues has demonstrated that knock-down of Akt2 using anti-sense technology led to the under-development of the liver during embryogenesis (Liu Lihui, unpublished data). This implies the importance of Akt2 in regulating liver development. We could assess the effect of Akt2 knock-down in our oncogenic Kras transgenic to study its role in liver overgrowth in our transgenic model.

The isoform specificity of the activation by the PI3K downstream of RAS signaling remains poorly defined to date (Gonzalez and McGraw, 2009). The knock-down of the three isoforms can be carried out separately in the Tg(*lfabp*-rtTA2s-M2; *TRE2*-eGFP-Kras G12V) line to assess its individual role in oncogenic Kras signaling. These could provide more insight into the specificity of the different AKT isoform in driving oncogenic Ras signaling.

Crosstalk of Ras and Rho in other tissues

Aberrant KRAS signaling caused by the activating mutation of the KRAS can be found in approximately 25% of all human cancers (Bos, 1989; Karnoub and Weinberg, 2008; Pylayeva-Gupta et al., 2011). Approximately 60% of all pancreatic cancers were found to be attributed to the mutation in the KRAS (Table 1). Other studies have also demonstrated the oncogenicity of Kras in eliciting pancreas tumorigenesis in zebrafish (Park et al., 2008). Thus, it will be interesting to address the crosstalk of RAS and Rho in

the pancreas, or any other organs in Kras-mediated transformation. This will ultimately help us better understand whether cell type specificity exists for this crosstalk.

Interactions with other oncogenes and tumor suppressor genes

My study showed that transgenic zebrafish are useful for studying signaling crosstalk and functional interplay of two different proteins. I also verified that the Kras transgenic line is a good model for studying liver tumorigenesis. Making the oncogenic Kras as the focus, we can study functional interplay of other oncogenes (C-myc gene, WNT, RTK, cyclin D1, cyclin E) and tumor suppressor genes (DLC-1, PTEN, Retinoblastoma protein, p53) with oncogenic Kras in causing and preventing HCC formation.

Knockdown and knockout of RhoA

The suppression of RhoA signaling, through the use of a dominant-negative mutant, augmented the oncogenic Kras effects on liver growth and HCC development as demonstrated in this study. To further ascertain the specificity of this interaction, a knockout or knockdown will be complementary. So far, the knockout technology in the zebrafish is still very much at its infant stage, with the likes of zinc finger nucleases and TALENs showing promising results. However, this technology is not readily available to the community due to its high cost and complexity. Therefore, the best way is to focus on the larvae liver growth. Morpholino anti-sense technology can be employed to

knockdown RhoA in the Kras transgenic to assess the effects of the loss of RhoA signaling on Kras-induced liver overgrowth. However, it must be noted that RhoA is an important regulator of processes during early embryogenesis. Therefore there is a possibility that the knockdown of RhoA could result in early developmental defects that could confound the results.

How is oncogenic Kras-activated RAF/MAPK signaling affected by RhoA signaling during liver overgrowth?

I reported the decreased activities of the PI3K/AKT2, as one of the effectors of Kras, being affected by the activation/inactivation of RhoA (Section 3.2.6, Figure 3.14) in the double transgenic lines (liver), which manifested in the reduction/increase of liver overgrowth caused by Kras G12V. There are many other important effectors of Kras that have not been studied in this study, namely, the RAF/MAPK pathway. Future works can seek to address the perturbation of this pathway activated by oncogenic Kras signaling by active RhoA through Western analysis.

Transgenic zebrafish larvae as an excellent drug screening tool

To have a better understanding of the pathways involved, specific chemical inhibitors of various pathways can be applied to the transgenic fish. For example, in this study, the RAF/MAPK/Erk and PI3K/AKT2 pathways were upregulated in the presence of oncogenic Kras signaling. Chemical inhibitors such as the U0126 and Wortmannin

which inhibit the MEK1/2 and PI3K respectively can be employed. These could provide evidences on the requirements of various pathways in driving Kras-mediated liver overgrowth. This would provide the proof of concept that the model is suitable for small chemical screening.

The oncogenic Kras transgenic line is a unique model where there is high correlation of the phenotypic changes in the larvae with the development of HCC in the adult. Thus, this raises the feasibility of using it as a high throughput drug screening tool. Small chemical compound libraries can be readily applied to the transgenic larvae to assess the effect of the various compounds on oncogenic Kras signaling. In addition, the compound can be screened for their teratogenic effects simultaneously.

IHC approaches to a more accurate diagnosis

In order to achieve a higher level of confidence in the diagnosis of the histological samples, we could perform IHC for certain prognostic and diagnostic markers on the specimens of interest. It was demonstrated in a study that E-cadherin, matrix metalloproteinase-7 and matrix metalloproteinase-9 immuno-histochemistry can be used to differentiate human normal liver, HCC and HCA based on the differences in the staining intensity of the three antibodies (Tretiakova et al., 2009). If applicable to the zebrafish liver cancer model, it can greatly improve the accuracy of the diagnosis of the histological samples by complementing the visual observations.

Chapter 5 References

Ahmed, M. M., Sheldon, D., Fruitwala, M. A., Venkatasubbarao, K., Lee, E. Y., Gupta, S., Wood, C., Mohiuddin, M. and Strodel, W. E. (2008). Downregulation of PAR-4, a pro-apoptotic gene, in pancreatic tumors harboring K-ras mutation. *Int J Cancer* **122**, 63-70.

Altomare, D. A. and Testa, J. R. (2005). Perturbations of the AKT signaling pathway in human cancer. *Oncogene* **24**, 7455-64.

Amano, M., Ito, M., Kimura, K., Fukata, Y., Chihara, K., Nakano, T., Matsuura, Y. and Kaibuchi, K. (1996). Phosphorylation and activation of myosin by Rho-associated kinase (Rho-kinase). *J Biol Chem* **271**, 20246-9.

Amatruda, J. F., Shepard, J. L., Stern, H. M. and Zon, L. I. (2002). Zebrafish as a cancer model system. *Cancer Cell* **1**, 229-31.

Aspenstrom, P., Ruusala, A. and Pacholsky, D. (2007). Taking Rho GTPases to the next level: the cellular functions of atypical Rho GTPases. *Exp Cell Res* **313**, 3673-9.

Augsten, M., Pusch, R., Biskup, C., Rennert, K., Wittig, U., Beyer, K., Blume, A., Wetzker, R., Friedrich, K. and Rubio, I. (2006). Live-cell imaging of endogenous Ras-GTP illustrates predominant Ras activation at the plasma membrane. *EMBO Rep* **7**, 46-51.

Beckwith, L. G., Moore, J. L., Tsao-Wu, G. S., Harshbarger, J. C. and Cheng, K. C. (2000). Ethylnitrosourea induces neoplasia in zebrafish (Danio rerio). *Lab Invest* **80**, 379-85.

Beis, D. and Stainier, D. Y. (2006). In vivo cell biology: following the zebrafish trend. *Trends Cell Biol* **16**, 105-12.

Besson, A., Gurian-West, M., Schmidt, A., Hall, A. and Roberts, J. M. (2004). p27Kip1 modulates cell migration through the regulation of RhoA activation. *Genes Dev* **18**, 862-76.

Bishop, A. L. and Hall, A. (2000). Rho GTPases and their effector proteins. *Biochem J* **348 Pt 2**, 241-55.

Bivona, T. G., Quatela, S. E., Bodemann, B. O., Ahearn, I. M., Soskis, M. J., Mor, A., Miura, J., Wiener, H. H., Wright, L., Saba, S. G. et al. (2006). PKC regulates a farnesyl-electrostatic switch on K-Ras that promotes its association with Bcl-XL on mitochondria and induces apoptosis. *Mol Cell* **21**, 481-93.

Blechinger, S. R., Evans, T. G., Tang, P. T., Kuwada, J. Y., Warren, J. T., Jr. and Krone, P. H. (2002). The heat-inducible zebrafish hsp70 gene is expressed during normal lens development under non-stress conditions. *Mech Dev* **112**, 213-5.

Boch, J. and Bonas, U. (2010). Xanthomonas AvrBs3 family-type III effectors: discovery and function. *Annu Rev Phytopathol* **48**, 419-36.

Bos, J. L. (1989). ras oncogenes in human cancer: a review. *Cancer Res* **49**, 4682-9.

Bourne, H. R., Sanders, D. A. and McCormick, F. (1991). The GTPase superfamily: conserved structure and molecular mechanism. *Nature* **349**, 117-27.

Brumby, A. M., Goulding, K. R., Schlosser, T., Loi, S., Galea, R., Khoo, P., Bolden, J. E., Aigaki, T., Humbert, P. O. and Richardson, H. E. (2011). Identification of novel Ras-cooperating oncogenes in Drosophila melanogaster: a RhoGEF/Rho-family/JNK pathway is a central driver of tumorigenesis. *Genetics* **188**, 105-25.

Bryan, B., Cai, Y., Wrighton, K., Wu, G., Feng, X. H. and Liu, M. (2005). Ubiquitination of RhoA by Smurf1 promotes neurite outgrowth. *FEBS Lett* **579**, 1015-9.

Chang, J. H., Pratt, J. C., Sawasdikosol, S., Kapeller, R. and Burakoff, S. J. (1998). The small GTP-binding protein Rho potentiates AP-1 transcription in T cells. *Mol Cell Biol* **18**, 4986-93.

Charron, F., Tsimiklis, G., Arcand, M., Robitaille, L., Liang, Q., Molkentin, J. D., Meloche, S. and Nemer, M. (2001). Tissue-specific GATA factors are transcriptional effectors of the small GTPase RhoA. *Genes Dev* **15**, 2702-19.

Chen, J. C., Zhuang, S., Nguyen, T. H., Boss, G. R. and Pilz, R. B. (2003). Oncogenic Ras leads to Rho activation by activating the mitogen-activated protein kinase pathway and decreasing Rho-GTPase-activating protein activity. *J Biol Chem* **278**, 2807-18.

Chien, Y. and White, M. A. (2003). RAL GTPases are linchpin modulators of human tumour-cell proliferation and survival. *EMBO Rep* **4**, 800-6.

Chiu, V. K., Bivona, T., Hach, A., Sajous, J. B., Silletti, J., Wiener, H., Johnson, R. L., 2nd, Cox, A. D. and Philips, M. R. (2002). Ras signalling on the endoplasmic reticulum and the Golgi. *Nat Cell Biol* **4**, 343-50.

Cleverley, S. C., Costello, P. S., Henning, S. W. and Cantrell, D. A. (2000). Loss of Rho function in the thymus is accompanied by the development of thymic lymphoma. *Oncogene* **19**, 13-20.

Colicelli, J. (2004). Human RAS superfamily proteins and related GTPases. *Sci STKE* **2004**, RE13.

Covian-Nares, F., Martinez-Cadena, G., Lopez-Godinez, J., Voronina, E., Wessel, G. M. and Garcia-Soto, J. (2004). A Rho-signaling pathway mediates cortical granule translocation in the sea urchin oocyte. *Mech Dev* **121**, 225-35.

Cox, A. D. and Der, C. J. (2002). Ras family signaling: therapeutic targeting. *Cancer Biol Ther* **1**, 599-606.

Cox, A. D. and Der, C. J. (2010). Ras history: The saga continues. *Small Gtpases* **1**, 2-27.

Datta, S. R., Dudek, H., Tao, X., Masters, S., Fu, H., Gotoh, Y. and Greenberg, M. E. (1997). Akt phosphorylation of BAD couples survival signals to the cell-intrinsic death machinery. *Cell* **91**, 231-41.

Davidson, A. E., Balciunas, D., Mohn, D., Shaffer, J., Hermanson, S., Sivasubbu, S., Cliff, M. P., Hackett, P. B. and Ekker, S. C. (2003). Efficient gene delivery and gene expression in zebrafish using the Sleeping Beauty transposon. *Dev Biol* **263**, 191-202.

Deiters, A. and Yoder, J. A. (2006). Conditional transgene and gene targeting methodologies in zebrafish. *Zebrafish* **3**, 415-29.

Diehl, J. A., Cheng, M., Roussel, M. F. and Sherr, C. J. (1998). Glycogen synthase kinase-3beta regulates cyclin D1 proteolysis and subcellular localization. *Genes Dev* **12**, 3499-511.

Dovey, M., White, R. M. and Zon, L. I. (2009). Oncogenic NRAS cooperates with p53 loss to generate melanoma in zebrafish. *Zebrafish* **6**, 397-404.

Doyon, Y., McCammon, J. M., Miller, J. C., Faraji, F., Ngo, C., Katibah, G. E., Amora, R., Hocking, T. D., Zhang, L., Rebar, E. J. et al. (2008). Heritable targeted gene disruption in zebrafish using designed zinc-finger nucleases. *Nat Biotechnol* **26**, 702-8.

Dreissigacker, U., Mueller, M. S., Unger, M., Siegert, P., Genze, F., Gierschik, P. and Giehl, K. (2006). Oncogenic K-Ras down-regulates Rac1 and RhoA activity and enhances migration and invasion of pancreatic carcinoma cells through activation of p38. *Cell Signal* **18**, 1156-68.

Duivenvoorden, W. C., Popovic, S. V., Lhotak, S., Seidlitz, E., Hirte, H. W., Tozer, R. G. and Singh, G. (2002). Doxycycline decreases tumor burden in a bone metastasis model of human breast cancer. *Cancer Res* **62**, 1588-91.

Emelyanov, A., Gao, Y., Naqvi, N. I. and Parinov, S. (2006). Trans-kingdom transposition of the maize dissociation element. *Genetics* **174**, 1095-104.

Fang, X., Yu, S., Eder, A., Mao, M., Bast, R. C., Jr., Boyd, D. and Mills, G. B. (1999). Regulation of BAD phosphorylation at serine 112 by the Ras-mitogen-activated protein kinase pathway. *Oncogene* **18**, 6635-40.

Farazi, P. A. and DePinho, R. A. (2006). Hepatocellular carcinoma pathogenesis: from genes to environment. *Nat Rev Cancer* **6**, 674-87.

Feitsma, H. and Cuppen, E. (2008). Zebrafish as a cancer model. *Mol Cancer Res* **6**, 685-94.

Feng, H., Langenau, D. M., Madge, J. A., Quinkertz, A., Gutierrez, A., Neuberg, D. S., Kanki, J. P. and Look, A. T. (2007). Heat-shock induction of T-cell lymphoma/leukaemia in conditional Cre/lox-regulated transgenic zebrafish. *Br J Haematol* **138**, 169-75.

Feramisco, J. R., Gross, M., Kamata, T., Rosenberg, M. and Sweet, R. W. (1984). Microinjection of the oncogene form of the human H-ras (T-24) protein results in rapid proliferation of quiescent cells. *Cell* **38**, 109-17.

Fernandez-Borja, M., Janssen, L., Verwoerd, D., Hordijk, P. and Neefjes, J. (2005). RhoB regulates endosome transport by promoting actin assembly on endosomal membranes through Dia1. *J Cell Sci* **118**, 2661-70.

Filmus, J., Robles, A. I., Shi, W., Wong, M. J., Colombo, L. L. and Conti, C. J. (1994). Induction of cyclin D1 overexpression by activated ras. *Oncogene* **9**, 3627-33.

Fleming, Y. M., Ferguson, G. J., Spender, L. C., Larsson, J., Karlsson, S., Ozanne, B. W., Grosse, R. and Inman, G. J. (2009). TGF-beta-mediated activation of RhoA signalling is required for efficient (V12)HaRas and (V600E)BRAF transformation. *Oncogene* **28**, 983-93.

Forti, F. L. and Armelin, H. A. (2007). Vasopressin triggers senescence in K-ras transformed cells via RhoA-dependent downregulation of cyclin D1. *Endocr Relat Cancer* **14**, 1117-25.

Frau, M., Biasi, F., Feo, F. and Pascale, R. M. (2010). Prognostic markers and putative therapeutic targets for hepatocellular carcinoma. *Mol Aspects Med* **31**, 179-93.

Fukui, K., Tamura, S., Wada, A., Kamada, Y., Sawai, Y., Imanaka, K., Kudara, T., Shimomura, I. and Hayashi, N. (2006). Expression and prognostic role of RhoA GTPases in hepatocellular carcinoma. *J Cancer Res Clin Oncol* **132**, 627-33.

Ghiaur, G., Lee, A., Bailey, J., Cancelas, J. A., Zheng, Y. and Williams, D. A. (2006). Inhibition of RhoA GTPase activity enhances hematopoietic stem and progenitor cell proliferation and engraftment. *Blood* **108**, 2087-94.

Ghosh, P. M., Bedolla, R., Mikhailova, M. and Kreisberg, J. I. (2002). RhoA-dependent murine prostate cancer cell proliferation and apoptosis: role of protein kinase Czeta. *Cancer Res* **62**, 2630-6.

Goessling, W., North, T. E. and Zon, L. I. (2007). New waves of discovery: modeling cancer in zebrafish. *J Clin Oncol* **25**, 2473-9.

Gomaa, A. I., Khan, S. A., Toledano, M. B., Waked, I. and Taylor-Robinson, S. D. (2008). Hepatocellular carcinoma: epidemiology, risk factors and pathogenesis. *World J Gastroenterol* **14**, 4300-8.

Gomez del Pulgar, T., Benitah, S. A., Valeron, P. F., Espina, C. and Lacal, J. C. (2005). Rho GTPase expression in tumourigenesis: evidence for a significant link. *Bioessays* **27**, 602-13.

Gonzalez, E. and McGraw, T. E. (2009). The Akt kinases: isoform specificity in metabolism and cancer. *Cell Cycle* **8**, 2502-8.

Gossen, M. and Bujard, H. (1992). Tight control of gene expression in mammalian cells by tetracycline-responsive promoters. *Proc Natl Acad Sci U S A* **89**, 5547-51.

Gossen, M., Freundlieb, S., Bender, G., Muller, G., Hillen, W. and Bujard, H. (1995). Transcriptional activation by tetracyclines in mammalian cells. *Science* **268**, 1766-9.

Gou, L., Wang, W., Tong, A., Yao, Y., Zhou, Y., Yi, C. and Yang, J. (2011). Proteomic identification of RhoA as a potential biomarker for proliferation and metastasis in hepatocellular carcinoma. *J Mol Med (Berl)* **89**, 817-27.

Grewal, T., Koese, M., Tebar, F. and Enrich, C. (2011). Differential Regulation of RasGAPs in Cancer. *Genes Cancer* **2**, 288-97.

Gupta, S., Plattner, R., Der, C. J. and Stanbridge, E. J. (2000). Dissection of Ras-dependent signaling pathways controlling aggressive tumor growth of human fibrosarcoma cells: evidence for a potential novel pathway. *Mol Cell Biol* **20**, 9294-306.

Gutierrez, A., Snyder, E. L., Marino-Enriquez, A., Zhang, Y. X., Sioletic, S., Kozakewich, E., Grebliunaite, R., Ou, W. B., Sicinska, E., Raut, C. P. et al. (2011). Aberrant AKT activation drives well-differentiated liposarcoma. *Proc Natl Acad Sci U S A* **108**, 16386-91.

Hall, A. (1998). Rho GTPases and the actin cytoskeleton. *Science* **279**, 509-14.

Halloran, M. C., Sato-Maeda, M., Warren, J. T., Su, F., Lele, Z., Krone, P. H., Kuwada, J. Y. and Shoji, W. (2000). Laser-induced gene expression in specific cells of transgenic zebrafish. *Development* **127**, 1953-60.

Hamad, N. M., Elconin, J. H., Karnoub, A. E., Bai, W., Rich, J. N., Abraham, R. T., Der, C. J. and Counter, C. M. (2002). Distinct requirements for Ras oncogenesis in human versus mouse cells. *Genes Dev* **16**, 2045-57.

Hanahan, D. and Weinberg, R. A. (2011). Hallmarks of cancer: the next generation. *Cell* **144**, 646-74.

Hancock, J. F. (2003). Ras proteins: different signals from different locations. *Nat Rev Mol Cell Biol* **4**, 373-84.

Hancock, J. F., Paterson, H. and Marshall, C. J. (1990). A polybasic domain or palmitoylation is required in addition to the CAAX motif to localize p21ras to the plasma membrane. *Cell* **63**, 133-9.

Harada, N., Oshima, H., Katoh, M., Tamai, Y., Oshima, M. and Taketo, M. M. (2004). Hepatocarcinogenesis in mice with beta-catenin and Ha-ras gene mutations. *Cancer Res* **64**, 48-54.

Heasman, S. J. and Ridley, A. J. (2008). Mammalian Rho GTPases: new insights into their functions from in vivo studies. *Nat Rev Mol Cell Biol* **9**, 690-701.

Hehnly, H., Longhini, K. M., Chen, J. L. and Stamnes, M. (2009). Retrograde Shiga toxin trafficking is regulated by ARHGAP21 and Cdc42. *Mol Biol Cell* **20**, 4303-12.

Heron-Milhavet, L., Khouya, N., Fernandez, A. and Lamb, N. J. (2011). Akt1 and Akt2: differentiating the aktion. *Histol Histopathol* **26**, 651-62.

Hill, C. S., Wynne, J. and Treisman, R. (1995). The Rho family GTPases RhoA, Rac1, and CDC42Hs regulate transcriptional activation by SRF. *Cell* **81**, 1159-70.

Horiguchi, K., Shirakihara, T., Nakano, A., Imamura, T., Miyazono, K. and Saitoh, M. (2009). Role of Ras signaling in the induction of snail by transforming growth factor-beta. *J Biol Chem* **284**, 245-53.

Hoshida, Y., Toffanin, S., Lachenmayer, A., Villanueva, A., Minguez, B. and Llovet, J. M. (2010). Molecular classification and novel targets in hepatocellular carcinoma: recent advancements. *Semin Liver Dis* **30**, 35-51.

Huang, C. J., Jou, T. S., Ho, Y. L., Lee, W. H., Jeng, Y. T., Hsieh, F. J. and Tsai, H. J. (2005). Conditional expression of a myocardium-specific transgene in zebrafish transgenic lines. *Dev Dyn* **233**, 1294-303.

Huang, P., Xiao, A., Zhou, M., Zhu, Z., Lin, S. and Zhang, B. (2011). Heritable gene targeting in zebrafish using customized TALENs. *Nat Biotechnol* **29**, 699-700.

Ishizaki, T., Maekawa, M., Fujisawa, K., Okawa, K., Iwamatsu, A., Fujita, A., Watanabe, N., Saito, Y., Kakizuka, A., Morii, N. et al. (1996). The small GTP-binding protein Rho binds to and activates a 160 kDa Ser/Thr protein kinase homologous to myotonic dystrophy kinase. *EMBO J* **15**, 1885-93.

Itoh, K., Yoshioka, K., Akedo, H., Uehata, M., Ishizaki, T. and Narumiya, S. (1999). An essential part for Rho-associated kinase in the transcellular invasion of tumor cells. *Nat Med* **5**, 221-5.

Izawa, I., Amano, M., Chihara, K., Yamamoto, T. and Kaibuchi, K. (1998). Possible involvement of the inactivation of the Rho-Rho-kinase pathway in oncogenic Ras-induced transformation. *Oncogene* **17**, 2863-71.

Jaffe, A. B. and Hall, A. (2002). Rho GTPases in transformation and metastasis. *Adv Cancer Res* **84**, 57-80.

Janssen, K. P., Abal, M., El Marjou, F., Louvard, D. and Robine, S. (2005). Mouse models of K-ras-initiated carcinogenesis. *Biochim Biophys Acta* **1756**, 145-54.

Jensen, P. J., Gunter, L. B. and Carayannopoulos, M. O. (2010). Akt2 modulates glucose availability and downstream apoptotic pathways during development. *J Biol Chem* **285**, 17673-80.

Kaibuchi, K., Kuroda, S. and Amano, M. (1999). Regulation of the cytoskeleton and cell adhesion by the Rho family GTPases in mammalian cells. *Annu Rev Biochem* **68**, 459-86.

Karaguni, I. M., Herter, P., Debruyne, P., Chtarbova, S., Kasprzynski, A., Herbrand, U., Ahmadian, M. R., Glusenkamp, K. H., Winde, G., Mareel, M. et al. (2002). The new sulindac derivative IND 12 reverses Ras-induced cell transformation. *Cancer Res* **62**, 1718-23.

Karlsson, R., Pedersen, E. D., Wang, Z. and Brakebusch, C. (2009). Rho GTPase function in tumorigenesis. *Biochim Biophys Acta* **1796**, 91-8.

Karnoub, A. E. and Weinberg, R. A. (2008). Ras oncogenes: split personalities. *Nat Rev Mol Cell Biol* **9**, 517-31.

Karreth, F. A. and Tuveson, D. A. (2009). Modelling oncogenic Ras/Raf signalling in the mouse. *Curr Opin Genet Dev* **19**, 4-11.

Khosravi-Far, R., Solski, P. A., Clark, G. J., Kinch, M. S. and Der, C. J. (1995). Activation of Rac1, RhoA, and mitogen-activated protein kinases is required for Ras transformation. *Mol Cell Biol* **15**, 6443-53.

Khosravi-Far, R., White, M. A., Westwick, J. K., Solski, P. A., Chrzanowska-Wodnicka, M., Van Aelst, L., Wigler, M. H. and Der, C. J. (1996). Oncogenic Ras activation of Raf/mitogen-activated protein kinase-independent pathways is sufficient to cause tumorigenic transformation. *Mol Cell Biol* **16**, 3923-33.

Kikuta, H. and Kawakami, K. (2009). Transient and stable transgenesis using tol2 transposon vectors. *Methods Mol Biol* **546**, 69-84.

Kimura, K., Ito, M., Amano, M., Chihara, K., Fukata, Y., Nakafuku, M., Yamamori, B., Feng, J., Nakano, T., Okawa, K. et al. (1996). Regulation of myosin phosphatase by Rho and Rho-associated kinase (Rho-kinase). *Science* **273**, 245-8.

Kinoshita, T., Yokota, T., Arai, K. and Miyajima, A. (1995). Regulation of Bcl-2 expression by oncogenic Ras protein in hematopoietic cells. *Oncogene* **10**, 2207-12.

Korzh, S., Pan, X., Garcia-Lecea, M., Winata, C. L., Wohland, T., Korzh, V. and Gong, Z. (2008). Requirement of vasculogenesis and blood circulation in late stages of liver growth in zebrafish. *BMC Dev Biol* **8**, 84.

Kranenburg, O., Gebbink, M. F. and Voest, E. E. (2004). Stimulation of angiogenesis by Ras proteins. *Biochim Biophys Acta* **1654**, 23-37.

Kulkarni, S., Goll, D. E. and Fox, J. E. (2002). Calpain cleaves RhoA generating a dominant-negative form that inhibits integrin-induced actin filament assembly and cell spreading. *J Biol Chem* **277**, 24435-41.

Kwan, K. M., Fujimoto, E., Grabher, C., Mangum, B. D., Hardy, M. E., Campbell, D. S., Parant, J. M., Yost, H. J., Kanki, J. P. and Chien, C. B. (2007). The Tol2kit: a multisite gateway-based construction kit for Tol2 transposon transgenesis constructs. *Dev Dyn* **236**, 3088-99.

Lahoz, A. and Hall, A. (2008). DLC1: a significant GAP in the cancer genome. *Genes Dev* **22**, 1724-30.

Lam, S. H. and Gong, Z. (2006). Modeling liver cancer using zebrafish: a comparative oncogenomics approach. *Cell Cycle* **5**, 573-7.

Lam, S. H., Wu, Y. L., Vega, V. B., Miller, L. D., Spitsbergen, J., Tong, Y., Zhan, H., Govindarajan, K. R., Lee, S., Mathavan, S. et al. (2006). Conservation of gene expression signatures between zebrafish and human liver tumors and tumor progression. *Nat Biotechnol* **24**, 73-5.

Langenau, D. M., Keefe, M. D., Storer, N. Y., Guyon, J. R., Kutok, J. L., Le, X., Goessling, W., Neuberg, D. S., Kunkel, L. M. and Zon, L. I. (2007). Effects of RAS on the genesis of embryonal rhabdomyosarcoma. *Genes Dev* **21**, 1382-95.

Langenau, D. M., Traver, D., Ferrando, A. A., Kutok, J. L., Aster, J. C., Kanki, J. P., Lin, S., Prochownik, E., Trede, N. S., Zon, L. I. et al. (2003). Myc-induced T cell leukemia in transgenic zebrafish. *Science* **299**, 887-90.

Lawson, N. D. and Wolfe, S. A. (2011). Forward and reverse genetic approaches for the analysis of vertebrate development in the zebrafish. *Dev Cell* **21**, 48-64.

Le, X., Langenau, D. M., Keefe, M. D., Kutok, J. L., Neuberg, D. S. and Zon, L. I. (2007). Heat shock-inducible Cre/Lox approaches to induce diverse types of tumors and hyperplasia in transgenic zebrafish. *Proc Natl Acad Sci U S A* **104**, 9410-5.

Lee, E., Yim, S., Lee, S. K. and Park, H. (2002). Two transactivation domains of hypoxia-inducible factor-1alpha regulated by the MEK-1/p42/p44 MAPK pathway. *Mol Cells* **14**, 9-15.

Leevers, S. J., Paterson, H. F. and Marshall, C. J. (1994). Requirement for Ras in Raf activation is overcome by targeting Raf to the plasma membrane. *Nature* **369**, 411-4.

Leung, T., Manser, E., Tan, L. and Lim, L. (1995). A novel serine/threonine kinase binding the Ras-related RhoA GTPase which translocates the kinase to peripheral membranes. *J Biol Chem* **270**, 29051-4.

Li, X. R., Ji, F., Ouyang, J., Wu, W., Qian, L. Y. and Yang, K. Y. (2006). Overexpression of RhoA is associated with poor prognosis in hepatocellular carcinoma. *Eur J Surg Oncol* **32**, 1130-4.

Li, Y., Dowbenko, D. and Lasky, L. A. (2002). AKT/PKB phosphorylation of p21Cip/WAF1 enhances protein stability of p21Cip/WAF1 and promotes cell survival. *J Biol Chem* **277**, 11352-61.

Li, Z., Huang, X., Zhan, H., Zeng, Z., Li, C., Spitsbergen, J. M., Meierjohann, S., Schartl, M. and Gong, Z. (2011). Inducible and repressable oncogene-addicted hepatocellular carcinoma in Tet-on xmrk transgenic zebrafish. *J Hepatol*.

Liu, A. X., Rane, N., Liu, J. P. and Prendergast, G. C. (2001). RhoB is dispensable for mouse development, but it modifies susceptibility to tumor formation as well as cell adhesion and growth factor signaling in transformed cells. *Mol Cell Biol* **21**, 6906-12.

Liu, J. J., Chao, J. R., Jiang, M. C., Ng, S. Y., Yen, J. J. and Yang-Yen, H. F. (1995). Ras transformation results in an elevated level of cyclin D1 and acceleration of G1 progression in NIH 3T3 cells. *Mol Cell Biol* **15**, 3654-63.

Liu, L., Zhu, S., Gong, Z. and Low, B. C. (2008). K-ras/PI3K-Akt signaling is essential for zebrafish hematopoiesis and angiogenesis. *PLoS One* **3**, e2850.

Liu, S. and Leach, S. D. (2011). Zebrafish models for cancer. *Annu Rev Pathol* **6**, 71-93.

Llovet, J. M., Burroughs, A. and Bruix, J. (2003). Hepatocellular carcinoma. *Lancet* **362**, 1907-17.

Llovet, J. M., Ricci, S., Mazzaferro, V., Hilgard, P., Gane, E., Blanc, J. F., de Oliveira, A. C., Santoro, A., Raoul, J. L., Forner, A. et al. (2008). Sorafenib in advanced hepatocellular carcinoma. *N Engl J Med* **359**, 378-90.

Lokeshwar, B. L. (1999). MMP inhibition in prostate cancer. *Ann N Y Acad Sci* **878**, 271-89.

Madaule, P. and Axel, R. (1985). A novel ras-related gene family. *Cell* **41**, 31-40.

Madaule, P., Eda, M., Watanabe, N., Fujisawa, K., Matsuoka, T., Bito, H., Ishizaki, T. and Narumiya, S. (1998). Role of citron kinase as a target of the small GTPase Rho in cytokinesis. *Nature* **394**, 491-4.

Maekawa, M., Ishizaki, T., Boku, S., Watanabe, N., Fujita, A., Iwamatsu, A., Obinata, T., Ohashi, K., Mizuno, K. and Narumiya, S. (1999). Signaling from Rho to the actin cytoskeleton through protein kinases ROCK and LIM-kinase. *Science* **285**, 895-8.

Malliri, A., van der Kammen, R. A., Clark, K., van der Valk, M., Michiels, F. and Collard, J. G. (2002). Mice deficient in the Rac activator Tiam1 are resistant to Ras-induced skin tumours. *Nature* **417**, 867-71.

Malumbres, M. and Barbacid, M. (2003). RAS oncogenes: the first 30 years. *Nat Rev Cancer* **3**, 459-65.

Man, J. H., Liang, B., Gu, Y. X., Zhou, T., Li, A. L., Li, T., Jin, B. F., Bai, B., Zhang, H. Y., Zhang, W. N. et al. (2010). Gankyrin plays an essential role in Ras-induced tumorigenesis through regulation of the RhoA/ROCK pathway in mammalian cells. *J Clin Invest* **120**, 2829-41.

Mebratu, Y. and Tesfaigzi, Y. (2009). How ERK1/2 activation controls cell proliferation and cell death: Is subcellular localization the answer? *Cell Cycle* **8**, 1168-75.

Meng, X., Noyes, M. B., Zhu, L. J., Lawson, N. D. and Wolfe, S. A. (2008). Targeted gene inactivation in zebrafish using engineered zinc-finger nucleases. *Nat Biotechnol* **26**, 695-701.

Meyer, V., Wanka, F., van Gent, J., Arentshorst, M., van den Hondel, C. A. and Ram, A. F. (2011). Fungal gene expression on demand: an inducible, tunable, and metabolism-independent expression system for Aspergillus niger. *Appl Environ Microbiol* **77**, 2975-83.

Michailidou, C., Jones, M., Walker, P., Kamarashev, J., Kelly, A. and Hurlstone, A. F. (2009). Dissecting the roles of Raf- and PI3K-signalling pathways in melanoma formation and progression in a zebrafish model. *Dis Model Mech* **2**, 399-411.

Miller, J. C., Tan, S., Qiao, G., Barlow, K. A., Wang, J., Xia, D. F., Meng, X., Paschon, D. E., Leung, E., Hinkley, S. J. et al. (2011). A TALE nuclease architecture for efficient genome editing. *Nat Biotechnol* **29**, 143-8.

Ming, X. F., Viswambharan, H., Barandier, C., Ruffieux, J., Kaibuchi, K., Rusconi, S. and Yang, Z. (2002). Rho GTPase/Rho kinase negatively regulates endothelial nitric oxide synthase phosphorylation through the inhibition of protein kinase B/Akt in human endothelial cells. *Mol Cell Biol* **22**, 8467-77.

Mizgireuv, I. V., Majorova, I. G., Gorodinskaya, V. M., Khudoley, V. V. and Revskoy, S. Y. (2004). Carcinogenic effect of N-nitrosodimethylamine on diploid and triploid zebrafish (Danio rerio). *Toxicol Pathol* **32**, 514-8.

Morin, P., Flors, C. and Olson, M. F. (2009). Constitutively active RhoA inhibits proliferation by retarding G(1) to S phase cell cycle progression and impairing cytokinesis. *Eur J Cell Biol* **88**, 495-507.

Motti, M. L., De Marco, C., Califano, D., De Gisi, S., Malanga, D., Troncone, G., Persico, A., Losito, S., Fabiani, F., Santoro, M. et al. (2007). Loss of p27

expression through RAS-->BRAF-->MAP kinase-dependent pathway in human thyroid carcinomas. *Cell Cycle* **6**, 2817-25.

Mure, H., Matsuzaki, K., Kitazato, K. T., Mizobuchi, Y., Kuwayama, K., Kageji, T. and Nagahiro, S. (2010). Akt2 and Akt3 play a pivotal role in malignant gliomas. *Neuro Oncol* **12**, 221-32.

Murtha, J. M. and Keller, E. T. (2003). Characterization of the heat shock response in mature zebrafish (Danio rerio). *Exp Gerontol* **38**, 683-91.

Nagayoshi, S., Hayashi, E., Abe, G., Osato, N., Asakawa, K., Urasaki, A., Horikawa, K., Ikeo, K., Takeda, H. and Kawakami, K. (2008). Insertional mutagenesis by the Tol2 transposon-mediated enhancer trap approach generated mutations in two developmental genes: tcf7 and synembryn-like. *Development* **135**, 159-69.

Nakashima, M., Adachi, S., Yasuda, I., Yamauchi, T., Kawaguchi, J., Hanamatsu, T., Yoshioka, T., Okano, Y., Hirose, Y., Kozawa, O. et al. (2011). Inhibition of Rho-associated coiled-coil containing protein kinase enhances the activation of epidermal growth factor receptor in pancreatic cancer cells. *Mol Cancer* **10**, 79.

Nakashima, M., Adachi, S., Yasuda, I., Yamauchi, T., Kozawa, O. and Moriwaki, H. (2010). Rho-kinase regulates negatively the epidermal growth factor-stimulated colon cancer cell proliferation. *Int J Oncol* **36**, 585-92.

Narumiya, S., Tanji, M. and Ishizaki, T. (2009). Rho signaling, ROCK and mDia1, in transformation, metastasis and invasion. *Cancer Metastasis Rev* **28**, 65-76.

Nasevicius, A. and Ekker, S. C. (2000). Effective targeted gene 'knockdown' in zebrafish. *Nat Genet* **26**, 216-20.

Nonomura, A., Ohta, G., Hayashi, M., Izumi, R., Watanabe, K., Takayanagi, N., Mizukami, Y. and Matsubara, F. (1987). Immunohistochemical detection of ras oncogene p21 product in liver cirrhosis and hepatocellular carcinoma. *Am J Gastroenterol* **82**, 512-8.

O'Shaughnessy, R. F., Akgul, B., Storey, A., Pfister, H., Harwood, C. A. and Byrne, C. (2007). Cutaneous human papillomaviruses down-regulate AKT1, whereas AKT2 up-regulation and activation associates with tumors. *Cancer Res* **67**, 8207-15.

Olofsson, B. (1999). Rho guanine dissociation inhibitors: pivotal molecules in cellular signalling. *Cell Signal* **11**, 545-54.

Olson, M. F., Paterson, H. F. and Marshall, C. J. (1998). Signals from Ras and Rho GTPases interact to regulate expression of p21Waf1/Cip1. *Nature* **394**, 295-9.

Onnebo, S. M., Condron, M. M., McPhee, D. O., Lieschke, G. J. and Ward, A. C. (2005). Hematopoietic perturbation in zebrafish expressing a tel-jak2a fusion. *Exp Hematol* **33**, 182-8.

Onoda, T., Ono, T., Dhar, D. K., Yamanoi, A., Fujii, T. and Nagasue, N. (2004). Doxycycline inhibits cell proliferation and invasive potential: combination therapy with cyclooxygenase-2 inhibitor in human colorectal cancer cells. *J Lab Clin Med* **143**, 207-16.

Osterop, A. P., Medema, R. H., vd Zon, G. C., Bos, J. L., Moller, W. and Maassen, J. A. (1993). Epidermal-growth-factor receptors generate Ras.GTP more efficiently than insulin receptors. *Eur J Biochem* **212**, 477-82.

Park, S. W., Davison, J. M., Rhee, J., Hruban, R. H., Maitra, A. and Leach, S. D. (2008). Oncogenic KRAS induces progenitor cell expansion and malignant transformation in zebrafish exocrine pancreas. *Gastroenterology* **134**, 2080-90.

Parkin, D. M., Bray, F., Ferlay, J. and Pisani, P. (2005). Global cancer statistics, 2002. *CA Cancer J Clin* **55**, 74-108.

Patton, E. E., Widlund, H. R., Kutok, J. L., Kopani, K. R., Amatruda, J. F., Murphey, R. D., Berghmans, S., Mayhall, E. A., Traver, D., Fletcher, C. D. et al. (2005). BRAF mutations are sufficient to promote nevi formation and cooperate with p53 in the genesis of melanoma. *Curr Biol* **15**, 249-54.

Pawlak, G. and Helfman, D. M. (2002). Post-transcriptional down-regulation of ROCKI/Rho-kinase through an MEK-dependent pathway leads to cytoskeleton disruption in Ras-transformed fibroblasts. *Mol Biol Cell* **13**, 336-47.

Perona, R., Montaner, S., Saniger, L., Sanchez-Perez, I., Bravo, R. and Lacal, J. C. (1997). Activation of the nuclear factor-kappaB by Rho, CDC42, and Rac-1 proteins. *Genes Dev* **11**, 463-75.

Pylayeva-Gupta, Y., Grabocka, E. and Bar-Sagi, D. (2011). RAS oncogenes: weaving a tumorigenic web. *Nat Rev Cancer*.

Qiu, R. G., Chen, J., McCormick, F. and Symons, M. (1995). A role for Rho in Ras transformation. *Proc Natl Acad Sci U S A* **92**, 11781-5.

Rekha, R. D., Amali, A. A., Her, G. M., Yeh, Y. H., Gong, H. Y., Hu, S. Y., Lin, G. H. and Wu, J. L. (2008). Thioacetamide accelerates steatohepatitis, cirrhosis and HCC by expressing HCV core protein in transgenic zebrafish Danio rerio. *Toxicology* **243**, 11-22.

Rembold, M., Lahiri, K., Foulkes, N. S. and Wittbrodt, J. (2006). Transgenesis in fish: efficient selection of transgenic fish by co-injection with a fluorescent reporter construct. *Nat Protoc* **1**, 1133-9.

Richard, D. E., Berra, E., Gothie, E., Roux, D. and Pouyssegur, J. (1999). p42/p44 mitogen-activated protein kinases phosphorylate hypoxia-inducible factor 1alpha (HIF-1alpha) and enhance the transcriptional activity of HIF-1. *J Biol Chem* **274**, 32631-7.

Riento, K. and Ridley, A. J. (2003). Rocks: multifunctional kinases in cell behaviour. *Nat Rev Mol Cell Biol* **4**, 446-56.

Robles, A. I., Rodriguez-Puebla, M. L., Glick, A. B., Trempus, C., Hansen, L., Sicinski, P., Tennant, R. W., Weinberg, R. A., Yuspa, S. H. and Conti, C. J. (1998). Reduced skin tumor development in cyclin D1-deficient mice highlights the oncogenic ras pathway in vivo. *Genes Dev* **12**, 2469-74.

Roomi, M. W., Monterrey, J. C., Kalinovsky, T., Rath, M. and Niedzwiecki, A. (2010). In vitro modulation of MMP-2 and MMP-9 in human cervical and ovarian cancer cell lines by cytokines, inducers and inhibitors. *Oncol Rep* **23**, 605-14.

Rossig, L., Jadidi, A. S., Urbich, C., Badorff, C., Zeiher, A. M. and Dimmeler, S. (2001). Akt-dependent phosphorylation of p21(Cip1) regulates PCNA binding and proliferation of endothelial cells. *Mol Cell Biol* **21**, 5644-57.

Roy, H. K., Olusola, B. F., Clemens, D. L., Karolski, W. J., Ratashak, A., Lynch, H. T. and Smyrk, T. C. (2002). AKT proto-oncogene overexpression is an early event during sporadic colon carcinogenesis. *Carcinogenesis* **23**, 201-5.

Sabaawy, H. E., Azuma, M., Embree, L. J., Tsai, H. J., Starost, M. F. and Hickstein, D. D. (2006). TEL-AML1 transgenic zebrafish model of precursor B cell acute lymphoblastic leukemia. *Proc Natl Acad Sci U S A* **103**, 15166-71.

Sahai, E., Garcia-Medina, R., Pouyssegur, J. and Vial, E. (2007). Smurf1 regulates tumor cell plasticity and motility through degradation of RhoA leading to localized inhibition of contractility. *J Cell Biol* **176**, 35-42.

Sahai, E. and Marshall, C. J. (2002). RHO-GTPases and cancer. *Nat Rev Cancer* **2**, 133-42.

Sahai, E., Olson, M. F. and Marshall, C. J. (2001). Cross-talk between Ras and Rho signalling pathways in transformation favours proliferation and increased motility. *EMBO J* **20**, 755-66.

Saikali, Z. and Singh, G. (2003). Doxycycline and other tetracyclines in the treatment of bone metastasis. *Anticancer Drugs* **14**, 773-8.

Sander, J. D., Cade, L., Khayter, C., Reyon, D., Peterson, R. T., Joung, J. K. and Yeh, J. R. (2011). Targeted gene disruption in somatic zebrafish cells using engineered TALENs. *Nat Biotechnol* **29**, 697-8.

Sandgren, E. P., Quaife, C. J., Pinkert, C. A., Palmiter, R. D. and Brinster, R. L. (1989). Oncogene-induced liver neoplasia in transgenic mice. *Oncogene* **4**, 715-24.

Santoriello, C., Gennaro, E., Anelli, V., Distel, M., Kelly, A., Koster, R. W., Hurlstone, A. and Mione, M. (2010). Kita driven expression of oncogenic HRAS leads to early onset and highly penetrant melanoma in zebrafish. *PLoS One* **5**, e15170.

Schagdarsurengin, U., Wilkens, L., Steinemann, D., Flemming, P., Kreipe, H. H., Pfeifer, G. P., Schlegelberger, B. and Dammann, R. (2003). Frequent epigenetic inactivation of the RASSF1A gene in hepatocellular carcinoma. *Oncogene* **22**, 1866-71.

Scheer, N. and Campos-Ortega, J. A. (1999). Use of the Gal4-UAS technique for targeted gene expression in the zebrafish. *Mech Dev* **80**, 153-8.

Schmidt, C. R., Gi, Y. J., Patel, T. A., Coffey, R. J., Beauchamp, R. D. and Pearson, A. S. (2005). E-cadherin is regulated by the transcriptional repressor SLUG during Ras-mediated transformation of intestinal epithelial cells. *Surgery* **138**, 306-12.

Schramm, K., Krause, K., Bittroff-Leben, A., Goldin-Lang, P., Thiel, E. and Kreuser, E. D. (2000). Activated K-ras is involved in regulation of integrin expression in human colon carcinoma cells. *Int J Cancer* **87**, 155-64.

Shah, V., Bharadwaj, S., Kaibuchi, K. and Prasad, G. L. (2001). Cytoskeletal organization in tropomyosin-mediated reversion of ras-transformation: Evidence for Rho kinase pathway. *Oncogene* **20**, 2112-21.

Shen, L. C., Chen, Y. K., Lin, L. M. and Shaw, S. Y. (2010). Anti-invasion and anti-tumor growth effect of doxycycline treatment for human oral squamous-cell carcinoma--in vitro and in vivo studies. *Oral Oncol* **46**, 178-84.

Shih, C. and Weinberg, R. A. (1982). Isolation of a transforming sequence from a human bladder carcinoma cell line. *Cell* **29**, 161-9.

Shive, H. R., West, R. R., Embree, L. J., Azuma, M., Sood, R., Liu, P. and Hickstein, D. D. (2010). brca2 in zebrafish ovarian development, spermatogenesis, and tumorigenesis. *Proc Natl Acad Sci U S A* **107**, 19350-5.

Sivasubbu, S., Balciunas, D., Davidson, A. E., Pickart, M. A., Hermanson, S. B., Wangensteen, K. J., Wolbrink, D. C. and Ekker, S. C. (2006). Gene-breaking

transposon mutagenesis reveals an essential role for histone H2afza in zebrafish larval development. *Mech Dev* **123**, 513-29.

Skinner, J., Bounacer, A., Bond, J. A., Haughton, M. F., deMicco, C. and Wynford-Thomas, D. (2004). Opposing effects of mutant ras oncoprotein on human fibroblast and epithelial cell proliferation: implications for models of human tumorigenesis. *Oncogene* **23**, 5994-9.

Spitsbergen, J. M., Tsai, H. W., Reddy, A., Miller, T., Arbogast, D., Hendricks, J. D. and Bailey, G. S. (2000a). Neoplasia in zebrafish (Danio rerio) treated with 7,12-dimethylbenz[a]anthracene by two exposure routes at different developmental stages. *Toxicol Pathol* **28**, 705-15.

Spitsbergen, J. M., Tsai, H. W., Reddy, A., Miller, T., Arbogast, D., Hendricks, J. D. and Bailey, G. S. (2000b). Neoplasia in zebrafish (Danio rerio) treated with N-methyl-N'-nitro-N-nitrosoguanidine by three exposure routes at different developmental stages. *Toxicol Pathol* **28**, 716-25.

Stacey, D. W. and Kung, H. F. (1984). Transformation of NIH 3T3 cells by microinjection of Ha-ras p21 protein. *Nature* **310**, 508-11.

Stanton, M. F. (1965). Diethylnitrosamine-Induced Hepatic Degeneration and Neoplasia in the Aquarium Fish, Brachydanio Rerio. *J Natl Cancer Inst* **34**, 117-30.

Stern, H. M. and Zon, L. I. (2003). Cancer genetics and drug discovery in the zebrafish. *Nat Rev Cancer* **3**, 533-9.

Stokoe, D., Macdonald, S. G., Cadwallader, K., Symons, M. and Hancock, J. F. (1994). Activation of Raf as a result of recruitment to the plasma membrane. *Science* **264**, 1463-7.

Stoletov, K. and Klemke, R. (2008). Catch of the day: zebrafish as a human cancer model. *Oncogene* **27**, 4509-20.

Takai, Y., Sasaki, T. and Matozaki, T. (2001). Small GTP-binding proteins. *Physiol Rev* **81**, 153-208.

Tretiakova, M. S., Hart, J., Shabani-Rad, M. T., Zhang, J. and Gao, Z. H. (2009). Distinction of hepatocellular adenoma from hepatocellular carcinoma with and without cirrhosis using E-cadherin and matrix metalloproteinase immunohistochemistry. *Mod Pathol* **22**, 1113-20.

Valencia, A., Chardin, P., Wittinghofer, A. and Sander, C. (1991). The ras protein family: evolutionary tree and role of conserved amino acids. *Biochemistry* **30**, 4637-48.

van Hengel, J., D'Hooge, P., Hooghe, B., Wu, X., Libbrecht, L., De Vos, R., Quondamatteo, F., Klempt, M., Brakebusch, C. and van Roy, F. (2008). Continuous cell injury promotes hepatic tumorigenesis in cdc42-deficient mouse liver. *Gastroenterology* **134**, 781-92.

Vega, F. M. and Ridley, A. J. (2008). Rho GTPases in cancer cell biology. *FEBS Lett* **582**, 2093-101.

Vidal, A., Millard, S. S., Miller, J. P. and Koff, A. (2002). Rho activity can alter the translation of p27 mRNA and is important for RasV12-induced transformation in a manner dependent on p27 status. *J Biol Chem* **277**, 16433-40.

Vitale-Cross, L., Amornphimoltham, P., Fisher, G., Molinolo, A. A. and Gutkind, J. S. (2004). Conditional expression of K-ras in an epithelial compartment that

includes the stem cells is sufficient to promote squamous cell carcinogenesis. *Cancer Res* **64**, 8804-7.

Wang, D., Dou, K., Xiang, H., Song, Z., Zhao, Q., Chen, Y. and Li, Y. (2007). Involvement of RhoA in progression of human hepatocellular carcinoma. *J Gastroenterol Hepatol* **22**, 1916-20.

Wang, L. and Zheng, Y. (2007). Cell type-specific functions of Rho GTPases revealed by gene targeting in mice. *Trends Cell Biol* **17**, 58-64.

Wennerberg, K., Rossman, K. L. and Der, C. J. (2005). The Ras superfamily at a glance. *J Cell Sci* **118**, 843-6.

Westerfield. (2000). The zebrafish book. A guide for the laboratory use of zebrafish (*Danio rerio*). In *University of Oregon Press*.

Westerfield, M., Wegner, J., Jegalian, B. G., DeRobertis, E. M. and Puschel, A. W. (1992). Specific activation of mammalian Hox promoters in mosaic transgenic zebrafish. *Genes Dev* **6**, 591-8.

Wheeler, A. P. and Ridley, A. J. (2004). Why three Rho proteins? RhoA, RhoB, RhoC, and cell motility. *Exp Cell Res* **301**, 43-9.

White, M. A., Nicolette, C., Minden, A., Polverino, A., Van Aelst, L., Karin, M. and Wigler, M. H. (1995). Multiple Ras functions can contribute to mammalian cell transformation. *Cell* **80**, 533-41.

Whittaker, S., Marais, R. and Zhu, A. X. (2010). The role of signaling pathways in the development and treatment of hepatocellular carcinoma. *Oncogene* **29**, 4989-5005.

Wienholds, E., Schulte-Merker, S., Walderich, B. and Plasterk, R. H. (2002). Target-selected inactivation of the zebrafish rag1 gene. *Science* **297**, 99-102.

Wienholds, E., van Eeden, F., Kosters, M., Mudde, J., Plasterk, R. H. and Cuppen, E. (2003). Efficient target-selected mutagenesis in zebrafish. *Genome Res* **13**, 2700-7.

Wong, C. C., Wong, C. M., Ko, F. C., Chan, L. K., Ching, Y. P., Yam, J. W. and Ng, I. O. (2008). Deleted in liver cancer 1 (DLC1) negatively regulates Rho/ROCK/MLC pathway in hepatocellular carcinoma. *PLoS One* **3**, e2779.

Wong, C. M. and Ng, I. O. (2008). Molecular pathogenesis of hepatocellular carcinoma. *Liver Int* **28**, 160-74.

Woodside, D. G., Wooten, D. K., Teague, T. K., Miyamoto, Y. J., Caudell, E. G., Udagawa, T., Andruss, B. F. and McIntyre, B. W. (2003). Control of T lymphocyte morphology by the GTPase Rho. *BMC Cell Biol* **4**, 2.

Xia, M. and Land, H. (2007). Tumor suppressor p53 restricts Ras stimulation of RhoA and cancer cell motility. *Nat Struct Mol Biol* **14**, 215-23.

Xu, X., Sakon, M., Nagano, H., Hiraoka, N., Yamamoto, H., Hayashi, N., Dono, K., Nakamori, S., Umeshita, K., Ito, Y. et al. (2004). Akt2 expression correlates with prognosis of human hepatocellular carcinoma. *Oncol Rep* **11**, 25-32.

Xue, W., Krasnitz, A., Lucito, R., Sordella, R., Vanaelst, L., Cordon-Cardo, C., Singer, S., Kuehnel, F., Wigler, M., Powers, S. et al. (2008). DLC1 is a chromosome 8p tumor suppressor whose loss promotes hepatocellular carcinoma. *Genes Dev* **22**, 1439-44.

Yang, H. W., Kutok, J. L., Lee, N. H., Piao, H. Y., Fletcher, C. D., Kanki, J. P. and Look, A. T. (2004). Targeted expression of human MYCN selectively causes pancreatic neuroendocrine tumors in transgenic zebrafish. *Cancer Res* **64**, 7256-62.

Yang, S., Tian, Y. S., Lee, Y. J., Yu, F. H. and Kim, H. M. (2011). Mechanisms by which the inhibition of specific intracellular signaling pathways increase osteoblast proliferation on apatite surfaces. *Biomaterials* **32**, 2851-61.

Yoshioka, K., Matsumura, F., Akedo, H. and Itoh, K. (1998). Small GTP-binding protein Rho stimulates the actomyosin system, leading to invasion of tumor cells. *J Biol Chem* **273**, 5146-54.

Zhang, Y., Wang, Z. and Magnuson, N. S. (2007). Pim-1 kinase-dependent phosphorylation of p21Cip1/WAF1 regulates its stability and cellular localization in H1299 cells. *Mol Cancer Res* **5**, 909-22.

Zhou, B. P., Liao, Y., Xia, W., Spohn, B., Lee, M. H. and Hung, M. C. (2001). Cytoplasmic localization of p21Cip1/WAF1 by Akt-induced phosphorylation in HER-2/neu-overexpressing cells. *Nat Cell Biol* **3**, 245-52.

Zhu, S., Korzh, V., Gong, Z. and Low, B. C. (2008). RhoA prevents apoptosis during zebrafish embryogenesis through activation of Mek/Erk pathway. *Oncogene* **27**, 1580-9.

Zhu, S., Liu, L., Korzh, V., Gong, Z. and Low, B. C. (2006). RhoA acts downstream of Wnt5 and Wnt11 to regulate convergence and extension movements by involving effectors Rho kinase and Diaphanous: use of zebrafish as an in vivo model for GTPase signaling. *Cell Signal* **18**, 359-72.

Zhuravleva, J., Paggetti, J., Martin, L., Hammann, A., Solary, E., Bastie, J. N. and Delva, L. (2008). MOZ/TIF2-induced acute myeloid leukaemia in transgenic fish. *Br J Haematol* **143**, 378-82.

Zondag, G. C., Evers, E. E., ten Klooster, J. P., Janssen, L., van der Kammen, R. A. and Collard, J. G. (2000). Oncogenic Ras downregulates Rac activity, which leads to increased Rho activity and epithelial-mesenchymal transition. *J Cell Biol* **149**, 775-82.